Unclassified

SECURITY CLASSIFICATION OF THIS PAGE (When Data Entered)

REPORT DOCUMENTATION PAGE	READ INSTRUCTIONS BEFORE COMPLETING FORM
1. REPORT NUMBER AFGL-TR-82-0350	2. GOVT ACCESSION NO. AD-A127553	3. RECIPIENT'S CATALOG NUMBER
4. TITLE (and Subtitle) POLYETHYLENE FREE BALLOON DESIGN FROM THE PERSPECTIVES OF USER AND DESIGNER		5. TYPE OF REPORT & PERIOD COVERED Scientific, Final. 6. PERFORMING ORG. REPORT NUMBER IP No. 314
7. AUTHOR(s) James F. Dwyer		8. CONTRACT OR GRANT NUMBER(s)
9. PERFORMING ORGANIZATION NAME AND ADDRESS Air Force Geophysics Laboratory (LCA) Hanscom AFB Massachusetts 01731		10. PROGRAM ELEMENT, PROJECT, TASK AREA & WORK UNIT NUMBERS 62101F 78591108
11. CONTROLLING OFFICE NAME AND ADDRESS Air Force Geophysics Laboratory (LCA) Hanscom AFB Massachusetts 01731		12. REPORT DATE 12 November 1982 13. NUMBER OF PAGES 119
14. MONITORING AGENCY NAME & ADDRESS(if different from Controlling Office)		15. SECURITY CLASS. (of this report) Unclassified 15a. DECLASSIFICATION/DOWNGRADING SCHEDULE

16. DISTRIBUTION STATEMENT (of this Report)

Approved for public release; distribution unlimited.

17. DISTRIBUTION STATEMENT (of the abstract entered in Block 20, if different from Report)

18. SUPPLEMENTARY NOTES

19. KEY WORDS (Continue on reverse side if necessary and identify by block number)

Free balloons
Polyethylene film
Balloon design
Balloon systems
Stress analysis
Balloon performance statistics
Balloon selection

20. ABSTRACT (Continue on reverse side if necessary and identify by block number)

Those who use large polyethylene balloons for experimental programs are presented with background information on the processes of selecting and designing balloons to meet their respective mission requirements. The effects of payload weight, altitude, duration, and vertical control on both the total payload weight and the balloon size are discussed with respect to these processes. The need to define mission success in terms of realistic requirements is emphasized and a mission planning procedure is proposed.

DD FORM 1 JAN 73 1473 EDITION OF 1 NOV 65 IS OBSOLETE

Unclassified

SECURITY CLASSIFICATION OF THIS PAGE (When Data Entered)

20. Abstract (Continued)

Assumptions and problems in contemporary balloon design are discussed, and design and analysis procedures based on the loads and geometry at the time of launch are developed. Dynamic launch shock is proposed as a criterion for shell thickness, and a model of polyethylene film modulus is developed to account for strain rate and stress and strain relaxation at a launch temperature of 23°C.

Computer codes have been written for the processes of balloon selection and balloon design to meet mission requirements. They are intended to be a basis for more efficient, interactive mission planning.

Finally, improvements to the balloon design process are proposed and discussed.

Preface

Successful balloon operations start with the definition of essential and realistic balloon flight requirements. Project scientists and program directors do not have to be conversant with the details of ballooning from either the design or operational perspectives, but they do have both a legitimate need and an obligation to understand the impact of their mission requirements on the selection, design, and performance of the balloons for their programs. In addition, they should be aware of the standards, processes, and historical perspectives that enter into the choice of the balloon to which they will eventually entrust their payload.

Because of the structural design of the balloon, the characteristics of its materials, and the nature of its use environment, performance and design are best examined statistically. Accordingly, and because the greater the variety of designs and experiences that are available to the designer, the better will be his understanding of and confidence in the decisions that he must make, a significant design and performance data base is included.

It is hoped that this report will serve as an initial ground upon which users and designer can meet in productive interaction. If such becomes the case, it will in no small part have been made possible by Mr. Jean R. Nelson, Vice President of Engineering, Winzen International, Incorporated, who made available much of the balloon design data and most of the performance data base for the larger balloons. Finally, Mrs. Catherine L. Rice deserves considerable credit for her technical suggestion and assistance in the effective organization of the material.

Contents

Contents

Illustrations

Tables

Polyethylene Free Balloon Design From the Perspectives of User and Designer

1. INTRODUCTION

Structurally the balloon (see Figure 1) is not a complicated device; for the most part it consists of panels (gores) and ribbons (load tapes) welded (heat sealed) together and clamped together at the apex and nadir ends of its vertical axis. The shapes, as constructed, are nearly axially symmetric, and each shape resembles a classical spinning top.

Performancewise, however, the balloon is an extremely complex thermodynamic machine. This is true not only with respect to its vertical motions, but also with respect to the distribution and dissipation of forces within its load bearing structural membranes and tape reinforcements; this is the case because the membranes are almost universally a high quality polyethylene, a strongly non-linear viscoelastic polymeric material.

It is not important for the user to understand these latter aspects on an esoteric level. However, with respect to the desired degree of conservatism and level of confidence, both the user and designer should be aware of the major assumptions and limitations underlying the design and the statistics of tested designs viewed uniformly from the same perspectives.

(Received for publication 9 November 1982)

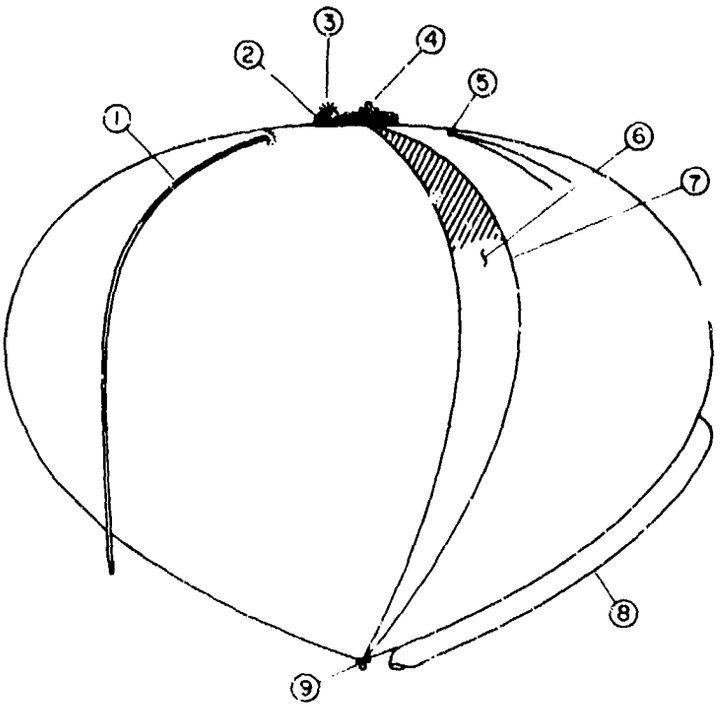

Figure 1. Conventional Modern Plastic Balloon. Components consist of: 1) inflation or fill tube, 2) apex fitting, 3) strobe light, 4) electric valve, 5) destruct button at apex of rip panel "V" tapes (two of these are usual and they are activated by a line that passes from the payload-parachute up through the balloon and is secured to them), 6) gore panel (usually about 100 in. wide at balloon's maximum diameter), 7) load tapes, 8) pressure relief duct, and 9) base end fitting with load ring for payload suspension. Very thin film balloons and heavy load balloons frequently have multiple wall construction in the crown region. These multiple layers are called caps. The hatched area shows a typical cap panel

Balloon designs are not originated on anything like a daily basis, but in forecasting, system planning, operations, and post-operational analyses, questions relative to balloon capability arise on an almost daily basis. Answers to these questions involve (some to a greater extent than others) a knowledge and understanding of the criteria and processes used in establishing the operational limits for existing or potential designs.

Considerable attention to the user's mission requirements is necessary, both to impress upon the user the need to assess the impact of his decisions concerning

payload design on the ultimate balloon design decision, and to serve as a bridge in discussions between user and designer.

The literature lacks an integrated compendious treatment of design procedures, criteria, and actual performance data suited for independent use by both the user and designer. The research results presented herein are intended as a first step in satisfying the need for a common reference to produce productive interaction between the two during the often critical phase of balloon payload conceptual design.

The analyses and criteria developed herein are not the ultimate answers. They are based on admittedly incomplete understanding of the materials and somewhat oversimplified methods of load distribution within the balloon load bearing structure. However, they are comparable with other present efforts, are more revealing than most, and are consistent with previously postulated causes of ascent failure and recent inflight measurements.

2. BALLOON MISSION REQUIREMENTS

2.1 General

Although use of the term "requirement" is customary, it can convey an undeserved priority. In practice, requirements range from 1) essential, through 2) if possible, to 3) desirable if practical. Also, in practice it has been found that some user requirements gravitate to the bottom of the described scale as critical timetables and operational windows exert their psychological pressures. In this regard, pre-definition of mission success in terms of realistic requirements can and should be made in the low pressure mission-planning phase, rather than in the most often highly stressful balloon flight operations environment. Cost and the probability of mission success should, accordingly, be improved. NASA, in their heavyload balloon program critique, took due note of the advantages of such a strategy. [1]

User requirements can be met in three ways: 1) use of a balloon from an existing inventory; 2) purchase of a balloon using existing specifications for a proven design; and 3) purchase of a balloon using a new set of specifications developed specifically to meet the mission requirements. Ideally, the latter option might appear to be optimum. However, the demonstrated reliability of existing designs, time, cost, priority, and other mission constraints are also

1. Cuddihy, W. F., et. al. (1979) A review of heavy lift balloon failures, Proceedings, Tenth AFGL Scientific Balloon Symposium, Catherine L. Rice, Ed., AFGL-TR-79-0053, AD A074459.

factors that frequently affect the choice of an option. All other factors notwithstanding, adequacy with respect to meeting the essential mission requirements is the overriding factor.

The adequacy of a specific balloon for a proposed mission is determined by its potential ability to carry the mission payload in the prescribed space-time profile, without adversely affecting the functions of the user's payload. This latter aspect of adequacy is not reflected in the balloon design unless it affects launch-related design features or necessitates added payload capacity for mechanical or thermal isolation of the payload. Other aspects of adequacy are expressable as requirements and can be translated by the balloon designer into balloon size, shape, structural materials and reinforcements, and, to a greater or lesser degree, construction features related to the launch method.

In an idealized case, the mission payload could be treated as "cargo" and the balloon system could be treated as a "carrier" consisting of the balloon proper, Figure 1, and its essential payload subsystems, Figure 2. In practice, however, such isolation rarely exists. Interfacing ranges from simply providing (in the carrier payload subsystems) command-activated circuit closures to full electro-mechanical integration of the mission and carrier payloads, exemplified in Figure 3. In general, regardless of the degree of isolation, the necessary rigging, mission payload, and carrier payload subsystems can be co-configured and the combined weight estimated independently of the balloon. Thus, there is no loss in generality in assuming a fully integrated payload. It is important to note that the payload recovery subsystem, normally a parachute, is, at this point, excluded from the carrier payload subsystem because the recovery parachute subsystem must be sized to accommodate the total suspended payload, including ballast. See Appendix B.

Most important but frequently overlooked in early planning, is the relative uniqueness of the mission payload and/or the lack of balloon experience within mission management. These factors create a tendency for mission planners to underestimate the final payload weight. The balloon system designer is thus well advised to include a factor to accommodate such growth and its effect on total payload weight. When appropriate, design experience should be used, but for general purposes a growth allowance factor of 10 percent is used.

2.2 Flight Profile Considerations

The space-time mission profile of a zero-pressure free balloon system, beyond attainment of the initial ceiling altitude, is normally achieved by

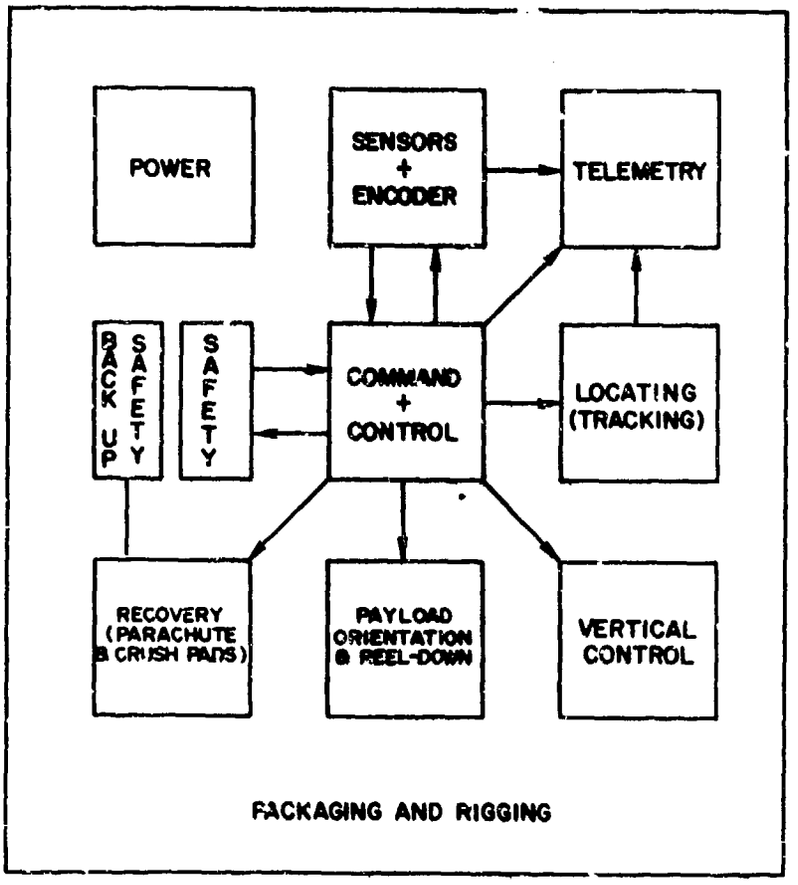

Figure 2. Essential Free Balloon Subsystems, Diagrammed to Show Interactions. The back-up safety system has its own power source, whereas the main power source services all of the other subsystems

deballasting and valving*: deballasting to slow or stop descent and to re-start ascent, and valving of lifting gas to slow or stop ascent and to accelerate or start descent. Figure 4 shows a typical profile and the control functions exercised to achieve it. It is clear that both profile and duration are dependent on the number of deballasting exercises, n, and the demand, d_i, of each exercise. The latter is expressed as a fraction of the gross system weight and is generally accepted as the dominant factor in the determination of both vertical velocity and total

*Alternative cryogenic gas replenishment systems are still in an experimental stage.

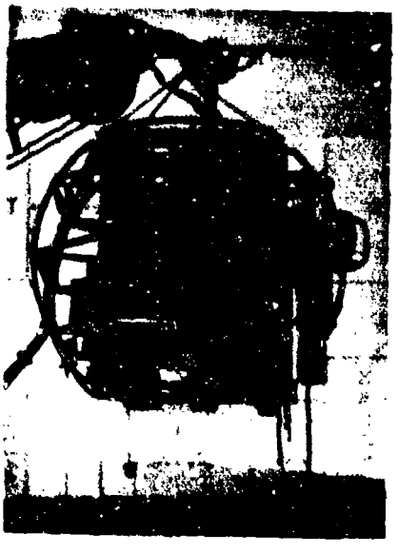

Figure 3. An Electro-Mechanically Integrated Payload. Shock-absorbing suspension frame is designed to provide mountings for the integrated experiment and carrier functions. The gondola, about 7 ft in diameter is shown suspended from the boom of the launch vehicle, a 60-ton crane

sunset ballast weight. Mission profile is thus translated into added system weight (ballast) according to the following:

$$W_s = \left[-1 + \prod_{i=1}^{n} (1 - d_i)^{-1} \right] (W_P^* + W_b) \quad , \tag{1}$$

where

W_s is the ballast weight

W_P^* is the irreducible payload weight

W_b is the balloon weight

d_i is the i^{th} fractional ballast drop .

Assignment of a value to each d_i is dependent, for the most part, on experience and statistical evidence, colored by the degree of conservatism of the mission planner.

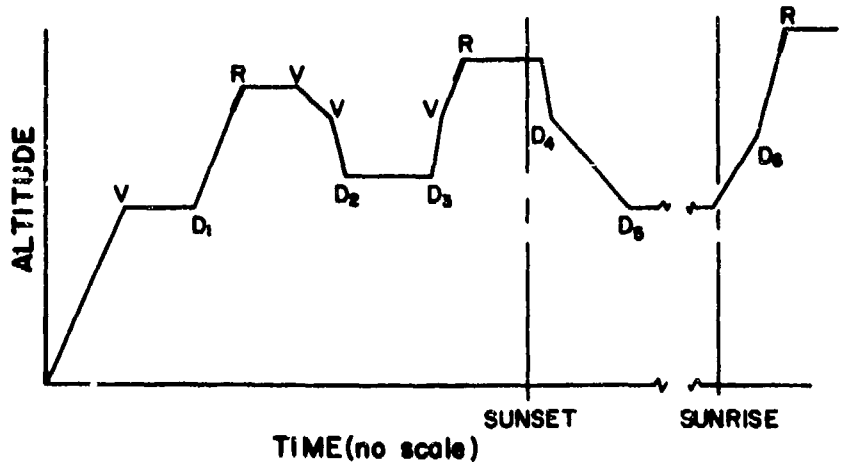

Figure 4. Typical Multilevel Flight Profile For a Zero-Pressure Free Balloon System. Symbols: V denotes valving through apex valve; R denotes the conclusion of the period of venting of excess lifting gas through the overpressure relief ducts; D denotes deballasting. For simplicity the very slow protracted descent following solar noon (but prior to sunset on the balloon) is not shown

Equation (1) expresses only the interdependence of the principal system weights, the balloon weight, the ballast weight, and the combined instrumentation and parachute weights. It does not address compatability between the parachute weight, implicit in W_P^*, and the required parachute size and strength.

If a mission requires a large amount of ballast, the parachute size required to support the initial flight payload in an emergency flight termination might exceed by far the parachute size required by the deballasted system. In such cases, dead weight ballast to ensure parachute stability and to minimize drift may be desirable. This need also arises from the availability of only discrete parachute sizes.

Figure 4 omits an essential reference in the space-time mission profile example; this is the reference to the initial space-time launch coordinates: geographical location, time of year, and time of day. These factors, except for time of day, influence both the size of the balloon and the statistical ballast needs with respect to flight duration. Time of day has a definite effect on ascent performance and could, thereby, place added ballast demands on the system. In addition, all of these factors influence the balloon structural design.

2.3 Establishing Mission Requirements

Users are familiar with the problems and limitations relative to the design of their own payload subsystems, but often lack a healthy appreciation of related balloon system problems. Aside from the sometimes complex electromechanical and electromagnetic interface problems, the most prevalent problem associated with present high altitude systems is runaway final payload weight with its consequent increased balloon size requirement. This is sometimes quite serious - balloons with volumes in the tens of millions of cubic feet are most often fabricated from thin polyethylene film and appear to have a greater number of failure modes than do smaller balloons made from thicker films.

The inter-relationship of mission requirements and balloon system design, and an interactive procedure to establish realistic and acceptable mission requirements are described schematically in Figure 5. The successful and efficient functioning of this planning procedure depends in great measure upon the user's ability both to establish a firm priority list of mission requirements and to define mission success in terms of these requirements (steps 2 and 3). Input from a balloon instrumentation engineer in step 4, use of interactive automated decision aids to accomplish step 5, and a team (user, instrumentation engineer, balloon design specialist, and balloon operations specialist) to effect step 6 are necessary and sufficient to implement such a procedure. Realism, as introduced in step 6, implies considerations of both time and other essential resources.

The planning document, Appendix A, typifies the first step in the procedure that moves from a conceptualized mission, through the negotiated establishment of mission requirements to design selection, whether new or existing. In summary form the information needed to arrive at a final decision includes, but is not limited to:

a) user payload weight

b) flight profile (altitudes, durations, vertical motion rates, and horizontal trajectories)

c) location, time of year, and time of day of proposed flight

d) launch and recovery shock restrictions

e) payload configuration

f) isolation of user's payload from influence of balloon temperature field and from balloon induced motions (including orientation of user's payload)

g) shielding from electromagnetic interference

h) electro-mechanical interfaces

i) command and data channels

j) special handling and support (such as required for delicate and hazardous payloads)

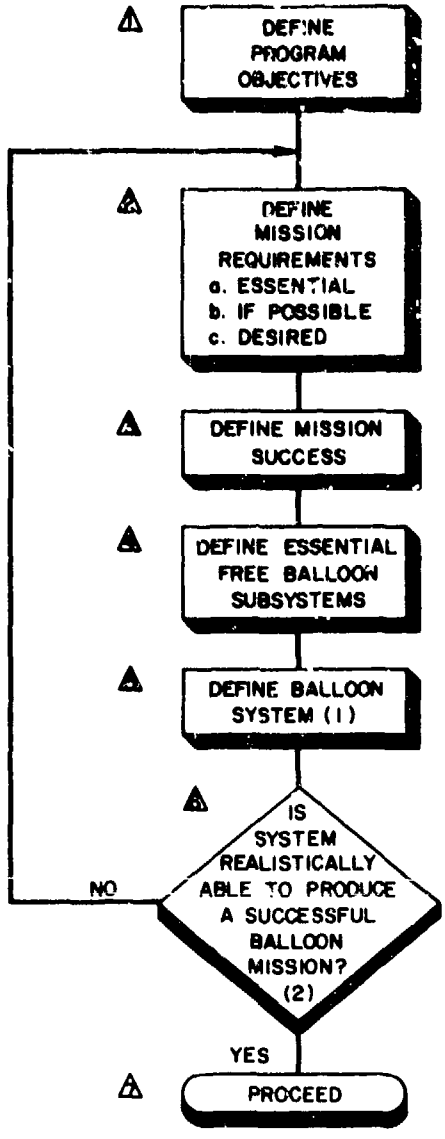

Figure 5. Mission Requirements Planning Procedure. (1) Balloon, ballast, and parachute can be defined by routines in Section 3 and/or 6. (2) There are no hard and fast rules for this decision. "YES" is equivalent to a high degree of confidence and "NO" to a low degree of confidence. Stress levels performance of systems with comparable features (film thickness, payload, grossload, balloon size, etc.) and general complexity of launch-recovery operation should be among the considerations

k) general description of payload functions

l) miscellaneous (frequencies, optical or radar tracking, etc.).

3. ADEQUACY OF EXISTING DESIGNS

There are many possible iterative sequences of computations and checks by which one might determine the adequacy or inadequacy of any particular balloon with respect to any particular set of mission requirements. One such sequence is depicted in Figure 6, the flow diagram for the computer program "ADEQUATE" (Appendix C). This program, developed under this study, when used with the table of tested and proven balloon designs, Appendix H, produces a sub-list of balloons adequate for a specified mission, and further indicates which of the sub-listed balloons yields the minimum system weight and therefore the optimum solution based on efficiency.

The quantitative input for the program listed in Appendix C is generated interactively on the basis of a series of questions appearing sequentially on the computer display. The first question offers a choice between metric and English units for the input; internal computations and output are in English units. Succeeding questions and their respective sample input values appear in Table 1. The entry, 0.050, following "BALLAST FRACTION" is the value input to satisfy the single sample requirement of the "BALLAST DROPS FOR CONTROL" entry.

The sample search of the tabulated designs for the balloon design that would best fulfill the requirements set forth in Table 1 yielded the entries in Table 2. AFGL models SV-016A and SV-020 have margin comments indicating that, although they meet the needs, they have not been flown with the required payloads. The asterisk opposite the entry for model LTV-006 indicates, as shown, that use of this model yields the minimum system weight.

The minimum system weight criterion is one of many that could be applied. For example, cost tables could be provided and accessed to make a decision on the most economical system. Even better perhaps, the stress level at launch could be computed for each adequate system configuration and selection could be based on minimum stress (on the premise that minimum stress equates with maximum reliability).

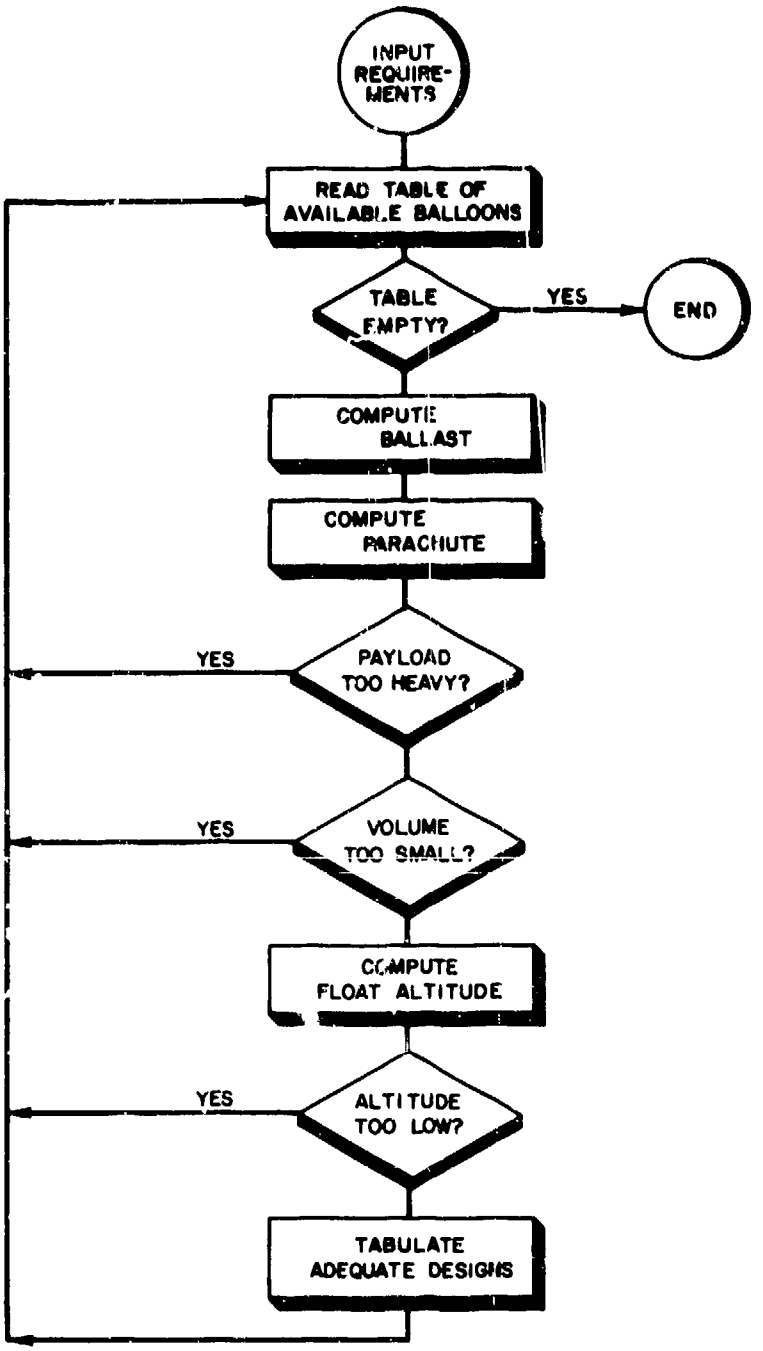

Figure 6. Flow Diagram for Interactive Determination of Adequate Existing Balloon Designs. Table of existing designs includes rated and tested payloads. This routine is the basis of "ADEQUATE", the program included as Appendix C

Table 1. Listing of Interactive Input for "ADEQUATE"

Input Parameter	Value
Altitude (ft)	100000
Payload (lb)	800
Descent Ballast Fraction	0.1
Ballast Fraction for Drive-up	0.07
Payload Growth Fraction	0.2
Sunset Ballast Drops	2
Fractional Sunset Ballast	0.08
Ballast Drops for Control	1
Chute Impact Speed (ft/sec)	20
Standard Atm. (1966)	
Ballast Fraction 0.050	

4. PAYLOADS AND THEIR SIGNIFICANCE WITH RESPECT TO PERFORMANCE AND DESIGN OF NATURAL SHAPE BALLOONS

4.1 The Natural Shape

Some background information on the "natural shape" balloon concept is necessary to an understanding of balloon shape and payload interaction. Minimally, this information consists of a definition of natural shape and an enumeration of certain shape-dependent characteristics.

The natural shape (Figure 1 for example) is a relatively uncomplicated and logical concept. It is based on simple membrane theory and upon the following assumptions: 1) the shapes are rotationally symmetric about the vertical axis; 2) the envelope is thin, homogeneous, inextensible, and incapable of supporting bending or compression; 3) the density difference between the atmosphere and the inflatant is constant over the height of the balloon; 4) the circumferential stress for any horizontal cross section is zero; and 5) there is no shear force. For a given payload weight, floating altitude, lifting gas, and unit envelope weight a unique zero-pressure shape exists and is characterized by a dimensionless number Σ, defined as:

$$\Sigma = \left(\frac{2\pi w^3}{W_{P,O} b_0^2} \right)^{1/3} .$$

Table 2. Output From "ADEQUATE". Dimensions are in English Units. Drift speed is terminal parachute speed when all ballast has been used

MODEL NO	VOLUME	MAXIMUM PAYLOAD	BALLOON WEIGHT	BALLAST WEIGHT	CHUTE WEIGHT	CHUTE SIZE	DRIFT SPEED	
SV-001A	5033609	4500	1340	1199	163	91	8*	
SV-006	25000000	4200	2635	1876	215	104	7	
SV-007	6677900	3600	2470	1767	208	102	7	
SV-008	8740030	7300	2430	1733	208	102	7	
SV-009	10576059	3500	2150	1506	136	99	7	
SV-014	15600000	3400	1890	1477	189	97	7	
SV-015	21580000	3100	2145	1504	196	99	7	
SV-016A	11620000	2400	1240	1149	165	90	8*	ABOVE TESTED LOAD
SV-017B	5142712	5000	1600	1330	178	94	7	
SV-019	5136000	5000	1470	1266	175	93	7	
SV-020	11617429	2400	1240	1149	165	90	8*	ABOVE TESTED LOAD
LTV-006	5033809	3000	1120	1089	162	89	8*	
SV-500	26085893	3800	2588	1828	215	104	7	
SV-501	27938324	5400	3416	2245	244	111	7	
SV-502	29008952	3400	2470	1767	208	102	7	
SV-503	33325200	3900	3041	2056	231	108	7	
SV-504	25690000	3000	2113	1583	196	99	7	
SV-505	25930000	4000	2607	1838	215	104	7	
SV-506	28048674	7250	4507	2794	284	120	7	
SV-508	28463000	4500	2853	1961	223	106	7	
SV-509	30390020	7500	4650	2866	288	121	7	
SV-510	31210000	4000	2733	1901	219	105	7	
SV-513	33120000	3400	2425	1745	208	102	7	
SV-514	31150000	3800	2800	1933	219	105	7	
SV-515	33500000	6000	4300	2689	274	118	7	
SV-517	34090000	5050	3732	2404	257	114	7	
SV-518	34311500	6000	4306	2692	274	118	7	
SV-521	39590000	7500	5064	3074	303	124	7	
SV-523	45840000	3900	3089	2080	231	108	7	
SV-524	47012000	6300	4064	2570	265	116	7	
SV-531	26400000	4000	2706	1888	219	105	7	
SV-522	42500000	5900	5300	3043	303	124	7	
SV-526	33100000	4500	3660	2367	252	113	7	

LAST * YIELDS LOWEST GROSS, 3331 POUNDS.

where

w is the unit weight of the shell film (lb/ft^2);

$W_{P,O}$ is the payload (lb) at the design point, and

b_0 is the specific lift of the inflatant (lb/ft^3), a function of the temperature and pressure at the design point altitude.

For each natural shape Σ there exists a family of dimensionless constants f_i, among which are:

f_1, the ratio of balloon weight to design-point payload weight;

f_2, the ratio of balloon maximum volume to the cube of the gorelength;

f_3, the ratio of the balloon surface area to the square of the gorelength;

f_4, the ratio of the balloon's maximum horizontal diameter to the gorelength; and

f_5, the ratio of the height of the fully inflated shape to the gorelength.

A most significant assumption about the natural shape balloon is that for payloads in excess of the design-point payload, the shape becomes less oblate - the limiting case being an approximation of the shape for which sigma is zero (in which case either the balloon film is weightless or the payload is infinitely heavy with respect to the balloon). With reduced oblateness every point on the original surface shifts so that its radial distance from the vertical axis of symmetry is reduced; the shell thus exhibits vertical wrinkles and the volume is decreased. Observed balloon performance seems to verify this important assumption.

4.2 Payload Designations

There are several "payload" designations with which we are concerned as a result of their significance in the design and selection of a balloon for any specific mission. In the usual order* of ascending weight, they are:

a) the design-point payload designated $W_{P,O}$;

b) the design payload;

c) the irreducible payload;

d) the mission payload designated $W_{P,M}$;

e) the maximum payload designated $W_{P,X}$.

*Mission payloads less than the design-point payload have been flown successfully for the purposes of increased efficiency and constancy of shape and volume; the required design and selection procedures for these specialized cases are not included, but there is additional commentary in the following text.

The design-point payload is not only a factor in the determination of Σ, it is the payload weight above which the balloon becomes less efficient by virtue of its change in shape and attendant reduction in volume. Further, it is that payload below which the fully inflated volume is constant and there is a re-orientation of the shell stresses - an increase in circumferential stress. This condition was unacceptable in the early days when it was difficult to obtain high strength gore seams, but it is no longer a problem.

The design payload, not to be confused with the design-point payload, consists of the user's experimental payload, the command and telemetry system to control the flight, and the rigging or gondola.

The irreducible payload consists of the design payload and the payload recovery parachute system; it is the total suspended payload after all flight control ballast has been dropped.

The mission payload includes the irreducible payload and the flight control ballast required to accomplish the mission objectives.

The maximum payload is that payload for which the tape and film loadings meet but do not exceed the design stress limits. This load is the principal factor affecting the required film thickness and load tape strength.

In general the range $W_{P,O}$ to $W_{P,X}$ is small enough to ensure efficiency with respect to reduced volume at high payloads and yet large enough to make the designs applicable to a reasonable range of requirements.

4.3 Payload – Altitude Relationship

Altitude per se does not appear in the models or functions that relate payload and altitude; rather it is b, the specific lift of the inflatant (lb/ft^3) that is a function of ambient pressure and temperature.

The weights in pounds of the maximum payload, mission payload, and design-point payload are subject to the relationship

$$W_{P,X} \geq W_{P,M} \geq W_{P,O} ,$$

and in the extreme case, when $W_{P,X} = W_{P,M} = W_{P,O}$, the balloon volume is constant and the altitude indicator b is numerically equal to the ratio of the system weight in pounds and balloon maximum volume in cubic feet.

For the natural shape balloon with a payload W_P in the range $W_{P,O} \leq W_P \leq W_{P,X}$ the payload-altitude relationship is best expressed by the function

$$\left[\frac{W_P - W_{P,O}}{b - b_0} \right] = 0.12605\, S^3 , \qquad (2)$$

where S is the balloon gorelength in feet.

The origin of this simple function is unknown, but its accuracy by actual comparison is as good as other standard methods for relating payload and altitude for natural shape balloons. Further it is nearly an ultimate formula for demonstrating the design options with respect to allowable payload and altitude combinations for natural shape balloons.

For an existing natural shape design, the gorelength is fixed, as are the balloon weight and balloon maximum volume. Thus the ratio f_1 (balloon weight to design-point payload weight) fixes both the design-point payload and the specific lift at the floating altitude for that payload. Therefore, for a fixed design, the variables in Eq. (2) are reduced to only W_P and b, and we are provided with a simple expression of altitude (corresponding to b) in terms of the suspended payload. The correspondence of altitude and b is, of course, governed by the use-atmosphere.

Now where W_b is the balloon weight in pounds, and the other terms are as previously defined in this section, we can express W_b in the following ways:

$$W_b = f_1 \cdot W_{P,O} \cdot \tag{3}$$

$$W_b = b_0 \cdot f_2 \cdot S^3 - W_{P,O} \cdot \tag{4}$$

$$W_b = w \cdot f_3 \cdot S^2 \, . \tag{5}$$

Since Eqs. (3) and (4) combine to yield

$$f^* = \left[\frac{f_1 + 1}{f_2} \right] = \left[\frac{b_0 S^3}{W_{P,O}} \right] \tag{6}$$

and since f* is a monotonic function, Σ is uniquely determined by specifying $W_{P,M}$, $W_{P,O}$ and b_M in Eq. (2) and then estimating the gorelength S. Equations (3) and (5) can then be solved to yield the film weight w and consequently the film thickness.† These relationships, in conjunction with Eq. (1), ensure that the mission payload and altitude requirements are consistent with natural shape balloon performance theory. Iteratively solving Eqs. (1) through (4) together with Eq. (6) and Eq. (5) (modified to include other balloon component weights) produces a design that guarantees a set of weights consistent with the prescribed mission altitude. Details of this procedure along with models of the ratios f_1 are covered in Section 6 and in Appendix G.

†Weights of components other than gores are excluded here for reasons of clarity of presentation. These components include, for the most part, tapes, caps, seams, and ducts.

5. GENERAL BALLOON DESIGN CONSIDERATIONS

Balloon selection and balloon design both depend on identical loading criteria; both likewise depend on compromises. Balloon selection compromises are most frequently forced, practical compromises of mission objectives based on available balloons and, most importantly, on proven or demonstrated capabilities. Design compromises, on the other hand, involve decisions on materials and structural variations to accommodate often conflicting requirements. (For example, balloon envelope durability for remote launch conditions presents a problem if the balloon payload-altitude requirement mandates, on the basis of weight, a very thin film for the shell.) The nature of the synthetic structural materials, the statistical nature of the atmosphere and the random deployment of the load bearing structure during ascent force decisions based on engineering principles, intuition, extrapolation, and willingness to risk.

End fittings, inflation tubes, destruct systems, reefing sleeves, and ducts no longer present critical design or installation problems. However, overdesign of duct-valving area presents a potentially significant reduction in payload capacity and reliability for very high altitude balloons to carry small payloads (Appendix F). The components that present the significant design problems are the caps, gores, and load tapes, each of which will be discussed in some detail.

5.1 The Load Cap

The problem of cap design is in reality the problem of determining the thickness of the crown of the balloon. This thickness is the sum of the shell (gore) film thickness and the film thickness of the cap(s). The cap length is generally accepted as:

$$L_c = C\,(G/b)^{1/3}, \tag{7}$$

where

L_c is the cap length (ft);

C is a constant;

G is the gross lift (lbs); and

b is the specific lift of the inflatant at S. T. P. (lb/ft^3).

Although C is a constant, there is no agreement on its value, but the accepted range is small, $3 \leq C \leq 3.18$. The larger value is probably the result of an investigation of failures of large balloons. This investigation was conducted by the Office of Naval Research in 1971. Launch films were reviewed and it was recommended to "... lengthen the present cap material to insure that most of the dynamic forces realized during the initial launch phases are contained within the capped area of the balloon ..."*

When there is no cap, the crown thickness is, of course, the shell (gore) thickness, but with most new designs either the load is sufficiently heavy or the altitude sufficiently high to justify the use of a cap with its attendant costs and added risks.**

Criteria for determining crown film thickness have not evolved commensurately along with the improvements in balloon capabilities, manufacturing techniques, materials, and designs.[2,3] For the most part, crown thickness has been based on the function

$$G = 1260(\sigma_m t)^{3/2} , \tag{8}$$

where

G is the gross lift of the system (lb/ft^3);

σ_m is the meridional film stress ($lb/in.^2$); and

t is the crown thickness (in.).

This function was developed to approximate the meridional stress at the maximum diameter of a helium-filled, tapeless, uncapped balloon at an altitude of 1000 ft (Schwoebel[4]). The allowable value of σ_m for contemporary designs (discussed in Section 5.3) appears to be based on experience and on the degree of conservatism of the designer.

---

*The quotation is from the 18 August 1971 Memorandum on the conclusions of the meeting of 9 August 1971. The Memorandum was entitled "Problems Concerning Large Volume Balloons", and was signed by F. B. Isakson, Director, Physics Program.

**Added structural complexity and added manufacturing handling provide (respectively) added modes of failure and added opportunities for damage and therefore added risks.

2. Dwyer, J. F. (1974) Free balloon capabilities: A critical perspective, Proceedings (Supplement), Eighth AFCRL Scientific Balloon Symposium, 30 September to 3 October 1974, Andrew S. Carten, Jr., Ed., pp. 123, 161.

3. Dwyer, J. F. (1973) Zero pressure balloon shapes, past, present, and future, Scientific Ballooning (COSPAR), W. Riedler, Ed., Pergamon Press, pp. 9, 19.

4. Schwoebel, R. L. (1956) Strato-lab Development, Final Technical Report, Contract No. NONR 1589(06).

Schwoebel considered the stress to be at its maximum for the conditions for which the approximation function was derived. Okamoto[5] likewise suggested that the film stresses at this point in the balloon flight were maximum. Certainly the differential pressure acting on the material in the crown is the greatest at the completion of inflation, and the modulus and yield strength of the film are minimum at launch temperatures. These being so, one might speculate why all failures do not occur at launch.

Some failures do occur at launch and some failures do occur at high altitudes, but historically most failures occur at tropopause (minimum temperature) altitudes. Photographic evidence of such tropopause-failures indicates that the crown is the region of failure. Photographic evidence and meteorological data indicate that wind shears and turbulence acting on the rising balloon cause dynamic loading of the undeployed film at tropopause altitudes. Weissmann[6] offered laboratory tests and a theory that appears to explain the role of such dynamics in tropopause-failures, but he concluded that the deformation history of the film also probably played a significant role.

Anderson[7], Dwyer[8], Kerr[9, 10, 11], Alexander[12], Webb[13], and Rand[14] have also addressed aspects of the relationships among film stress history, material properties, balloon designs, and balloon failures. The most significant conclusions appear to be:

1) "... environmental temperatures at or below the cold brittle transition temperature of polyethylene are not sufficient to produce balloon burst," but "ambient launch temperature appears to be a critical factor both statistically and from an engineering viewpoint." (Dwyer[8]). (See Figure 7

2) Polyethylene film performance "appears to have a strong dependence on stress history." (Webb[13]).

3) "... path dependency has been demonstrated to influence the behavior of polyethylene films ..." (Rand[14]).

4) It "appears that the observed correlation of the ductile-brittle transition to a preload strain state is only valid for one loading history, creep. It would seem that there is a material state associated with this transition that can be reached through different loading histories at different strain states." (Alexander[12]). (See Figures 8 through 11).

5) "In a balloon system the influence of rates, histories, temperature and the like can be even more important than indicated by laboratory tests. The balloon skin must work as a system to uniformly distribute loads. When a few gores (or even segments within one gore) see a history at variance with the rest,

---

Because of the large number of references cited above, they will not be listed here See References, page 57.

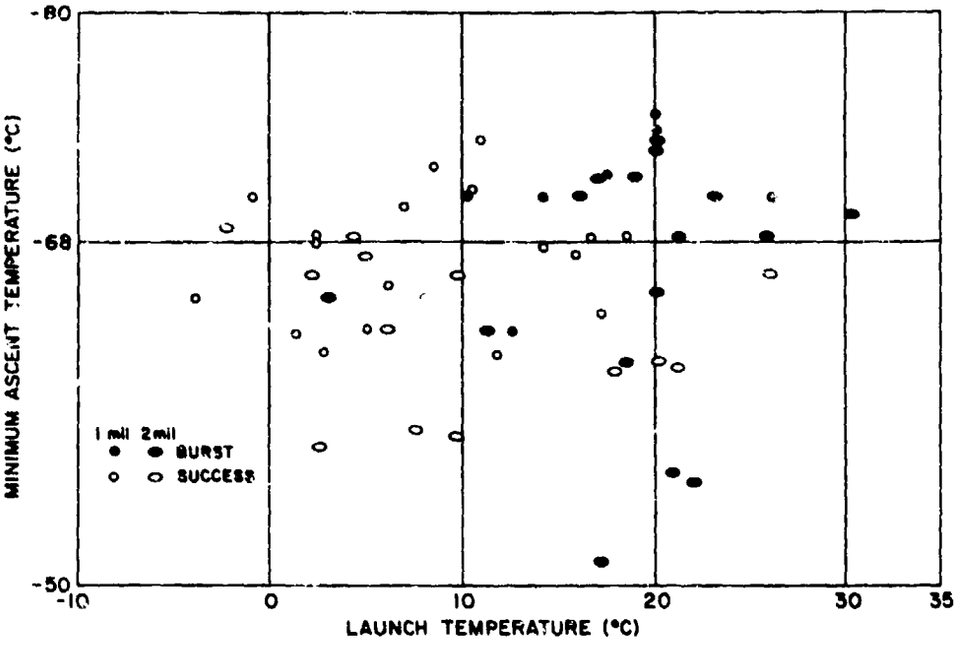

Figure 7. Balloon Performance Classification With Respect to Significant Temperatures

then uniformity of behavior is destroyed. Unusual and unexpected stresses will result and ordinarily adequate designs can fail." (Webb[13]). (Emphasis added).

The thickness determination problem thus appears incapable of direct solution; to know as a function of time the stresses in each small area of the shell (deployed and undeployed), even if possible, does not appear to be practical. Conceivably, however, such knowledge may be unnecessary, for failures are predominantly in two categories: those that occur during the dynamic erection of the bubble and those that occur in the vicinity of the tropopause. If we accept that the tropopause failures result from the dynamic interaction of the balloon and its environment and that the mechanical responses of the balloon film result in some statistically consistent manner from its initial deformation at launch, then we can use a pre-launch stress-strain state as the zero point in film crown stress history and as the crown stress design point. This is the initial point in flight history for dynamic launch failures, also the stress design point chosen by Okamoto and, for practical purposes, the stress design point chosen by Schwoebel. This is the stress design point we shall use.

The observed relationships (Figures 8 through 11) of failure mode and failure stress to preload temperature, stress, and axial extension ratio are

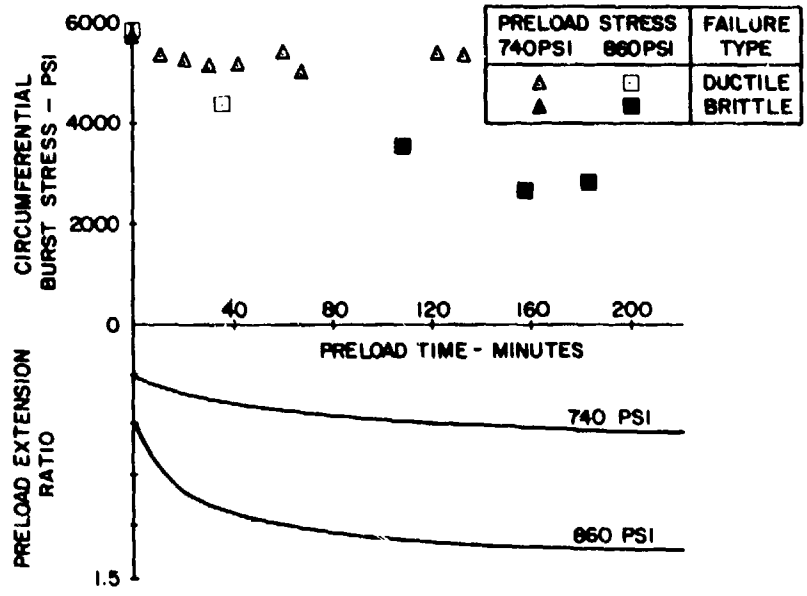

Figure 8. Effects of Preloading On Failure Mode and Failure Stress For 2.0 mil Stratofilm® at 92°F Preload Temperature

not meant to imply any quantitative criterion. Rather, they are intended to show conclusively that stress history, albeit uniaxial in these cases, significantly affects the mechanical responses of polyethylene film (Stratofilm® and X-124 are typical examples). Qualitative effects of biaxial prestress at elevated temperatures were also studied by Alexander[12] and dramatic changes in biaxial ultimate strain were observed at the -70°F test temperatures.

5.2 Shell Thickness

A criterion for the thickness of the shell (gore) material for capped balloons has not been found in the literature. The weight penalty, principally for higher altitude applications, has thus caused some designers to reduce this thickness beyond what may be reasonable, but balloons fabricated from very thin envelope material (as low as 0.35 mil) can and have been launched successfully. In general, however, where weight is not a problem film thicknesses of one mil or greater are used by Air Force Geophysics Laboratory to reduce the probability of damage due to required handling during layout and launch.

A criterion for shell thickness might be found in either of two flight phases: bubble erection in a dynamic launch or venting of free lift when entering float. The latter has not often been a problem and present duct sizes and quantities

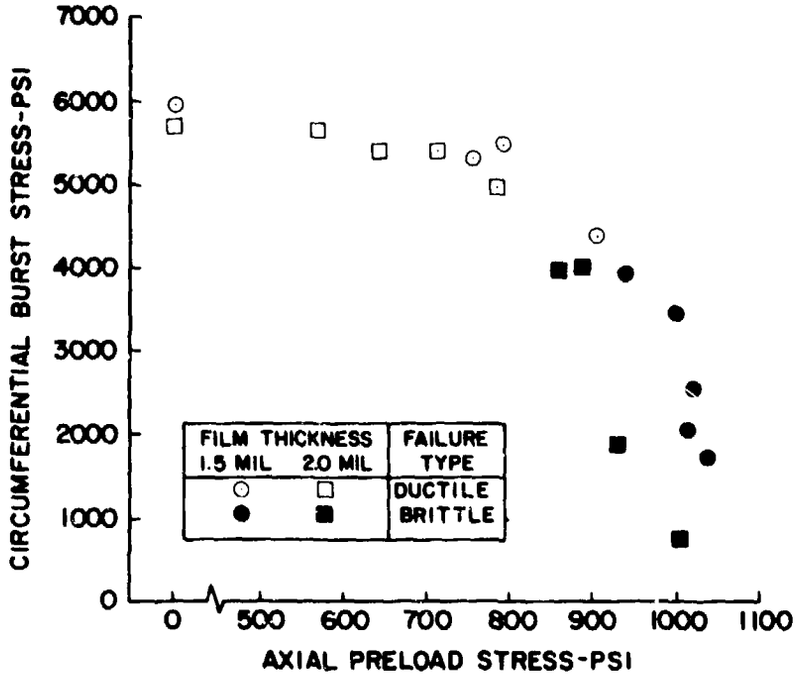

Figure 9. Effects of Preloading on Stratofilm® Failure Mode and Stress. Preloading was at 110°F for 120 min

appear to be more than adequate (see Appendix E). Arguments for and against the dynamic launch have traditionally been qualitative, but the potential requirement to fly a very expensive, moderately heavy (1000 lb) payload at 150,000 ft triggered the search for a quantitative approach, the result of which related shell thickness to dynamic launch failures.*

In a dynamic launch, the inflated upper portion of the balloon is held by a roller arm at a point roughly 100 ft below the balloon's apex. Since the in-line recovery parachute system is generally on the order of 100 ft long, the distance between the roller arm and the payload hold-down point is about equal to the gorelength of the balloon, which is proportional to the cube root of the balloon volume. This is roughly equal to the distance that the inflated bubble must move upward before it is erect over the payload, which is held by a payload release vehicle.

One perspective of the dynamic launch yielded results that were both quantitative and apparently significant with respect to discrimination between tendencies

*It should also be noted that launch dynamics have long been proposed as contributing to eventual bursts at and above the tropopause, but such a relationship will not be addressed herein.

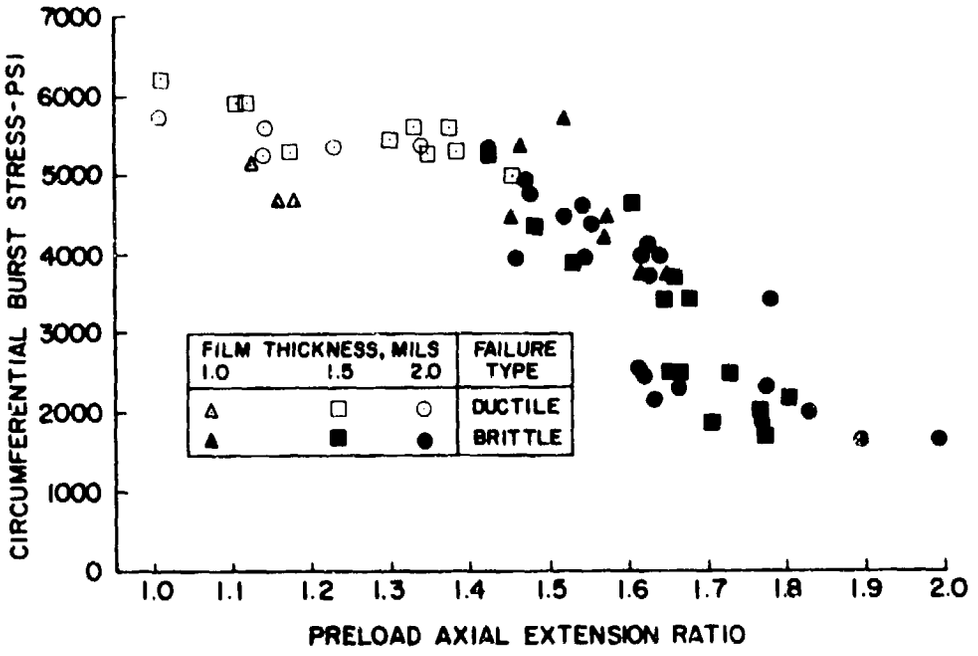

Figure 10. Effects of Preloading on Stratofilm® Failure Mode and Stress

toward success and failure. This perspective considered 1) the increased failure rate for large balloons (greater than 20×10^6 ft^3) reported by Cuddihy[1]; 2) the magnitude of the erecting force acting on the launch bubble; 3) the thickness of the film; 4) balloon construction; and 5) an assumption that thinner films are more subject to flaws and damage and thus reasonably of a probable lesser quality.

The force acting to erect the balloon (neglecting the parachute weight) is very simply the gross lift minus the balloon weight. That is, it is the sum of the free lift force and the payload. The product of the erecting force and the balloon gore-length thus approximates the energy absorbed by the balloon in the erection process. Because of normal manufacturing differences in the widths of envelope gores and adjacent cap gores, the dynamic loading can be assumed to be taken up by the envelope material. If one further argues from experience that film "quality" is proportional to t, the film thickness, then the "effective film thickness" is t^2, the product of the quality and the actual thickness. Thus F_D, an index of dynamic loading or shock, is an index that is directly proportional to erecting force and balloon size and inversely proportional to effective film thickness; it can be expressed as:

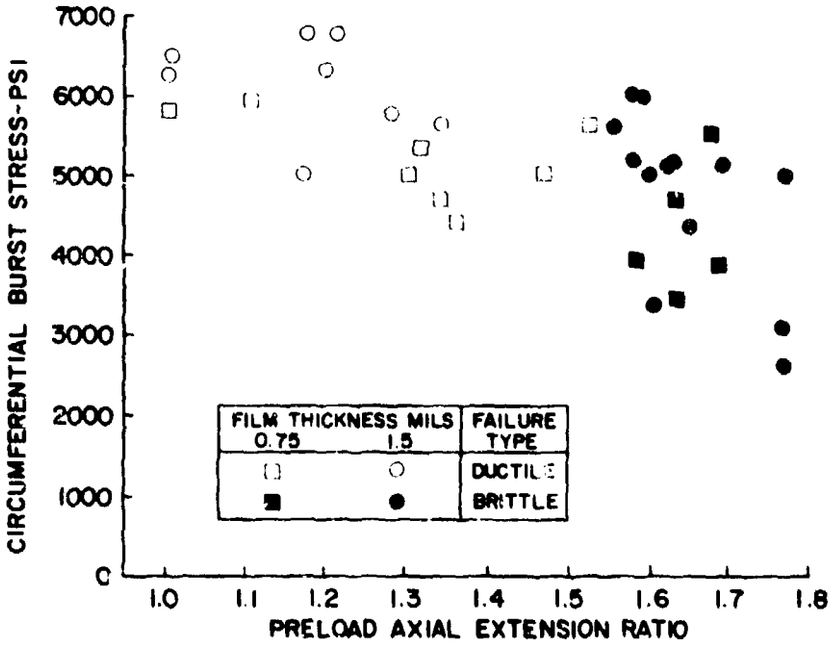

Figure 11. Effects of Preloading on Stratofilm® Failure Mode and Stress

$$F_D = (W_g - W_b)\ S/t^2 \ , \tag{9}$$

where

F_D is the dynamic loading index (ft lb/in^2);

W_g is the gross inflation (lb);

W_b is the balloon weight (lb);

t is the film thickness (in.); and

S is the balloon gorelength (ft) .

The results of this model for the launches of 93 balloons (volumes greater than 25×10^6 ft^3) appear in Figure 12. The sharp change in success rate suggests a maximum acceptable value of F_D of about 10. Gore film thickness in mils can then be determined by:

$$t \geq \sqrt{(W_g - W_b)\ S \cdot 10^{-1}} \ . \tag{10}$$

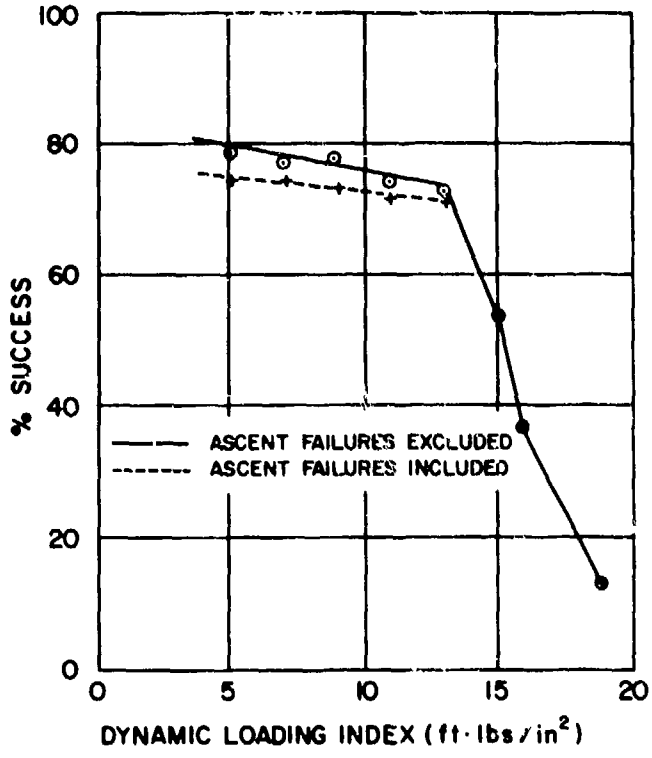

Figure 12. Statistical Basis of Shell Thickness Model. Based on balloons having volumes greater than or equal to 25×10^6 ft^3

The use of the model as it appears in Eq. (10) seems reasonable, but it does not explain the possible influence of launch temperature or launch wind speed. Both of these should contribute to launch failures: temperature, because both modulus and yield strength decrease with increasing temperature, and wind speed, because it directly affects the dynamic loading of the film.

5.3 Film Strength Considerations

Not stress alone, but stress in relation to temperature, time to failure, strength, and strain rate must be reflected in the criterion for crown film thickness. This suggests that creep strength and yield strength might be reasonably consistent film capability references. Alexander provides temperature related information on yield strength,[12] biaxial safe stress[15] (Figure 13) and uniaxial

15. Alexander, H., and Murthy, G.K.N. (1968) A Failure Stress Criterion For A Polyethylene Balloon Film, Scientific Report No. 4, Contract F19628-67-C-0241, AFCRL-TR-69-0103, AD 692516.

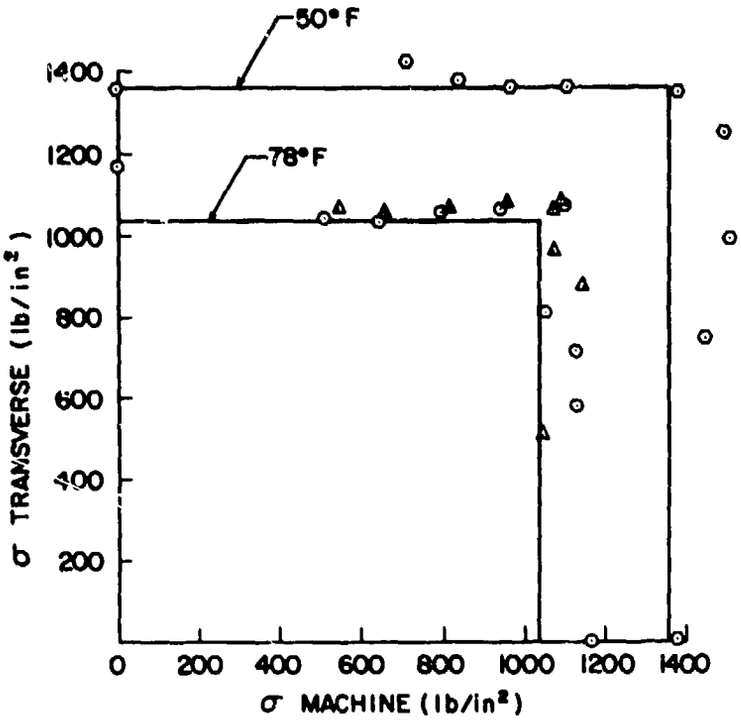

Figure 13. Safe Stress Chart for 2.0 mil Stratofilm®

creep strength[15] for Stratofilm® .

For a representative film thickness (0.75 mil), analysis of yield strength data in the temperature range $-40 \leq {}^{o}F \leq 120$ Alexander [12] (his figure 49) provides the relationship:

$$\sigma_y = 2262 - 19.185\,F + 0.025496\,F^2 + 0.00016979\,F^3 \quad , \tag{11}$$

where

σ_y is yield strength (lb/in^2) and

F is temperature (^{o}F) .

The actual rate of loading or straining during the inflation process is quite slow and inconstant and inflation temperatures are usually in the upper part of the range 20 to 80^{o}F. Although the rate of 100 percent per minute used in the yield strength tests is slow, it is considerably faster than that produced in the inflation process, and thus at the usually relatively warm launch temperatures the film yield strength will be lower than the computed yield strength. In the

absence of more refined data and because our analyses are intended primarily for quantitative comparability, values of roughly 95 percent of the yield strengths at 20°F and 80°F were used to generate the temperature dependent "Stress Limit" function (Figure 14):

$$\sigma_{SL} = EXP[7.7187 - 0.010986\ F] \tag{12}$$

or

$$\sigma_{SL} = EXP[7.367 - 0.01978\ C]\ , \tag{13}$$

where

σ_{SL} is the stress limit (lb/in^2);

F is the temperature (°F); and

C is the temperature (°C) .

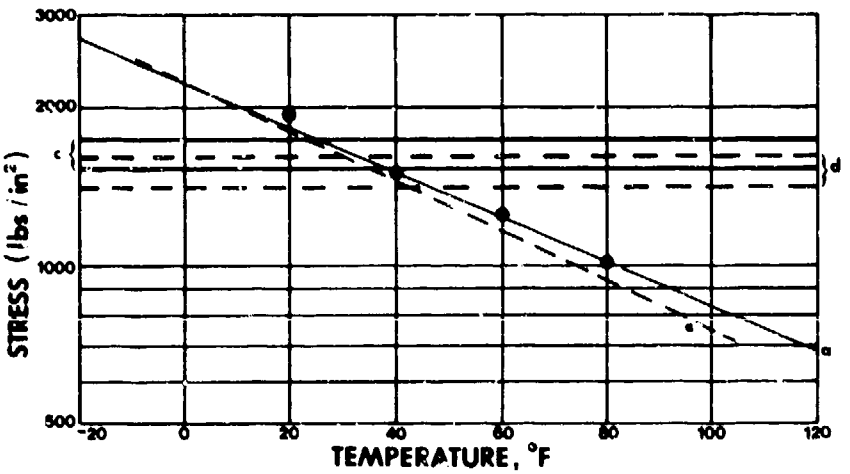

Figure 14. Proposed Stress Limit for Stratofilm® Balloons at an Approximately Static Loading Rate. This log-linear plot shows: a) safe stress from Figure 13, b) discrete stress values, represented by the symbol, ●, Eq. 11, c) nominal Stratofilm® yield strengths, 1733-psi machine direction and 1526-psi transverse direction, d) current design stress indicator range used with Schwoebel's approximation function, 1400 to 1600 psi, Eq. 8, and e) proposed Stress Limit function for Stratofilm® balloons, Eqs. 12 and 13

5.4 Load Tapes

Little engineering design effort has been undertaken with respect to the meridional load tapes used on polyethylene balloons. Perhaps this is because the tapes have always been considered strong in comparison to the balloon film, and confirmed tape failures, other than those associated with early semi-cylinder balloons during the inflation process, are unknown.* This disregard is somewhat inconsistent because the introduction of satisfactory tape attachment methods in the early to mid 1950s was hailed as a significant step toward improved balloon capabilities.

Ultimate tape strength as a function of temperature is not found in the literature and, for the most part, the types of fibers and methods of construction are not comparable. Further, both ultimate strength and ultimate elongation vary with test specimen length and most certainly with elongation rate; static loading (as during inflation) is known to be the most severe use test.[16]

Load tapes have been made from a variety of fibers and with a variety of construction practices. Materials used successfully include nylon, polyester, rayon, and glass. Kevlar is used on a very limited basis for experimental designs. At room temperature, a 100-lb (rated strength) tape made from each of these materials would have a modulus as follows:

Nylon	500 lbs
Polyester	1000 lbs
Rayon	1600 lbs
Kevlar	2000 lbs
Glass	3100 lbs .

These figures are nominal and, to an undetermined degree, dependent upon both the construction of the tape and material sub-type (Dacron and Fortrel are both polyester fibers but significantly different in mechanical response).

More important than the tape modulus itself is the natural "crimp" in the load tape fibers and the amount of tape elongation (and attendant meridional film strain) required to uncrimp the fibers before the theoretical modulus becomes

---

*A series of balloons 4,850,000 ft^3 in volume made from 0.75 mil polyethylene and having 300-lb. test Fortisan® load tapes did fail whereas the same balloon type with 100-lb. test Fortisan® load tapes had been successful. The balloon film in the former cases cannot, however, be ruled out as a cause of failure, but reorientation of stresses due to the tape modulus change (from 100 lb. to 300 lb.) is the suspected cause.

16. Parsons, W.B. (1965) Performance of Balloon Reinforcement Tapes Under Static and Dynamic Loading, Scientific Report No. 2, Contract AF19(628)-2944, AD 698758.

effective.[16] Figure 15 shows the effects of removing most of the crimp from one of two test specimens of Fortisan® (rayon) load tapes and further shows that the effects of variations in crimp along given fibers, fiber bundles, and load tapes appear to average out rather uniformly.

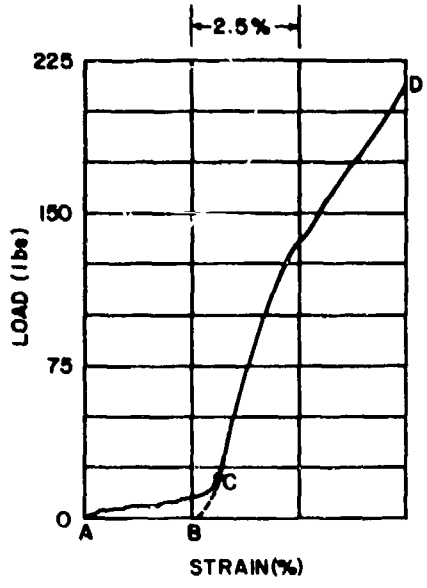

Figure 15. The Effect of Fiber Crimp on Load Tape Performance. The curves ACD and BCD are the load-strain responses of two distinct samples of rayon (Fortisan®) load tape. A and B are the respective zero-strain points for the curves that have been shifted horizontally to overlay one another. Note the extreme crimp effect in the early portion of curve ACD

Elimination of the effects of crimp can be accomplished in two ways. Either the fiber bundles can be encased under a uniform tension during tape construction, or the tapes can be attached to the gore seam hems while under a higher uniform tension. In either case, the value of the tension must be high enough to be in the uniformly common part of the load strain curve (see point C in Figure 15 for example). Only in this way can the tapes be forced to share the meridional loads at very low elongations.

Historically, this aspect of load tape construction has been ignored in practice by some designers and manufacturers; most likely this is because there has been no analysis in which this consideration could be used quantitatively to reveal its effects. This is no longer the case; the analysis proposed herein (see Appendix D) addresses the effect in Eq. (D3) by means of the term ϵ_o, defined as mechanical tape slack.

The maximum tape load occurs at the apex when the balloon enters float. It has been traditional to use this as the tape design point. However, this merely establishes a rated strength based on a load multiplication factor. This "rule" addresses neither an acceptable limit for tape modulus (which would control tape-film interaction) nor the temperature dependency of tape properties.

Nominal ultimate tape strength has been used as a tape "specification", but this does not ensure comparability between sources. Subtle evolutionary changes in tape construction surely continue to influence the mean statistical responses of nominally identical load tapes from a single source. When balloon failures are rare, these inconsistencies are overlooked, but when quantitative analyses of the structural stresses are attempted either for failure analysis or for more efficient design extrapolations, problems can arise.

Until reliable quantitative data on load tape behavior are obtained, design rules such as load multipliers (normally four to five times the apex region load at float altitude) will continue to be used. Similarly, tape modulus as a function of temperature as approximated in Eq. (D9) of Appendix D will have to suffice.

6. AFGL DESIGN PROCESS

The design process shown schematically in Figure 16 is the essence of the computer code developed under this study (Appendix G). Some of the design features and design criteria are contained as assumptions in the code and others are interactively input. What follows here is a general discussion of input; specific input instructions are discussed in Appendix G. The complete list of inputs include:

a. natural shape minimum payload (lb)
b. operational design payload (lb)
c. maximum payload (lb)
d. operational design altitude (ft)
e. fractional ballast requirements
f. terminal parachute speed (ft/sec)
g. shell thickness (mils)
h. cap thickness (mils)
i. load tape factor
j. maximum gore width (in.)

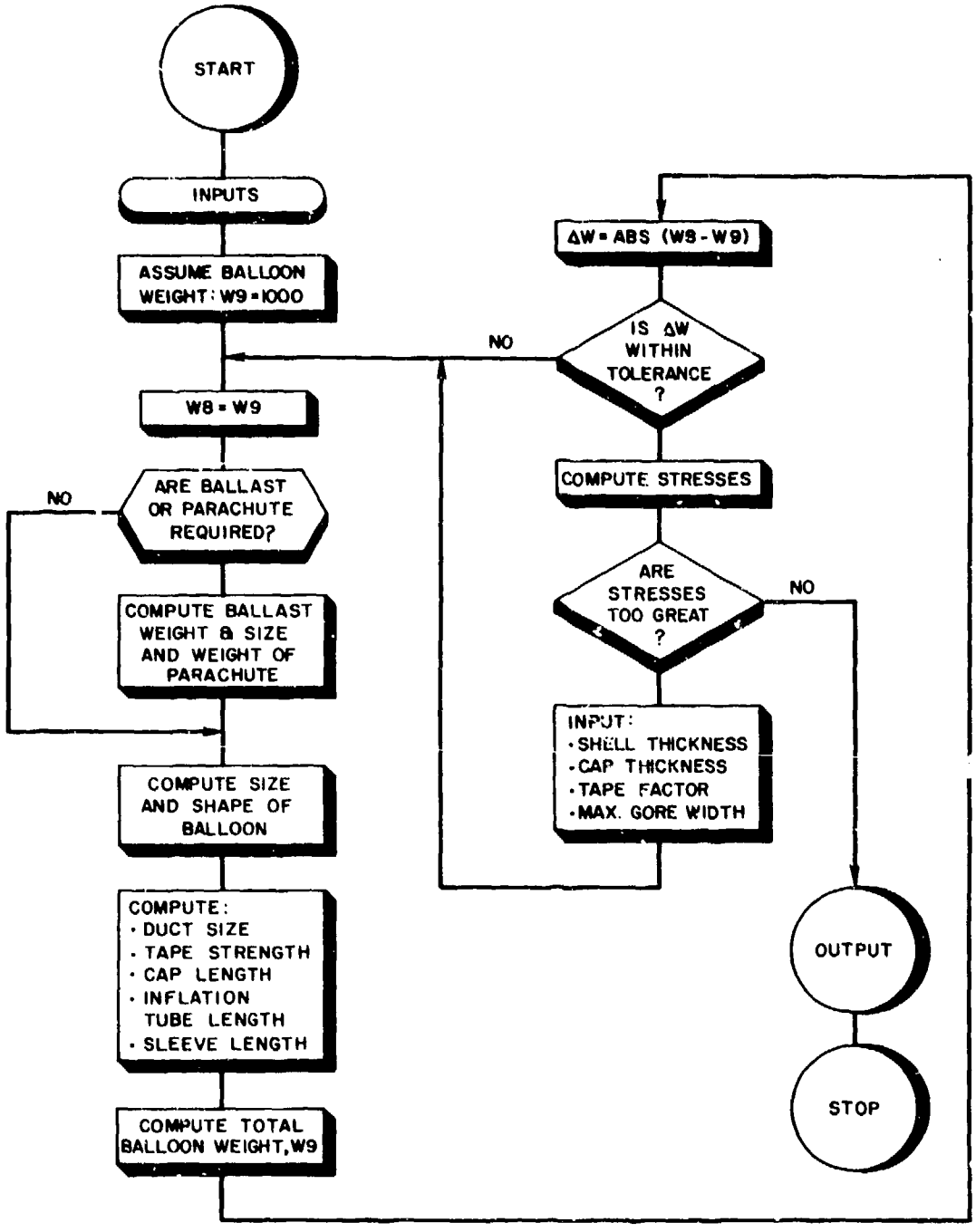

Figure 16. Interactive Balloon Design Procedure

Inputs a through f are related to the mission and descriptive of the capabilities and performance requirements. Film thickness inputs (g and h) are estimates based on experience and are interactively adjusted during the iterative design process. The load tape factor and maximum gorewidth (inputs i and j) are normally constant; the maximum gorewidth, usually about 101 in., is based on economic use of the standard 54-in. layflat width of the extruded polyethylene tube; and the load tape factor, about 5, is a value presently without a firm engineering rationale.

The last four inputs (g through j) significantly affect the computed stress level. Increases in the first two reduce stress but have the most adverse impact on balloon weight. Decreases in the maximum gorewidth also reduce stress, but increase balloon cost - labor is roughly proportional to the product of the number of gores and the gorelength (the total length of gore heat seals).

Minimum adverse impact is achieved by increasing the load tape factor (i) to achieve reduced stress levels. This was inferred in the earlier references to the effect of tape fiber crimp.

The minimum payload value governs the balloon shape and thus the values of the nondimensionalized shape characteristics f_1 through f_5 (see Section 4.1) and $\bar{R}_m$, the ratio of the meridional radius of curvature (at 0.17 gorelength units from the apex) to the launch bubble gorelength, and the related characteristics:

θ	the half cone angle at the nadir (degrees);
T/W_p	the ratio of the apex loading to the payload; and
T/G	the ratio of the apex loading to the grossload .

The design payload and altitude combined govern the balloon volume and thus the gorelength, whereas the maximum payload affects the selection of tape strength, film thickness, caplength, cap thickness, and total duct venting area. If the design payload weight is the weight of the functional payload only, then the design code requires input of both ballast needs for ascent, descent, and sunset control (expressed as decimal fractions), and allowable parachute impact speed, which governs the parachute size and thus weight. These inputs are covered in detail in Appendix G.

Balloon ducts allow the free lift gas to be vented and thereby prevent overpressurization and bursting when the balloon reaches its natural floating altitude. The length of the duct is selected so that the balloon will not take in air when ascending or floating at an altitude below its natural floating altitude. This is effected by ensuring that the duct entry in the balloon wall is always in the positive pressure region, except during the initial ascent when the ducts are still fully collapsed. Balloon duct length is selected so that the zero differential pressure level is at the upper end of the duct when the balloon is about 16,000 ft

below the natural floating altitude; that is, when the balloon is about half full.

The requirement for a reefing sleeve exists only when the volume exceeds four million ft^3 (an arbitrary volume based on experience). The sleeve extends from the base to within 5 ft of the cap. Endfitting sizes and thus weights are related to payload weight and number of gores, and are based on existing designs.

Selections of an adequate stress level and shock index as criteria for acceptance of a resulting design are basically at the discretion of the designer, but with due consideration to actual flight histories and regard for the margins of safety that appear appropriate for the relevant mission. For future designs, a stress level of about 600 psi and a shock index of 10 seem to be reasonable based on experience at this time.

7. CONCLUSIONS AND RECOMMENDATIONS

The single-cell polyethylene balloon is not structurally complex; aside from the endfittings, which are really in the nature of sophisticated fasteners, * there are only a few critical parts that affect the strength of the vehicle (load tapes, caps, and gores) or affect the loading of the structure (ducts). These critical parts have been researched with the following conclusions and recommendations.

7.1 Ducts

We have considered the function of the duct and the various ways in which its size has been determined (Appendix F). We have shown that the film strength and atmospheric scale height should be considered as functions of altitude and not as constants, and that the present duct sizes based on these considerations are consistent with the early University of Minnesota recommendation that the actual duct diameters should be twice the theoretical. Further, we have shown that the results of the venting back pressure model of the University of Minnesota, when the atmospheric scale height is considered to be altitude dependent, are consistent with those produced by the differential equations governing the ascent venting process; these pressures are small percentages of the differential pressure at the maximum horizontal diameter.

It is concluded that duct sizes today are more than adequate. The need to have ducts that have diameters twice what is theoretically required has been

*The plate, hoop, and ring apex fitting developed by Winzen, International, Inc., has probably been the single most important design improvement since the mid-1950s when the heat sealed tape was introduced; it, more than anything else, has made it possible to realize the load potential of capped- and uncapped-taped, fully-tailored polyethylene balloons.

questioned, and in this regard actual venting back-pressure measurements should be made to confirm this. Reducing the number of ducts by using the largest practical sizes and making the ducts from the thinnest film practical would reduce both weight and construction costs - this should be done.

A venting-stress model should be developed to accommodate newer understanding of the high stress regions of the fully inflated balloon and should be based on improved film characterization at loading rates consistent with peak pressurization rates during the expulsion of the free lift gas.

7.2 Load Tapes

Load tapes appear to have adequate ultimate strengths, dynamic loading responses (accommodating dynamic launch), and moduli. However, the difference between the modulus in theory and in practice (and between manufacturers) limits both design accuracy and confidence in the results of structural analyses of the balloon pre-launch load distributions. This is a problem that can be addressed confidently, easily, and without significant added cost to the balloon user. All that is required is stricter specifications for manufacturing and testing.

At present, the total tape strength requirement has been found to be based on a factor of four (NSBF) or five (AFGL) times the total meridional load in the balloon crown at float altitude. This seems to be a "rule of thumb" in both cases, rather than an engineering formula.

7.3 Gores

Gore thickness standards for a fully-tailored polyethylene balloon with load tapes, but without a cap are the same standards used for the crown of a capped balloon. Analysis of ground abort statistics suggested a criterion for the film thickness (in mils) of the gores of capped balloons, namely Eq. 10:

$$t \geq \sqrt{(W_g - W_b)\ S/10^7}\ .$$

It was noted that a final refined model should probably account for launch temperature and, if possible, launch wind speed.*

*Development of the "soft collar" dynamic launch method has, it appears, significantly improved the statistics for the large capped balloons, but, in the absence of this NSBF system, use of the model as a guide appears to offer a significant advantage.

7.4 Crown and Analytical Method

Criterion for the crown thickness is the essential part of this study. The NSBF model, or more properly the Schwoebel model, and the Okamoto analysis were reviewed and results compared with those of the author's model, which is based on modifications and additions to the analytic approach of Alexander[17] and the film model of Webb. The comparisons involved 81 distinct balloon designs, ranging in volume from about 1 to 70 million ft^3. All three approaches had in common the selection of the launch as the proper point for comparative stress analysis or application of design criteria. Only the proposed approach accounts for the film-tape interaction, for the orthotropic nature of the film, and for film modulus based both on temperature and accounting for relaxation of stresses and strains in the balloon crown.

Table 3 provides a comparison of the results of three approaches to design and analysis: the author's model (columns 3, 4, and 8 through 12); the NSBF model (columns 5 and 6); and the model suggested by Okamoto (column 7). For the most part, there are two payload entries for each balloon, the first in the pair being the suggested maximum and the second being the maximum flown successfully. The letter code following the entries in column 2 is the key to the source of the load rating. The tape indices, columns 3 and 6, are the ratios of total tape strength to total meridional load at the apex at float altitude (AFGL and NSBF computations differ slightly). For each payload the second entry in each pair for columns 4, 7, 8, and 9 are percentages. Thus column 4 shows the tape load at launch in pounds and as a percentage of the rated tape strength. Column 7 shows the computed Okamoto circumferential stress in psi and as a percentage of the author's computed circumferential stress. The circumferential and meridional stresses computed by the author's model are expressed in psi and as a percentage of the safe stress, 1004 psi. The second entry in each pair in columns 10 and 11 is the respective radius of curvature in feet.

In column 6 we have the NSBF stress index multiplied by 1000. The first entry in each pair is the effective value based on the column 2 payload. The second entry is the suggested index (multiplied by 1000) based on the actual film thickness, the load, and the size of the balloon. If the second value in each pair is less than the first it means that the suggested index is conservative.

One of the most remarkable results of the comparison of analyses is the consistency of the AFGL and Okamoto circumferential stress values; the Okamoto values are almost uniformly 3 to 5 percent greater than the AFGL values, except

17. Alexander, H., and Agrawal, P. (1974) Gore Panel Stress Analysis of High Altitude Balloons, Scientific Report No. 2, Contract F19628-72-C-0100, AFCRL-TR-74-0597, AD A009627.

Table 3. Comparison of the Results of Analyses of Balloon Load Tape and Film Loading at Launch. The launch temperature is 23°C and the assumed safe stress is 1004 psi. Altitude is sea level and the stress-strain relaxation time is assumed to be 1 hr

(1) Model Balloon	(2) Payload (LB)	(3) Tape Index	(4) Tape Load	(5) Number Tapes	(6) Radius Stress	(7) Overload Cir Str	(8) Stress Cir	(9) Stress Mer	(10) Strain/Radius Cir	(11) Strain/Radius Mer	(12) Shock Index
SV-001A	4503A	6.67	40.0	8.24	1439	546	524	516	0.01251	0.00817	1.695
			8.00		1400	104.17	52.2	51.4	4.670	49.094	
	4955	6.35	43.5	5.78	1576	575	551	544	0.01311	0.00888	1.351
			8.70		1400	104.25	54.9	54.2	4.804	49.677	
SV-002	4000	7.88	36.0	7.18	1356	497	476	469	0.01109	0.00735	1.221
			7.20		1400	104.46	47.4	46.7	4.477	43.659	
	2501	11.08	25.0	9.99	1103	402	386	377	0.00920	0.00510	0.306
			4.99		1600	104.14	38.4	37.6	4.005	41.731	
SV-004	750	5.45	8.6	4.71	1393	530	512	507	0.01143	0.00877	2.967
			8.60		1400	103.55	51.0	50.5	3.523	44.805	
	445	6.54	7.2	5.65	1265	468	452	447	0.01003	0.00740	1.977
			7.25		1400	103.42	45.1	44.5	3.276	43.204	
SV-005	2150#	7.15	21.4	6.38	1518	542	524	514	0.01328	0.00728	2.175
			7.14		1600	103.46	52.2	51.2	3.806	48.650	
	1658	8.46	17.9	7.49	1371	490	474	464	0.01214	0.00608	1.708
			5.96		1600	103.37	47.3	46.2	3.615	47.289	
SV-006	4200#	6.20	31.7	5.53	1394	518	500	494	0.01153	0.00808	5.865
			7.92		1400	103.59	49.8	49.2	4.975	62.158	
	3940	6.47	30.3	5.76	1359	504	486	480	0.01122	0.00774	5.525
			7.58		1400	103.55	48.4	47.8	4.894	61.660	
SV-007	8600#	4.59	83.5	4.17	1312	642	607	602	0.01408	0.01066	3.648
			10.44		1400	105.76	60.5	59.9	7.940	58.482	
	6300	5.86	64.2	5.29	1123	540	513	506	0.01199	0.00819	2.701
			8.03		1400	105.39	51.1	50.4	7.176	56.538	
SV-008	7000#	4.46	63.1	4.04	1373	645	613	607	0.01428	0.01074	3.251
			10.52		1400	105.23	61.0	60.5	7.156	59.024	
	5166	5.62	49.4	5.06	1188	549	523	516	0.01226	0.00840	2.429
			8.23		1400	104.91	52.1	51.4	6.510	57.075	
SV-009	3500	7.35	33.0	6.56	1173	477	459	451	0.01089	0.00673	1.734
			6.60		1600	104.09	45.7	44.9	5.136	54.811	
	3437	7.44	32.6	6.64	1164	474	455	447	0.01081	0.00664	1.705
			6.51		1600	104.08	45.3	44.5	5.114	54.715	
SV-010	725#	5.16	9.0	4.45	1411	539	520	516	0.01142	0.00920	3.263
			9.02		1400	103.57	51.8	51.4	3.717	47.209	
	674	5.29	8.8	4.56	1393	530	511	507	0.01121	0.00899	3.084
			8.81		1400	103.55	50.9	50.5	3.679	46.975	
SV-011	900#	5.84	12.2	5.04	1402	501	485	481	0.01063	0.00833	2.537
			8.16		1400	103.25	48.3	47.9	3.915	54.864	
	896	5.85	12.2	5.05	1401	500	484	480	0.01061	0.00832	2.529
			8.15		1400	103.25	48.2	47.8	3.912	54.853	

Table 3. Comparison of the Results of Analyses of Balloon Load Tape and Film Loading at Launch. The launch temperature is 23°C and the assumed safe stress is 1004 psi. Altitude is sea level and the stress-strain relaxation time is assumed to be 1 hr (Contd)

(1) MODEL NUMBER	(2) PAYLOAD (LB)	(3) TAPE INDEX	(4) TAPE LOAD	(5) NSBF TAPES	(6) INDICES STRESS	(7) OKAMOTO CIR STR	(8) STRESS CIR	(9) STRESS MER	(10) STRAIN/RADIUS CIR	(11) STRAIN/RADIUS MER	(12) SHOCK INDEX
SV-012	1050W	5.89	11.9	5.12	1396	525	508	501	0.01185	0.00810	2.035
			7.94		1400	103.42	50.6	49.9	3.697	48.548	
	1038	5.92	11.8	5.14	1392	523	506	499	0.01181	0.00806	2.015
			7.90		1400	103.42	50.4	49.7	3.690	48.503	
SV-014	3400W	4.92	28.0	4.40	1403	593	569	563	0.01335	0.00952	5.335
			9.33		1400	104.15	56.7	56.1	5.219	55.612	
	2312	6.33	21.5	5.61	1204	500	481	474	0.01136	0.00731	3.724
			7.16		1400	103.92	47.9	47.2	4.732	53.206	
SV-015	3100W	4.78	23.6	4.25	1395	581	559	554	0.01278	0.00964	5.539
			9.44		1400	103.99	55.7	55.1	5.115	57.165	
	2357	5.67	19.9	5.00	1260	517	497	492	0.01137	0.00811	4.303
			7.95		1400	103.84	49.5	49.0	4.769	55.370	
SV-016A	2400W	6.78	22.6	6.08	1563	560	541	531	0.01369	0.00769	4.857
			7.53		1600	103.50	53.9	52.9	3.881	49.130	
	2138	7.35	20.7	6.57	1487	533	515	505	0.01309	0.00705	4.355
			6.91		1600	103.46	51.3	50.3	3.784	48.392	
SV-017A	5000W	6.10	43.4	5.53	1414	560	536	530	0.01244	0.00885	1.929
			8.67		1400	104.56	53.4	52.8	5.317	50.984	
	4199	6.99	37.5	6.32	1297	511	489	482	0.01142	0.00766	1.630
			7.50		1400	104.40	48.7	48.1	5.047	50.003	
SV-018	1900W	4.35	20.2	3.95	1404	687	653	644	0.01652	0.01033	2.604
			10.12		1600	105.14	65.0	64.2	4.766	39.632	
	1738	4.67	18.7	4.24	1342	655	624	615	0.01584	0.00955	2.389
			9.36		1600	105.07	62.1	61.2	4.648	39.139	
SV-019	5000W	4.65	51.6	4.22	1396	658	624	617	0.01498	0.01053	1.914
			10.32		1400	105.37	62.2	61.5	6.357	50.544	
	2020	9.01	24.8	8.00	925	431	412	402	0.01035	0.00506	0.808
			4.96		1600	104.62	41.1	40.1	5.052	46.129	
SV-020	2400	6.49	23.2	5.83	1563	575	555	545	0.01413	0.00789	4.328
			7.73		1600	103.58	55.3	54.3	3.986	49.269	
	1313	9.61	15.2	8.47	1233	456	441	430	0.01148	0.00518	2.913
			5.08		1600	103.38	44.0	42.9	3.546	45.839	
SV-021	500W	4.08	6.3	3.53	1331	588	563	561	0.01193	0.01079	4.306
			10.57		1400	104.33	56.1	55.9	4.145	42.881	
	509	4.06	6.4	3.51	1335	590	565	563	0.01198	0.01084	4.362
			10.62		1400	104.34	56.3	56.1	4.153	42.936	
SV-022	900W	4.86	9.4	4.22	1425	569	548	544	0.01236	0.00958	3.430
			9.39		1400	103.75	54.6	54.2	3.743	44.906	
	432	6.41	7.3	5.53	1230	471	455	450	0.01015	0.00741	1.910
			7.26		1400	103.56	45.3	44.8	3.354	42.287	

Table 3. Comparison of the Results of Analyses of Balloon Load Tape and Film Loading at Launch. The launch temperature is 23°C and the assumed safe stress is 1004 psi. Altitude is sea level and the stress-strain relaxation time is assumed to be 1 hr (Contd)

(1) MODEL NUMBER	(2) PAYLOAD (LB)	(3) TAPE INDEX	(4) TAPE LOAD	(5) ASBS TAPES	(6) INDICES STRESS	(7) OKAMOTO CIR STR	(8) STRESS CIR	(9) STRESS MER	(10) STRAIN/RADIUS CIR	(11) STRAIN/RADIUS MER	(12) SHOCK INDEX
LTV-001	1000	3.77	12.9	3.29	2225	787	762	754	0.01917	0.01319	1.033
			12.93		1400	103.26	75.9	75.1	3.323	46.283	
	750	4.30	11.3	3.73	2069	721	699	691	0.01763	0.01154	0.809
			11.31		1400	103.16	69.7	68.8	3.160	45.451	
LTV-002	800A	4.06	10.7	3.58	1644	727	698	688	0.01813	0.01090	0.560
			10.68		1600	104.19	69.5	68.5	3.616	37.897	
	911	3.75	11.6	3.32	1722	765	733	724	0.01898	0.01185	0.631
			11.62		1600	104.27	73.0	72.1	3.721	38.338	
LTV-003C	2900W	8.21	42.8	7.42	1556	602	576	564	0.01613	0.00671	0.407
			6.58		1600	104.40	57.4	56.2	4.389	42.730	
	3000	8.00	44.0	7.24	1581	610	584	572	0.01632	0.00691	0.421
			6.78		1600	104.41	58.2	57.0	4.415	42.877	
LTV-005	750	9.25	10.9	8.32	659	405	380	370	0.00952	0.00445	0.066
			4.36		1600	106.69	37.8	36.8	4.704	27.396	
LTV-006	3000A	9.83	31.4	8.88	2376	600	584	571	0.01674	0.00640	1.132
			6.27		1600	102.75	58.2	56.9	2.830	46.080	
	3000	9.83	31.4	8.88	2376	600	584	571	0.01674	0.00640	1.132
			6.27		1600	102.75	58.2	56.9	2.830	46.080	
LTV-007	2300W	6.94	35.6	6.29	1310	609	579	567	0.01575	0.00727	0.286
			7.13		1600	105.31	57.6	56.5	4.909	38.551	
	2165	7.28	33.8	6.58	1272	594	564	552	0.01541	0.00689	0.270
			6.75		1600	105.28	56.2	55.0	4.850	38.312	
LTV-008	1200W	4.77	17.6	4.36	786	577	527	522	0.01193	0.00896	0.077
			8.78		1600	109.59	52.5	51.9	6.515	24.247	
	1104	5.13	16.2	4.68	750	548	501	495	0.01138	0.00828	0.071
			8.11		1600	109.41	49.9	49.3	6.301	24.040	
LTV-009	1 00W	4.68	16.8	4.26	822	576	531	524	0.01244	0.00858	0.096
			8.41		1600	108.45	52.9	52.2	6.182	27.543	
	949	5.64	13.6	5.11	730	506	468	461	0.01114	0.00692	0.076
			6.79		1600	108.05	46.6	45.9	5.720	26.934	
LTV-010B	1100W	4.92	15.1	4.44	822	552	513	505	0.01244	0.00770	0.105
			7.55		1600	107.50	51.1	50.3	5.809	30.150	
	952	5.48	13.3	4.93	768	514	479	470	0.01172	0.00678	0.091
			6.65		1600	107.30	47.7	46.8	5.573	29.765	
LTV-011A	1200W	5.02	13.8	4.53	1330	628	598	589	0.01478	0.00938	0.331
			9.19		1600	105.08	59.5	58.7	4.076	34.316	
	1145	5.20	13.2	4.68	1301	614	584	576	0.01448	0.00903	0.317
			8.85		1600	105.04	58.2	57.4	4.025	34.150	

Table 3. Comparison of the Results of Analyses of Balloon Load Tape and Film Loading at Launch. The launch temperature is 23°C and the assumed safe stress is 1004 psi. Altitude is sea level and the stress-strain relaxation time is assumed to be 1 hr (Contd)

(1) MODEL NUMBER	(2) PAYLOAD (LB)	(3) TAPE INDEX	(4) TAPE LOAD	(5) NSBF TAPES	(6) INDICES STRESS	(7) OKAMOTO CIR STR	(8) STRESS CIR	(9) STRESS MER	(10) STRAIN/RADIUS CIR	(11) STRAIN/RADIUS MER	(12) SHOCK INDEX
LTV-012	950W	5.30	12.5	4.67	1406	611	587	577	0.01502	0.00854	0.380
			8.37		1600	104.13	58.4	57.5	3.794	40.111	
	1237	4.52	14.9	4.01	1546	676	648	640	0.01645	0.01016	0.484
			9.96		1600	104.29	64.6	63.7	4.015	40.995	
LTV-013A	3000W	6.13	42.0	5.56	1552	658	628	616	0.01688	0.00856	0.425
			8.39		1600	104.83	62.5	61.4	4.835	42.732	
	2602	6.85	37.0	6.19	1447	617	590	578	0.01600	0.00756	0.371
			7.41		1600	104.74	58.7	57.6	4.691	42.083	
LTV-014	4000W	5.04	59.1	4.58	1366	683	644	635	0.01633	0.01004	0.283
			9.84		1400	106.17	64.1	63.2	6.309	42.175	
	3001	6.34	45.6	5.74	1180	592	559	549	0.01446	0.00776	0.215
			7.60		1600	105.88	55.7	54.7	5.851	40.966	
LTV-018	1875W	4.42	40.3	4.05	1022	721	659	650	0.01685	0.01027	0.132
			10.07		1600	109.42	65.6	64.7	7.130	26.911	
	1330	5.98	28.1	5.47	840	597	548	537	0.01446	0.00718	0.094
			7.04		1600	108.51	54.6	53.5	6.445	25.901	
LTV-019	1650W	4.25	28.5	3.88	982	681	628	619	0.01588	0.00970	0.141
			9.51		1600	108.46	62.5	61.6	6.703	29.678	
	1441	4.76	26.9	4.34	912	632	584	574	0.01493	0.00848	0.123
			8.31		1600	108.25	58.1	57.2	6.430	29.243	
LTV-020	750W	4.84	16.7	4.43	568	551	495	485	0.01239	0.00682	0.039
			6.68		1600	111.32	49.3	48.3	7.881	20.032	
	803	4.56	18.0	4.17	591	573	514	505	0.01277	0.00736	0.042
			7.21		1600	111.43	51.2	50.3	8.073	20.176	
LTV-021	900W	4.97	17.4	4.53	657	560	509	499	0.01277	0.00709	0.057
			6.94		1600	110.12	50.7	49.7	7.059	23.116	
	692	6.18	13.1	5.62	571	489	445	435	0.01151	0.00535	0.044
			5.25		1600	109.70	44.4	43.3	6.536	22.516	
LTV-022	800W	6.48	15.5	5.91	924	608	565	552	0.01592	0.00634	0.136
			6.21		1600	107.57	56.2	55.0	4.956	24.895	
	554	8.71	10.5	7.88	766	520	484	472	0.01409	0.00430	0.096
			4.21		1600	107.36	48.2	47.0	4.636	23.938	
LTV-023	1440W	5.96	20.3	5.41	1408	652	620	609	0.01676	0.00830	0.370
			8.14		1600	105.17	61.8	60.6	4.130	33.681	
	712	10.06	11.0	8.98	1016	491	468	456	0.01322	0.00445	0.189
			4.40		1600	104.84	46.6	45.4	3.632	31.298	
LTV-024	1550W	4.24	22.7	3.85	996	649	605	596	0.01518	0.00928	0.161
			9.10		1600	107.39	60.2	59.3	6.202	32.940	
	1525	4.30	22.4	3.90	988	644	600	591	0.01507	0.00914	0.159
			8.96		1600	107.37	59.7	58.8	6.172	32.884	

Table 3. Comparison of the Results of Analyses of Balloon Load Tape and Film Loading at Launch. The launch temperature is 23°C and the assumed safe stress is 1004 psi. Altitude is sea level and the stress-strain relaxation time is assumed to be 1 hr (Contd)

(1) Model Number	(2) Payload (LB)	(3) Tape Index	(4) Tape Load	(5) Msw Tapes	(6) Indices Stress	(7) Seamtu Cir Str	(8) Stress Cir	(9) Stress Mer	(10) Strain/Radius Cir	(11) Strain/Radius Mer	(12) Shock Index
LTV-026	3400#	5.29	48.4	4.83	1604	716	680	669	0.01818	0.00988	0.451
			9.69		1600	105.29	67.7	66.7	5.218	41.671	
	1311	10.97	20.7	9.80	1014	481	459	446	0.01303	0.00423	0.181
			4.15		1600	104.82	45.7	44.4	4.359	37.683	
SP-001	700#	5.02	6.7	4.51	891	522	454	485	0.01230	0.00689	1.872
			6.75		1600	105.56	49.2	48.3	4.270	31.938	
	413	7.20	4.5	6.38	714	418	397	387	0.01015	0.00456	1.140
			4.47		1600	105.24	39.6	38.5	3.798	29.814	
SP-002	100#	6.54	3.3	5.76	1120	459	443	436	0.01023	0.00670	0.688
			6.57		1400	103.67	44.1	43.4	2.709	32.705	
	93	6.63	3.2	5.85	1113	455	439	432	0.01014	0.00662	0.660
			6.49		1400	103.66	43.7	43.0	2.697	32.672	
SP-003	5000#	4.71	52.9	4.32	992	621	569	567	0.01221	0.01079	0.443
			10.58		1400	109.18	56.7	56.5	8.717	35.478	
	3856	5.91	41.7	5.40	857	519	478	475	0.01018	0.00851	0.343
			8.34		1600	108.56	47.7	47.3	7.736	34.551	
SV-500	3800#	5.03	27.4	4.48	1384	562	541	536	0.01223	0.00933	7.221
			9.15		1400	103.90	53.9	53.4	5.318	60.978	
	3004	5.94	23.6	5.16	1266	507	488	483	0.01103	0.00804	5.812
			7.88		1400	103.77	48.6	48.1	5.002	59.302	
SV-501	5400#	4.94	37.3	4.40	1360	563	541	537	0.01210	0.00950	7.686
			9.31		1400	104.05	53.9	53.5	6.051	66.755	
	3686	6.28	29.2	5.54	1178	475	458	453	0.01023	0.00745	5.401
			7.30		1400	103.81	45.6	45.1	5.464	64.054	
SV-502	3400#	5.71	24.9	5.08	1367	526	508	502	0.01151	0.00848	9.667
			8.31		1400	103.66	50.6	50.0	4.886	59.856	
	2287	7.24	19.7	6.36	1189	448	433	427	0.00983	0.00669	6.731
			6.55		1400	103.48	43.1	42.5	4.449	57.125	
SV-503	3900#	5.10	27.9	4.52	1463	563	543	539	0.01221	0.00948	8.078
			9.29		1400	103.67	54.1	53.6	5.167	63.439	
	3102	5.95	24.3	5.15	1348	511	494	489	0.01109	0.00826	6.552
			8.10		1400	103.56	49.2	48.7	4.878	61.803	
SV-504	3000#	4.15	21.1	3.69	1444	620	596	591	0.01345	0.01077	8.188
			10.55		1400	104.10	59.3	58.9	5.234	57.113	
	2788	4.35	20.2	3.86	1404	600	576	572	0.01300	0.01028	7.650
			10.08		1400	104.06	57.4	57.0	5.129	56.563	
SV-505	4000#	4.85	29.0	4.33	1480	587	566	561	0.01289	0.00986	7.581
			9.66		1400	103.84	56.3	55.8	5.255	61.450	
	3786	5.03	27.9	4.48	1447	573	552	546	0.01256	0.00951	7.202
			9.32		1400	103.80	54.5	54.4	5.176	61.026	

Table 3. Comparison of the Results of Analyses of Balloon Load Tape and Film Loading at Launch. The launch temperature is 23°C and the assumed safe stress is 1004 psi. Altitude is sea level and the stress-strain relaxation time is assumed to be 1 hr (Contd)

(1) MODEL NUMBER	(2) PAYLOAD (LB)	(3) TAPE INDEX	(4) TAPE LOAD	(5) MSBF TAPES	(6) INDICES ST ESS	(7) OKAMOTO CIR STR	(8) STRESS CIR	(9) STRESS MER	(10, STRAIN/RADIUS CIR	(11) STRAIN/RADIUS MER	(12) SHOCK INDEX
SV-506	7250W	5.51	53.0	4.92	1406	547	527	522	0.01188	0.00901	7.929
			8.83		1400	103.89	52.5	52.0	6.250	71.969	
	5800	6.37	45.6	5.[illegible]	1288	494	477	471	0.01076	0.00776	6.442
			7.61		1400	103.74	47.5	46.9	5.883	70.346	
SV-507	2000W	5.68	16.9	5.00	1441	538	520	514	0.01196	0.00860	5.541
			8.43		1400	103.49	51.8	51.2	4.139	53.343	
	2003	5.67	16.9	5.00	1442	529	520	515	0.01196	0.00861	5.549
			8.43		1400	103.49	51.8	51.3	4.140	53.352	
SV-508	4500W	4.44	30.2	3.96	1398	595	571	567	0.01278	0.01026	8.799
			10.05		1400	104.12	56.9	56.5	5.854	63.577	
	3697	5.04	26.6	4.47	1295	543	522	517	0.01164	0.00903	7.329
			8.85		1400	103.99	52.0	51.5	5.539	62.045	
SV-509	7500W	4.56	50.9	4.07	1437	598	574	570	0.01279	0.01038	6.676
			10.18		1400	104.14	57.1	56.7	6.770	73.084	
SV-510	4000W	5.02	27.9	4.47	1433	566	545	541	0.01229	0.00949	11.662
			9.30		1400	103.79	54.3	53.8	5.257	62.387	
SV-511	2700W	4.57	19.3	4.04	1365	573	551	547	0.01225	0.00983	7.953
			9.64		1400	103.95	54.9	54.5	5.089	57.756	
	2029	5.37	16.5	4.71	1242	511	492	488	0.01089	0.00840	6.146
			8.23		1400	103.81	49.0	48.6	4.749	55.891	
SV-512	2800W	6.49	22.9	5.73	1412	503	487	481	0.01121	0.00778	5.703
			7.62		1400	103.34	48.5	47.9	4.362	58.797	
	2305	7.25	20.5	6.36	1324	467	453	446	0.01043	0.00656	4.784
			6.82		1400	103.26	45.1	44.4	4.180	57.545	
SV-513	3400W	4.91	23.1	4.37	1360	557	536	532	0.01196	0.00941	10.149
			9.22		1400	103.90	53.4	53.0	5.201	59.833	
	2690	5.68	20.0	5.01	1247	503	485	480	0.01078	0.00816	8.180
			8.00		1400	103.78	48.3	47.8	4.895	57.977	
SV-514	3800W	5.28	27.3	4.69	1479	559	539	534	0.01220	0.00929	7.628
			9.11		1400	103.62	53.7	53.2	4.986	62.151	
	3420	5.64	25.6	4.99	1421	534	515	510	0.01165	0.00870	6.921
			8.52		1400	103.56	51.3	50.8	4.851	51.360	
SV-515	6000W	4.50	40.3	4.00	1412	590	567	563	0.01257	0.01028	5.543
			10.07		1400	104.07	56.5	56.1	6.429	70.860	
	6068	4.47	40.6	3.97	1418	593	570	566	0.01264	0.01035	5.601
			10.15		1400	104.07	[illegible]	[illegible]	[illegible]	[illegible]313	

Table 3. Comparison of the Results of Analyses of Balloon Load Tape and Film Loading at Launch. The launch temperature is 23°C and the assumed safe stress is 1004 psi. Altitude is sea level and the stress-strain relaxation time is assumed to be 1 hr (Contd)

(1) MODEL NUMBER	(2) PAYLOAD (LB)	(3) TAPE INDEX	(4) TAPE LOAD	(5) NSBF TAPES	(6) INDICES STRESS	(7) OKAMOTO CIR STR	(8) STRESS CIR	(9) STRESS MER	(10) STRAIN/RADIUS CIR	(11) STRAIN/RADIUS MER	(12) SHOCK INDEX
SV-516	2000#	4.31	15.1	3.78	1397	591	569	564	0.01262	0.01029	5.997
			10.08		1400	103.96	56.6	56.2	4.781	54.286	
	1528	4.96	13.2	4.33	1288	535	515	511	0.01137	0.00899	4.726
			8.81		1400	103.84	51.3	50.9	4.500	52.699	
SV-517	5050#	5.42	35.3	4.81	1405	540	521	516	0.01164	0.00899	5.952
			8.81		1400	103.70	51.9	51.5	5.581	67.937	
	4800	5.59	34.1	4.96	1379	528	509	505	0.01137	0.00871	5.679
			8.53		1400	103.67	50.7	50.2	5.505	67.543	
SV-518	6000#	5.66	43.0	5.03	1412	534	515	510	0.01156	0.00877	9.235
			8.59		1400	103.67	51.3	50.8	5.785	70.974	
	4813	6.49	37.4	5.73	1302	485	468	463	0.01053	0.00763	7.538
			7.48		1400	103.54	46.7	46.1	5.466	69.358	
SV-519	2000#	4.64	14.9	4.08	1473	582	561	558	0.01246	0.01012	9.975
			9.92		1400	103.74	55.9	55.5	4.441	53.650	
	1995	4.65	14.9	4.08	1472	582	561	557	0.01244	0.01011	9.952
			9.91		1400	103.74	55.9	55.5	4.438	53.632	
SV-520	1600#	4.98	13.8	4.34	1416	553	533	529	0.01183	0.00941	5.149
			9.22		1400	103.63	53.1	52.7	4.294	53.483	
	1364	5.37	12.3	4.66	1357	524	506	502	0.01120	0.00875	4.489
			8.58		1400	103.57	50.4	50.0	4.159	52.654	
SV-521	7500#	4.84	48.4	4.31	1428	571	550	546	0.01213	0.00968	9.262
			9.69		1400	103.92	54.7	54.4	6.565	75.392	
	6593	5.26	40.6	4.67	1358	538	518	514	0.01141	0.00919	8.218
			8.91		1400	103.83	51.6	51.2	6.327	74.327	
SV-523	3900#	4.65	24.4	4.12	1408	570	549	545	0.01202	0.00997	13.009
			9.77		1400	103.85	54.7	54.3	5.455	63.929	
SV-524	6300#	5.01	37.1	4.46	1373	548	528	524	0.01152	0.00947	20.913
			9.28		1400	103.86	52.6	52.2	6.140	71.771	
SV-525	2500#	5.81	17.0	5.09	1401	504	487	484	0.01041	0.00870	20.250
			8.52		1400	103.48	48.5	48.2	4.447	58.291	
SV-527	2800#	6.54	22.7	5.77	1405	501	485	478	0.01115	0.00773	5.679
			7.57		1400	103.35	48.3	47.6	4.353	58.588	
	2749	6.61	22.5	5.83	1396	497	481	475	0.01107	0.00764	5.584
			7.49		1400	103.34	47.9	47.3	4.335	58.461	

Table 3. Comparison of the Results of Analyses of Balloon Load Tape and Film Loading at Launch. The launch temperature is 23°C and the assumed safe stress is 1004 psi. Altitude is sea level and the stress-strain relaxation time is assumed to be 1 hr (Cont'd)

(1) MODEL NUMBER	(2) PAYLOAD (LB)	(3) TAPE INDEX	(4) TAPE LOAD	(5) HS&F TAPES	(6) INDICES STRESS	(7) CHAMOTO CIR STR	(8) STRESS CIR	(9) STRESS MER	(10) STRAIN/RADIUS CIR	(11) STRAIN/RADIUS MER	(12) SHOCK INDEX
SV-528	2420W	6.42	19.3	5.65	1403	496	480	475	0.01084	0.00786	7.583
			7.70		1400	103.31	47.0	47.3	4.201	57.462	
	1877	7.36	16.8	6.42	1298	452	438	432	0.00989	0.00688	6.049
			6.74		1400	103.22	43.7	43.1	3.982	55.850	
SV-529	2000W	5.72	16.9	4.98	1414	513	496	492	0.01088	0.00682	7.302
			8.45		1400	103.39	49.4	49.0	4.335	58.120	
	1609	6.31	15.4	5.47	1339	479	464	459	0.01012	0.00785	6.070
			7.69		1400	103.32	46.2	45.7	4.158	56.912	
SV-530	3200W	5.42	22.3	4.76	1453	534	515	512	0.01133	0.00910	11.373
			8.91		1400	103.47	51.4	51.0	4.791	62.705	
	1905	7.05	17.3	6.12	1250	444	430	425	0.00936	0.00707	7.219
			6.93		1400	103.29	42.8	42.4	4.289	59.186	
SV-531	4000W	4.79	28.3	4.27	1370	571	549	545	0.01235	0.00962	5.607
			9.43		1400	104.02	54.7	54.2	5.560	61.856	
SV-532	1000W	6.38	11.5	5.52	1399	492	476	471	0.01070	0.00783	3.422
			7.67		1400	103.24	47.5	46.9	3.586	50.150	
	1149	6.02	12.2	5.22	1444	512	495	490	0.01114	0.00828	3.838
			8.11		1400	103.28	49.3	48.8	3.671	50.735	
SV-533	2400W	5.00	18.5	4.39	1423	555	536	531	0.01191	0.00943	7.570
			9.24		1400	103.65	53.4	52.9	4.689	58.045	
	1960	5.56	16.7	4.35	1338	515	497	493	0.01102	0.00850	6.327
			8.33		1400	103.56	49.5	49.1	4.481	56.801	
SV-535	2000W	5.59	17.1	4.80	1411	519	502	498	0.01105	0.00871	7.072
			8.54		1400	103.42	50.0	49.6	4.393	58.314	
	1834	5.82	16.4	5.06	1379	505	488	484	0.01072	0.00838	6.565
			8.21		1400	103.39	48.6	48.2	4.317	57.830	
SV-536	800W	4.49	7.8	3.90	1341	571	549	545	0.01206	0.00992	3.074
			9.72		1400	104.03	54.6	54.3	3.884	43.227	
	896	4.26	8.2	3.71	1381	592	569	565	0.01255	0.01040	3.386
			10.19		1400	104.07	56.7	56.3	3.970	43.805	
SV-522	5900W	4.69	38.7	4.14	1377	565	544	540	0.01189	0.00986	7.534
			9.66		1400	103.93	54.2	53.8	6.418	73.486	
	4751	5.32	34.1	4.67	1279	515	497	493	0.01081	0.00870	6.189
			8.53		1400	103.79	49.5	49.1	6.062	72.961	
SV-526	4500W	4.27	30.7	3.78	1388	596	573	569	0.01268	0.01045	4.172
			10.24		1400	104.11	57.0	56.7	6.116	66.723	
	3615	4.86	27.0	4.28	1286	543	522	518	0.01151	0.00919	3.417
			9.01		1400	103.97	52.0	51.6	5.771	65.239	

Table 3. Comparison of the Results of Analyses of Balloon Load Tape and Film Loading at Launch. The launch temperature is 23°C and the assumed safe stress is 1004 psi. Altitude is sea level and the stress-strain relaxation time is assumed to be 1 hr (Contd)

(1) MODEL NUMBER	(2) PAYLOAD (LB)	(3) TAPE INDEX	(4) TAPE LOAD	(5) MSBF TAPE	(6) INDICES STRESS	(7) OKAMOTO CIR STR	(8) STRESS CIR	(9) STRESS MER	(10) STRAIN/RADIUS CIR	(11) STRAIN/RADIUS MER	(12) SHOCK INDEX	
SV-534	1600#	6.89	14.9	6.02	1498	496	481	475	0.01113	0.00759	6.135	1
			7.44		1400	103.08	48.0	47.3	3.545	52.059		
	1423	7.31	14.0	6.37	1448	477	463	456	0.01071	0.00716	5.536	1
			7.02		1400	103.05	46.1	45.5	3.467	51.386		

for a few cases where the difference is in the order of 10 percent. This uniformity is particularly interesting when one considers that the Okamoto model considers only differential pressure p, film thickness t, meridional radius of curvature R_1, and circumferential radius of curvature R_2 according to the relationship:*

$$\sigma_2 = \left(\frac{pR_2}{t}\right)\left(1 - \frac{R_2}{2R_1}\right) \quad .$$

The ranges of meridional and circumferential stress values (psi) for successful flights are very interesting when compared with the ranges of design (rated) values. These are shown in Table 4. In the absence of values for balloons that subsequently failed in flight, one could conclude that present designs are too conservative. However, a limit greater than 700 psi, when a reasonable safe stress is only about 1000 psi is probably inadvisable.

Table 4. Stress Range Summary of Data Base Designs

Balloon Type	Load Category	Meridional Stress		Circumferential Stress	
		Min	Max	Min	Max
No Cap	Rated	485	754	495	762
	Tested	435	724	445	733
Capped	Rated	436	669	443	653
	Tested	377	615	386	624

With respect to the NSBF stress index, there were three balloons in the study (all without caps) for which the index was greater than 1.6 in actual successful flights. The corresponding NSBF load tape factor (usually equal to 4) and the computed AFGL meridional stress values are shown in Table 5. The stress trends are opposite, but consistent with the noted tape factors. In fact, for a NSBF tape factor of about 5 and a NSBF stress index of about 1.4, the AFGL stresses appear to be consistently about 510 psi. This strongly indicates that any AFGL crown stress criterion could be translated into a comparable set of NSBF indices, and vice versa. However, this would apply at only one launch temperature.

*Because R_2 is part of the solution, this model cannot be used predictively, but it should provide a valuable check at other launch temperatures.

Table 5. Large NSBF Stress Indices

NSBF		AFGL
Stress Index	Tape Factor	Meridional Stress
1.722	3.32	724
2.069	3.73	691
2.376	7.24	572

Using analysis at the initial point in balloon flight histories as an operational predictor of subsequent success and failure, and as a decision model in an iterative design process is still a reasonable goal. The results of this study confirm it as historically viable, but design and operational use criteria require that acceptable stress levels be established not for one temperature (23°C in our case) but over the complete range of launch temperatures.

Useful film strength does decrease and meridional and circumferential film strains do increase with increasing temperature. Such deformations, locked in to some uncertain degree by the decreasing temperature accompanying the ascent to the tropopause, have been proposed as significant contributors to the so-called "tropopause burst" phenomenon. Indeed, in-flight strain measurements reported by Rand[18], suggest that such strains are "frozen in" up to the tropopause.

Webb's material characterization has been applied in the AFGL analysis model with limited success. It is not known whether further extrapolation to cover the complete range of launch temperatures will be successful. However, it is expected that recent work by Wilbeck[19] will be useful and, if fully developed, might meet the total Stratofilm® characterization requirements of the AFGL analysis model and thereby enable the realization of a simple and effective performance prediction model.

The method of stress analysis of the fully inflated balloon developed by Rand[20] and revised to take advantage of Wilbeck's material model offers the

18. Rand, J.L. (1982) Balloon film strain measurements, Workshop on Instrumentation and Technology for Scientific Ballooning, XXIV COSPAR Plenary Meeting, Ottawa, Canada, 16 May - 2 June 1982.

19. Wilbeck, J.S., and Rand, J.L. (1981) Balloon Material Characterization, AIAA 7th Aerodynamic Decelerator and Balloon Technology Conference.

20. Rand, J.L. (1978) Design and Analysis of Single Cell Balloons, Scientific Report No. 1, Contract F19628-76-C-0082, AFGL-TR-78-0258, AD A072828.

most promising approach to making the fully inflated shape more efficient. If it is further modified for use with the partially inflated bubble at launch, it should provide a description of the launch stresses and strains much more accurately than any method proposed to date.

References

1. Cuddihy, W.F., et. al. (1979) A review of heavy lift balloon failures, Proceedings, Tenth AFGL Scientific Balloon Symposium, Catherine L. Rice, Ed., AFGL-TR-79-0053, AD A074469, pp. 57, 80.

2. Dwyer, J.F. (1974) Free balloon capabilities: A critical perspective, Proceedings (Supplement), Eighth AFCRL Scientific Balloon Symposium, 30 September to 3 October 1974, Andrew S. Carten, Jr., Ed., pp. 123, 161.

3. Dwyer, J.F. (1978) Zero pressure balloon shapes, past, present, and future, Scientific Ballooning (COSPAR), W. Riedler, Ed., Pergamon Press, pp. 9, 19.

4. Schroebel, R.L. (1956) Strato-lab Development, Final Technical Report, Contract No. NONR 1589(06).

5. Okamoto, S. (1973) The effect of the number of longitudinal reinforcing tapes on a balloon and the development of thin balloon films, Institute of Space and Aeronautical Science: Bulletin, Tokyo, Japan 9(1B):142-158. (Translation, Emmanuel College, EMM-75-322, Contract F19628-74-C-0135).

6. Weissmann, D. (1972) The Ductile Brittle Transition of Low Density Polyethylene, Scientific Report No. 1, Contract No. F19628-72-C-0100, AD 757885.

7. Anderson, A.A., Jr., and Monfitt, G.L. (1958) Balloon Barrier Materials, Final Technical Report, Contract AF 19(604)-1393, AD 152504.

8. Dwyer, J.F. (1966) Some polyethylene balloon statistics, Proceedings, AFCRL Scientific Balloon Workshop, 1965, pp. 49-56, AD 634765.

9. Kerr, A.D. (1967) Stress and Deformation Analysis of Flexible Balloons, Final Report, Contract AF 19(628)-4990, AFCRL-TR-67-0345, AD 666437.

10. Kerr, A.D., and Alexander, H. (1967) On a Cause of Failure of High Altitude Plastic Balloons, Scientific Report No. 2, Contract F19628-67-C-0241, AFCRL-TR-67-0611, AD 667192.

11. Kerr, A.D. and Alexander, H. (1968) On a Cause of Failure of High Altitude Plastic Balloons, Scientific Report No. 5, Contract F19628-67-C-0241, AFCRL-TR-68-0486, AD 692173.

12. Alexander, H. and Weissmann, D. (1972) A Compendium of the Mechanical Properties of Polyethylene Balloon Films, Scientific Report No. 2, Contract F19628-69-C-0069, AFCRL-72-0068, AD 746678.

13. Webb, L.D. (1978) Mechanical Behavior of Balloon Films, Scientific Report No. 2, Contract F19628-76-C-0082, AFGL-TR-79-0026, AD A098937.

14. Rand, J.L. (1978) Define and Study Free Balloon Design Problems, Final Report, Contract F19628-76-C-0082, AFGL-TR-78-0295, AD A067716.

15. Alexander, H., and Murthy, G.K.N. (1968) A Failure Stress Criterion For A Polyethylene Balloon Film, Scientific Report No. 4, Contract F19628-67-C-0241, AFCRL-TR-69-0103, AD 692516.

16. Parsons, W.B. (1965) Performance of Balloon Reinforcement Tapes Under Static and Dynamic Loading, Scientific Report No. 2, Contract AF19(628)-2944, AD 698758.

17. Alexander, H., and Agrawal, P. (1974) Gore Panel Stress Analysis of High Altitude Balloons, Scientific Report No. 2, Contract F19628-72-C-0100, AFCRL-TR-74-0597, AD A009627.

18. Rand, J.L. (1982) Balloon film strain measurements, Workshop on Instrumentation and Technology for Scientific Ballooning, XXIV COSPAR Plenary Meeting, Ottawa, Canada, 16 May - 2 June 1982.

19. Wilbeck, J.S., and Rand, J.L. (1981) Balloon Material Characterization, AIAA 7th Aerodynamic Decelerator and Balloon Technology Conference.

20. Rand, J.L. (1978) Design and Analysis of Single Cell Balloons, Scientific Report No. 1, Contract F19628-76-C-0082, AFGL-TR-78-0258, AD A072828.

Appendix A

Balloon Program Planning Document

1. PROGRAM IDENTIFICATION AND COORDINATION

PROGRAM NAME _____

PROJECT NUMBER _____ TASK NUMBER _____

	RESPONSIBLE AGENCY	PRIME CONTRACTOR
NAME	_____	_____
ADDRESS	_____	_____
	_____	_____
TELEPHONE	_____	_____
COORDINATOR	_____	_____

2. FLIGHT REQUIREMENTS (List in order of priority. Identify as essential, if possible, and desirable.)

_____

_____

_____

_____

3. PROGRAM PAYLOAD

ESTIMATED WEIGHT RANGE, MAX _____ lb MIN _____ lb

COMPONENTS AND CONFIGURATIONS:

ITEM	HT. ×WT. ×LT (in.)	WEIGHT (lb)

4. FLIGHT PROFILE DESCRIPTION (Describe in terms of altitudes, durations, and ascent and descent rates, when applicable. See Figure A1.)

5. MISSION LOCATION AND TIMETABLE

DESIRED GEOGRAPHICAL LOCATION OF LAUNCH SITE _____

ESTIMATED LAUNCH DATE (Year, Month, Day) _____

LATEST LAUNCH DATE (Year, Month, Day) _____

DESIRED FLOAT ARRIVAL TIME _____ hours (local) ± _____ hours

6. SPECIAL LAUNCH, FLIGHT AND RECOVERY CONSIDERATIONS (launch and recovery shock, electromagnetic interference, reel-down of payload, command channels, data channels, payload pointing, horizontal trajectory, payload hazards, etc.)

7. DESCRIPTION OF PASSIVE AND COMMANDED PAYLOAD FUNCTIONS

8. ADDITIONAL COMMENTS AND QUESTIONS

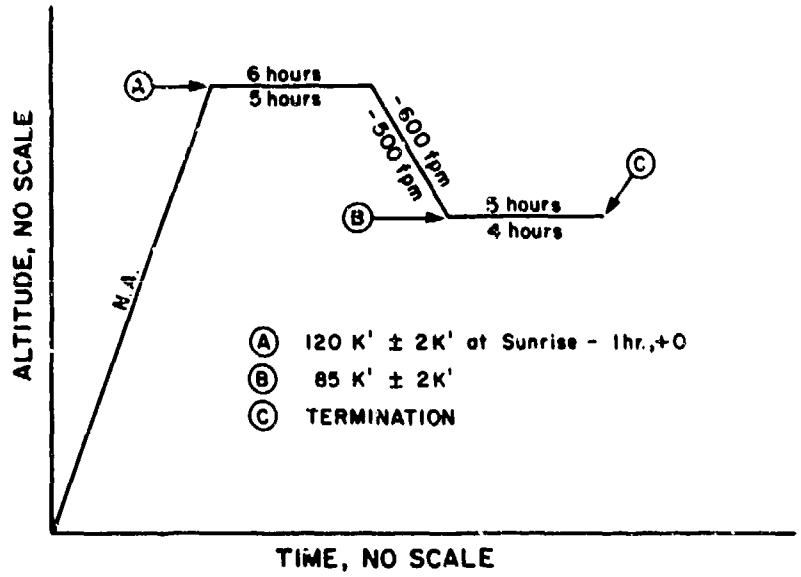

Figure A1. Sample Flight Profile Plan With Acceptable Ranges of Times, Altitudes, and Rates

Appendix B

Parachute Size

In many balloon systems the recovery parachute subsystem contributes a significant fraction of the payload weight, particularly for short-duration high-altitude flights. Weightwise, the principal components of the recovery subsystem are the canopy and the instrumentation cable. The latter services the balloon apex valve and the termination devices that separate the balloon and payload at the end of the flight. The combined weights can be adequately approximated in terms of the parachute diameter D_c by a second degree polynomial. Based on conventional instrumentation, cable weight, and parachutes 40, 60, and 100 ft in diameter, the parachute subsystem weight W_c becomes:

$$W_c = 0.02257\, D_c^2 - 0.7847\, D_c + 52.778 \ . \qquad \text{(B1)}$$

If the maximum load suspended from the parachute is represented by L_c, then the relationship between total descent weight, sea level terminal descent velocity V_c, and parachute diameter can be derived for standard flat circular parachutes using Hess' tables[B1] as:

$$D_c = (37.8/V_c)\sqrt{L_c + W_c} \ . \qquad \text{(B2)}$$

B1. Hess, J. (1963) Determination of Parachute Descent Times and Impact Locations for High Altitude Balloon Payloads, AFCRL-63-885.

Eliminating W_c between the latter two equations yields:

$$D_c = \frac{560.6 - \sqrt{(75411 + 1428.8\,L_c)V_c^2 - 46078.8\,L_c - 211773}}{32.25 - V_c^2} \quad , \qquad \text{(B3)}$$

which provides quite realistic values for diameters down to about 24 ft. Since the balloon selection procedure is based on a number of estimates, the need to compromise due to the availability of only discrete parachute sizes should not adversely affect balloon selection.

Since the parachute size must be large enough to accommodate the maximum payload, the descent time with all ballast expended may cause undesirable or even unacceptable drift. This can be overcome by using deadweight ballast if otherwise not precluded. Balloon selection programs should also (and the AFGL program does) compute the minimum descent rate as a caution to the systems designer.

Appendix C

Program "ADEQUATE"

C1. DESCRIPTION

This program takes balloon mission requirements and from them computes their compatability with balloons having tested capabilities. It determines the weight of ballast required and the size and weight of the required parachute. It creates a table of existing designs capable of performing the specified mission and indicates the most efficient solution (reference Table 2).

C2. METHOD

The method is described schematically in Figure 6 using the data base format described in Figure C1.

C3. SPECIAL CONSIDERATIONS

The following assumption underlies the solution process: 1962 U.S. Standard Atmosphere.

K	I	11 DIGIT NUMERICAL CODE											OUTPUT DESCRIPTION
1	1						X	Y	Y	Y	Z	Z	BALLOON TYPE (1)* NUMBER, 000 THRU 999 MODIFICATION (2)
2	2			X	X	X	X	X	X	X	X	X	VOLUME (FT^3)
3	3						X	X	X	X	X	Y	RATED PAYLOAD (LB) RATER (3)
4	4	X	X	X	X	X	Y	Z	Z	Z	Z	Z	TESTED PAYLOAD (LB) FLIGHT NO. REF (4)
5	5 6 7	X	Y	Y	Y	Y	Z	Z	Z	Z	Z	Z	GORELENGTH (FT) SIGMA SIGMA SOURCE REF (5)
6	8 9 10	X	X	Y	Y	Y	Y	Z	Z	Z	Z	Z	DUCT AREA (FT^2) DUCT LENGTH (FT) NO. OF DUCTS
7	11 12 13		X	X	X	Y	Y	Y	Z	Z	Z	Z	TAPE STRENGTH (LB) NO. OF GORES SHELL THICKNESS (MIL)
8	14 15	X	X	X	X	X	Y	Y	Y	Y	Y	Y	DESIGN POINT ALTITUDE (FT) DESIGN POINT PAYLOAD (LB)
9	16 17 18				X	Y	Y	Y	Z	Z	Z	Z	MAX. CAP LENGTH (FT) CROWN THICKNESS (MIL) NUMBER OF CAPS
10	19 20 21			X	X	Y	Y	Z	Z	Z	Z	Z	BALLOON WEIGHT (LB) APEX FITTING WEIGHT (LB) BASE FITTING WEIGHT (LB)

Figure C1. Coded Balloon Database. The input array is U(J, K) and the output array is A(I). The value stored in U(J, K) is the K^{th} coded integer for the J^{th} balloon in the file. The value output for A(I) when I is greater than 1 and not equal to 7 is a real number with the indicated number of digits and the decimal point on the far right of the number unless otherwise noted. (*See Section C6 of this appendix)

C4. SYSTEM

This program is written in BASIC programming language and is configured to run on an HP9830A (32308 word, Read-Write Memory) with an HP9871A impact printer.

C5. OPERATION

The program is stored on cassette number 4, file number 3. The scanned data base is stored on files 4 through 19 of the same cassette.

a. Press: LOAD, type: 3, press: EXECUTE

b. Press: RUN EXECUTE

c. The display reads: YYMMDD? Type in the date, for example, 821225 (Christmas 1982), press: EXECUTE

d. The display reads: METRIC INPUT? Type in answer, for example, YES. If input is anything but yes, inputs requested are in feet and pounds (force), not kilometers and kilograms (force). Press: EXECUTE (See Figure C2).

e. The display reads: ALTITUDE Type in the altitude in proper units, for example, 100000, press: EXECUTE

f. The display reads: PAYLOAD Type in the payload in the proper units (not including ballast or parachute weights), for example, 1000, press: EXECUTE

g. The display reads: DESCENT BALLAST FRACTION Type in the descent ballast requirement expressed as a decimal fraction, for example, 0.05, press: EXECUTE

h. The display reads: BALLAST FRACTION FOR DRIVE-UP Type in the ballast required as a decimal fraction, for example, 0.05, press: EXECUTE

i. The display reads: PAYLOAD GROWTH FRACTION Type in the allowable payload weight increase as a decimal fraction of the payload, for example, 0.06, press: EXECUTE This value allows for experimenter's underestimate of the project payload weight (ballast and parachute excluded)

j. The display reads: SUNSET BALLAST DROPS Type in the number of sunsets that must be counteracted by using ballast, for example, 2, press: EXECUTE

k. The display reads: FRACTIONAL SUNSET BALLAST Type in the average sunset effect ballast as a decimal fraction, for example, 0.075, press: EXECUTE This indicates that for each night, 7 1/2 percent of the gross system weight will be dropped as ballast to keep the system from descending to the ground.

l. The display reads: BALLAST DROPS FOR CONTROL Type in the number of non-sunset ballast drops (reference Figure 4), for example, 3, press: EXECUTE

m. The display reads: CHUTE IMPACT SPEED Type in the allowable parachute terminal velocity in ft/sec, for example, 20, press: EXECUTE

n. The display reads: BALLAST FRACTION Type in the decimal fraction for the first drop (reference l above), for example, 0.06, press: EXECUTE This display repeats for the number of times input in l above.

```
'ADEQUATE' (CF 4.03) 820808

ALTITUDE (Kilometers)           50
PAYLOAD (Kilograms)             200
DESCENT BALLAST FRACTION        0.05
BALLAST FRACTION FOR DRIVE-UP   0.1
PAYLOAD GROWTH FRACTION         0.06
SUNSET BALLAST DROPS            0
BALLAST DROPS FOR CONTROL       0
CHUTE IMPACT SPEED (Km/Sec)     18
STANDARD ATM.(1966)

'ADEQUATE' (CF 4.03) 820809

ALTITUDE (Feet)                 100000
PAYLOAD (Pounds)                1000
DESCENT BALLAST FRACTION        0.05
BALLAST FRACTION FOR DRIVE-UP   0.06
PAYLOAD GROWTH FRACTION         0.1
SUNSET BALLAST DROPS            2
FRACTIONAL SUNSET BALLAST       0.075
BALLAST DROPS FOR CONTROL       3
CHUTE IMPACT SPEED (Ft/Sec)     20
STANDARD ATM.(1966)

BALLAST FRACTION
 0.060
 0.060
 0.065
```

Figure C2. Examples of Metric and English Input

C6. DATA BASE FORMAT

The data base is divided into groups of ten balloons each, with ten separate packages of coded information on design and performance. The construction of a coded package is typically like XXXYYYZZZZ. If this number were decoded as U(J, 7), it would produce the following:

shell thickness = X.XX mil
number of gores = YYY.
tape strength = ZZZZ. lb .

There are five sets of alpha codes as follows:

(1) Balloon Model Codes

1	_SV-	capped balloons
2	LTV-	taped - uncapped balloons
3	TTV-	tapeless semi-cylinder balloons
4	_CV-	cylinder balloons
5	_SP-	special or experimental design balloons
6	WWW-	Winzen International, Inc., design balloons
7	RRR-	Raven Industries, Inc. design balloons

(2) Modification Code

1-26	A through Z

(3) Balloon Payload Rater

1	A	Air Force
2	N	Navy
3	P	Palestine
4	W	Winzen International, Inc.
5	R	Raven Industries, Inc.
6	blank	Unknown

(4) Flight Number Reference

1	H-	Hollom AFB
2	C-	Chic[illegible]A
3	S-	Special Series
4	AD-	Balloon Development Series (early AFGL)
5	WW-	Winzen International, Inc.
6	NF-	NSBF
7	blank	Numerical designation only

The value of ZZZZZ is input as an integer for certain flight series and as a real number for certain others: for example, AD-87 (input as integer), H-81-023 (input as real number, 81.023). The decoding and encoding take care of the retrieval and storage changes required to interchange decimal points and dashes.

(5) Sigma Source Reference

1	U/M SIGMA
2	Smalley
3	Not Tabulated

```
1000 REM "ADEQUATE" (CF 4.03 82AUG09)

1010 REM INTERNAL COMPUTATIONS AND OUTPUT IN ENGLISH UNITS.
1020 REM 1966 STD  ATM. IS USED.
1030 DIM A$[180],C$[35],D$[35],E$[35],G$[35]
1040 DIM A[21],E[10,2],X[9],U[10,10],Z1[10,8]

1050 A$="ALTITUDE PAYLOAD GROWTH FRACTIONAL SUNSET "
1060 A$[43]="BALLAST DROPS FOR CONTROLCHUTE IMPACT SPEED "
1070 A$[87]="DESCENT BALLAST FRACTION FOR DRIVE-UP"
1080 REM INPUT STRING ADDRESSES
1090 DATA 1,9,10,17,87,110,95,123,10,32,36,55,25,49,43,67,68,86,0,0,0
1100 REM DECODE II
1110 DATA 1,1,6,1,0,0.0,0,2,1,9,9,0,0,0,0,3,1,6,5,0,0,0,0
1120 DATA 4,1,11,5,0,0,0,0,5,3,6,4,4,1,1,1,8,3,5,3,4,3,2,2
1130 DATA 11,3,4,4,3,3,3,1,14,2,6,6,5,5,0,0,16,3,4,3,3,1,1,1
1140 DATA 19,3,5,5,2,2,2,2
1150 REM 1966 ATM.
1160 DATA 9,1013.25,0,288.15,11,216.65,20,216.65,32,228.65,47,270.65
1170 DATA 52,270.65,61,252.65,79,180.65,0,0

1180 MAT READ A
1190 MAT READ Z
1200 MAT READ E
1210 FORMAT B
1220 FORMAT 2B
1230 WRITE (15,1220)27,84;

1240 DISP "YYMMDD";
1250 INPUT D8
1260 PRINT "'ADEQUATE' (CF 4.03)"D8
1270 PRINT
1280 C1=6356766
1290 C2=0.3048037
1300 C3=34.163195
1310 C4=0.0217484
1320 C5=0.8018105
1330 STANDARD

1340 D$="(Feet)                "
1350 E$="(Pounds)                "
1360 G$="(ft/Sec)    "
1370 B=D=1
1380 DISP "METRIC INPUT ";
1390 INPUT C$
1400 IF C$#"YES" THEN 1460
1410 D$="(Kilometers)          "
1420 E$="(Kilograms)             "
1430 G$="(Km/Sec)    "
1440 B=3280.8
1450 D=2.2046
```

```
1000 REM "ADEQUATE" (CF 4.03 82AUG09)


1460 FOR I=1 TO 17 STEP 2
1470 IF I#13 THEN 1510
1480 IF A[6]#0 THEN 1510
1490 X[7]=0
1500 GOTO 1660
1510 C$=A$[A[I],A[I+1]]
1520 DISP C$;
1530 INPUT X[(I+1)/2]
1540 IF I>3 AND I#17 THEN 1650
1550 PRINT C$;
1560 IF I>1 THEN 1590
1570 PRINT D$;
1580 GOTO 1630
1590 IF I>3 THEN 1620
1600 PRINT E$;
1610 GOTO 1630
1620 PRINT G$;
1630 PRINT X[(I+1)/2]
1640 GOTO 1660
1650 PRINT C$,X[(I+1)/2]
1660 NEXT I


1670 PRINT "STANDARD ATM.(1966)"
1680 A=X[1]=B*X[1]
1690 X[2]=D*X[2]
1700 X[9]=B*X[9]
1710 F1=1/(1-X[3])/(1-X[4])
1720 IF X[8]=0 THEN 1830
1730 PRINT
1740 PRINT


1750 FIXED 3
1760 PRINT "BALLAST FRACTION"
1770 FOR I=1 TO X[8]
1780 DISP "FRACTION";
1790 INPUT H7
1800 PRINT H7
1810 F1=F1/(1-H7)
1820 NEXT I
1830 F1=-1+F1/((1-X[7])^X[6])


1840 DISP "ERROR";
1850 INPUT C$
1860 WRITE (15,1210)12
1870 IF C$="YES" THEN 1330
```

```
1000 REM "ADEQUATE" (CF 4.03 82AUG09)


1880 A$=" SV-LTV-TTV- CV- SP-WWW-RRR-0123456789"
1890 A$[39]=" ABCDEFGHIJKLMNOPQRSTUVWXYZ"
1900 GOSUB 2450
1910 B6=3
1920 K9=0
1930 H7=1E+06
1940 P8=80


1950 FOR O=4 TO 19
1960 LOAD  DATA 0,0
1970 FOR H=1 TO 10
1980 GOSUB 2780
1990 IF A[5]=0 THEN 2360
2000 IF K9>0 THEN 2050
2010 PRINT "MODEL NO  VOLUME MAXIMUM BALLOON BALLAST CHUTE  CHUTE DRIFT"
2020 PRINT "                  PAYLOAD WEIGHT  WEIGHT  WEIGHT SIZE  SPEED"
2030 PRINT
2040 K9=1
2050 W1=(1+X[5])*X[2]
2060 FOR J=1 TO 5
2070 B8=P1*(W1+P8+A[19])
2080 D9=0.090278-0.0028*X[9]*X[9]
2090 D9=INT(0.5+(1.5694-SQR(2.4632-4*D9*(B8+W1+52.778)))/D9)
2100 P8=D9/2
2110 P8=0.09027[illegible]*P8-1.5594*P8+52.778
2120 NEXT J
2130 S7=SQR(4*(P8+X[5]*X[2])/(D9*...*0.0028))
2140 W1=W1+B8+P8
2150 IF W1>INTA[3] THEN 2360
2160 A=A[14]
2170 GOSUB 2450
2180 B=A[15]+0.12605*(A[5]^3)*(B6-B)
2190 IF W1 <= A[15] THEN 2210
2200 B=B6*A[2]-A[19]
2210 IF W1>B THEN 2360
2220 GOSUB 2640
2230 WRITE (15,2240)C$,A[2],INTA[3],A[19],B8,P8,D9,S7;
2240 FORMAT F10.0,2X,F7.0,2X,F7.0,2X,F7.0,2X,F6.0,2X,F5.0,2X,F5.0
2250 IF H7<(W1+A[19]) THEN 2350
2260 IF INTA[3]>INTA[4] THEN 2290
2270 PRINT "*"
2280 GOTO 2300
2290 PRINT "* ABOVE TESTED LOAD"
2300 H7=A[19]+W1
2310 K9=K9+1
2320 IF K9<51 THEN 2360
2330 WRITE (15,1210)12
2340 K9=0
2350 PRINT
2360 NEXT H
2370 NEXT O
```

```
1000 REM "ADEQUATE" (CF 4.03 82AUG09)


2380 PRINT
2390 IF H7=1E+06 THEN 2430
2400 FORMAT F5.0
2410 WRITE (15,2400)"LAST * YIELDS LOWEST GROSS,"H7;
2420 PRINT " POUNDS."
2430 DISP "END"
2440 END


2450 REM MODEL ATM.
2460 M=E[1,1]
2470 P=E[1,2]
2480 X=C2*A
2490 X=0.001*C1*X/(C1+X)
2500 FOR I=2 TO M+1
2510 J=I
2520 E1=0
2530 IF E[I+1,2]#E[1,2] THEN 2550
2540 E1=0.0001
2550 R=(E1+E[I+1,2]-E[I,2])/(E[I+1,1]-E[I,1])
2560 IF X<E[I+1,1] THEN 2590
2570 P=P*((E[I,2]/(E1+E[I+1,2]))^(C3/R))
2580 NEXT I
2590 T=E[J,2]+R*(X-E[J,1])
2600 P=P*((E[J,2]/T)^(C3/R))
2610 D=C4*P/T
2620 B=C5*D
2630 RETURN


2640 REM DECODE I
2650 B=INTA[I]
2660 C$=A$[4*B-3,4*B]
2670 A=A[I]-B
2680 FOR D=1 TO 4
2690 IF D<4 THEN 2720
2700 B=-29-INT(A*100)
2710 GOTO 2740
2720 A=A*10
2730 B=INTA
2740 C$[4+D]=A$[B+29,B+29]
2750 A=A-B
2760 NEXT D
2770 RETURN
```

```
1000 REM "ADEQUATE" (CF 4.03 82AUG09)


2780 REM DECODE II
2790 FOR Y=1 TO 10
2800 B=U(B,Y)
2810 FOR M=1 TO Z(Y,2)
2820 X=-Z(Y,2*M+1)
2830 D=B*(10^X)
2840 B=INTD
2850 J=Z(Y,1)+M-1
2860 X=Z(Y,2*M+2)
2870 A(J)=(D-B)*(10^X)
2880 NEXT M
2890 NEXT Y
2900 RETURN
```

Appendix D

Equations Governing the Balance of Forces

Alexander[D1] assumed linearity between engineering stress and simple strain, acknowledged the orthotropic nature of current polyethylene balloon film and arrived at the following two-dimensional constitutive relation:

$$\epsilon_c = \frac{\sigma_c}{E_c} - \frac{\sigma_m}{E_m}\,\nu \tag{D1}$$

$$\epsilon_m = \frac{\sigma_m}{E_m} - \frac{\sigma_c}{E_c}\,\nu \tag{D2}$$

where ϵ is strain, σ is stress (lb ft^{-2}) and E is the film modulus (lb ft^{-2}). The subscripts c and m refer to the circumferential and meridional directions (mutually orthogonal) of the balloon gores and the corresponding circumferential and machine directions of the extruded tubular polyethylene film used to construct the balloon gores. The film is assumed incompressible under load and Poisson's ratio is assumed to be constant (ν = 0.679) over the range of balloon use temperatures.

D1. Alexander, H., and Agrawal, P. (1974) Gore Panel Stress Analysis of High Altitude Balloons, Scientific Report No. 2, Contract F19628-72-C-0100, AFCRL-TR-74-0597, AD A009627.

Force equilibrium in the meridional direction is satisfied by the relationship:

$$\sigma_m = \left[\frac{F_m}{Qwh} + \frac{M_t \epsilon_o}{wh}\right] - \left[\frac{M_t}{wh}\right] \epsilon_m \quad . \tag{D3}$$

where

- Q is the number of balloon gores
- w is the gorewidth at the analysis location (Figure D1) (ft)
- h is the balloon wall thickness at the analysis location (ft)
- ϵ_o is the mechanical slack built into the load tapes (dim)
- F_m is the total meridional load as determined from payload, balloon weight and geometrical considerations (lb)
- M_t is the elastic modulus of the load tapes (lb) .

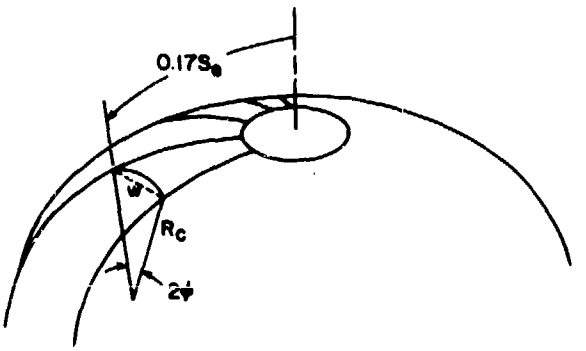

Figure D1. Balloon Crown Deployment During Inflation and at Launch

Alexander further assumed that the film would deform circumferentially under pressure, that the shape of deformation would be a circular arc, and that it would lie in the plane normal to the meridional stress (Figure D1). These assumptions are continued in the author's analysis, but unlike Alexander's analysis, the contribution of film weight is considered negligible and omitted. Force equilibrium normal to the surface is thus given by:

$$P = \frac{h\sigma_m}{R_m} + \frac{h\sigma_c}{R_c} \quad , \tag{D4}$$

where

P is the pressure differential across the film (lb ft^{-2})

R_m is the meridional radius of curvature of the balloon surface, assumed equal for both film and load tapes (ft)*

R_c is the radius of curvature of the deformed gorewidth (ft) .

In the fully deployed crown of the balloon, the geometry of the deformation (Figure D1) yields two additional relationships:

$$\sin\phi = (1 + \epsilon_m)\, w/[2R_c] \tag{D5}$$

$$\phi = (1 + \epsilon_c)\, \sin\phi\, /(1 + \epsilon_m) \quad . \tag{D6}$$

The two additional relationships needed to complete the set of 8 independent equations result from a material model suggested by Webb[D2] and modified as shown in Appendix E. These are:

$$E_c = 144\, E_{60}(\epsilon_c) \tag{D7}$$

$$E_m = 144\, E_{60}(\epsilon_m) \tag{D8}$$

The five remaining variables in these equations, M_t, F_m, P, w, and R_m are evaluated on the basis of geometrical, thermal, and environmental considerations. Models for these will vary according to the relative altitude of the balloon analysis, which for this study is taken as the launch site elevation.

Both Alexander[D1] and Rand[D3] provide similar models for polyester load tape modulus as a function of centigrade temperature. At 15°C their results agree to within 1.5 percent. Where L is the nominal load tape strength, Rand's model is:

$$M_t = [11.334 - {}^{\circ}C/15]\, L \quad . \tag{D9}$$

---

*For additional comments on this assumption see Rand.[D3]

D2. Webb, L. D. (1978) Mechanical Behavior of Balloon Films, Scientific Report No. 2, Contract F19628-76-C-0082, AFGL-TR-79-0026, AD A098937.

D3. Rand, J. L. (1978) Design and Analysis of Single Cell Balloons, Scientific Report No. 1, Contract F19628-76-C-0082, AFGL-TR-78-0258, AD A072828.

Smalley[D4] provides natural shape balloon tables which, for all practical values of Σ, yield corresponding values of $(T/P)_\Sigma$ and $(W/P)_\Sigma$. In these ratios, T is the total load at the balloon apex (lb), W is the balloon weight (lb), and P is payload (lb). Where G is the gross load (lb), the relationship $(G/P)_\Sigma = 1+(W/P)_\Sigma$ allows us to write $T = G(T/P)_\Sigma / (G/P)_\Sigma$.

Smalley[D5] shows, that for a balloon shape with $\Sigma = 0.2$, the ratio of apex loading at launch to apex loading at float for current altitudes of interest is approximately 0.716. Actually, the ratio is a function of both altitude (as inferred from b/b_d) and shape (Σ). Development of a functional relationship is possible and may become desirable, but Smalley's results (Figure D2) indicate that 0.716 is a reasonable first approximation and that the minimum of the probable range of values is greater than 0.639. Further, the quotient $(T/P)_\Sigma / (G/P)_\Sigma$ can be represented by a 5th-degree polynominal that is designated $F_1(\Sigma)$, such that the total meridional load at launch becomes:

$$F_m = 0.716\, G\, F_1(\Sigma) \quad . \tag{D10}$$

The differential pressure at the top of a balloon was shown by Dwyer[D6] to be proportional to the product $W_P^{1/3} b^{2/3}$ where W_P is the payload (lb) and b is the specific lift (lb ft^{-3}). Smalley[D4] presented a graphic relationship (Figure D3) between the non-dimensionalized pressure and variations in Σ as well as relative altitude. The following model approximates differential pressure for $b/b_d > 20$ and was derived from Smalley's graphical presentation by numerical methods:

$$P = \left[e^{\Sigma} - e^{-\pi} \right] W_P^{1/3} b^{2/3} \quad . \tag{D11}$$

An approximation to the solution of the problem of knowing the shape and effective gorelength S_e of a balloon at launch (the static fully erect balloon) was suggested by analysis of Smalley's tables of balloon dimensions for altitudes below design altitude ($b/b_d > 1$). For $b/b_d > 20$, more than 70,000 ft below float, these data reflect insignificant dependence on Σ (for normally used shapes) in so far as the relative gas bubble length is concerned. This is sufficient for nearly

---

D4. Smalley, J.H. (1963) Determination of the Shape of A Free Balloon, Scientific Report No. 2, Contract AF 19628-2783, AFCRL-64-734, AD 610125.

D5. Smalley, J.H. (1966) Balloon Shapes and Stresses Below the Design Altitude, NCAR-TN-25.

D6. Dwyer, J.F. (1973) Balloon Apex Pressure Differential, AFCRL-73-0632, AD 774399.

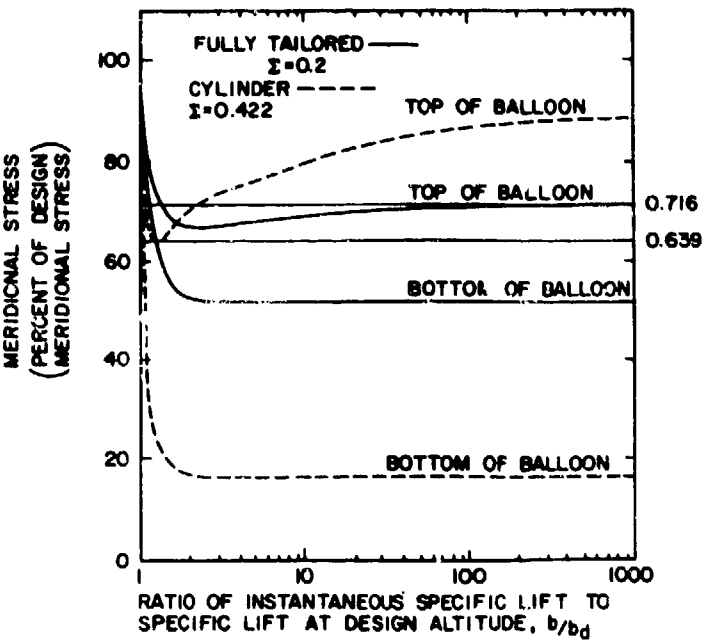

Figure D2. Relative Meridional Stress at the Top and Bottom of a Balloon That is Below its Design Altitude

all present balloon flights. The gas bubble length, or effective gorelength, is defined as the total gorelength S_λ minus the undeployed length (Figure D4). For large fully-tailored balloons, the type with which we are concerned, the weight of the undeployed film is effectively the same as added payload in so far as balloon shape is concerned. Numerical analysis of Smalley's data yielded the following approximation:

$$S_e = S_\lambda \left[0.8975 - 0.2325 \log_{10}(b/b_d) \right] \quad . \tag{D12}$$

Motion pictures of balloon ascent bursts (looking upward from the payload and downward inside the balloon from the apex fitting) indicate that failures occur high in the crown of the balloon. Upson[D7] in his analyses referred to this critical region as "the taut cap". Studies on the causes of such ascent bursts by Dwyer[D8]

D7. Upson, R. H. (1939) Stresses in a partially inflated free balloon, J. Aero. Sci. 6(4):153-156.

D8. Dwyer, J. F. (1965) Some Polyethylene Balloon Statistics, Proceedings AFCRL Scientific Balloon Workshop, AFCRL-66-309, AD 634765.

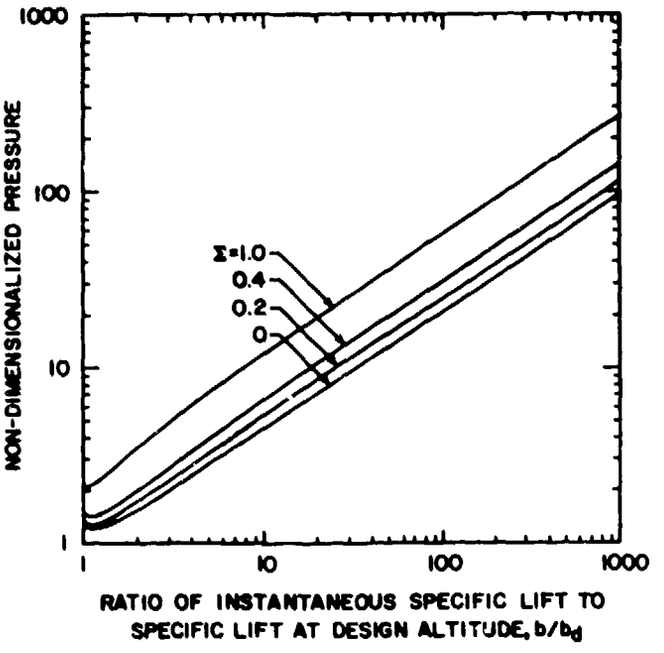

Figure D3. Pressure Trend at Top of Fully-Tailored, Natural Shape Balloon at Altitudes Below Natural Float Altitude

and Kerr[D9] indicate that this most highly stressed region at launch is potentially the key to success or failure during passage through the minimum temperature region of the tropopause.

Observations of launches of fully-tailored balloons and experience with hangar inflation tests indicated that the crown of the balloon at launch was fully deployed for a distance of about $0.17\ S_e$, measured from the apex. Alexander, as shown in Figure D5, found launch stress in some cases to peak in this very region. Consequently, the point ($0.17\ S_e$ measured from the apex) is chosen as the launch stress analysis point. Since the number of gores is large and the crown area is flat (for practical purposes), the gore width at this point can be expressed as:

$$w = 2\pi[0.170\,S_e]/Q \quad . \tag{D13}$$

D9. Kerr, A. D., and Alexander, H. (1967) On a Cause of Failure of High Altitude Plastic Balloons, Scientific Report No. 2, Contract F19328-67-C-0241, AFCRL-67-0611, AD 667192.

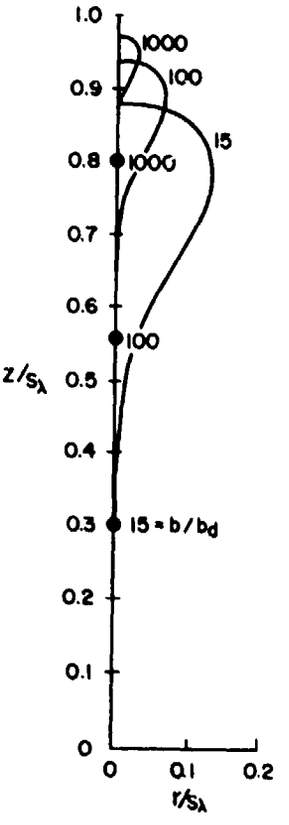

Figure D4. Representative Shapes of a Fully-Tailored Balloon, Below Design Altitude, According to Smalley[D5]. The effective gorelength S_e is the difference between the manufactured gorelength S_λ and the value of Z/S_λ at and below which $r/S_\lambda = 0$. The symbol ● represents the effective base endfitting location corresponding to S_e and b/b_d

From the natural-shape balloon tables, the meridional radius of curvature, R_m, has been computed at a gore position about 0.17 S_e ft from the apex for the useful range of the Σ shape factor. A model relating R_m to Σ for a full balloon has been numerically developed. Adjustment for the launch shape is not thought to be necessary. However, the necessity can easily be verified by determining the sensitivity of the computed stresses to variations of C_m in the following developed model (see line 1270, Appendix G for values of coefficients):

$$R_m = C_m S_e \underset{i=0}{\overset{i=6}{SUM}} (a_i \Sigma^i) \quad . \tag{D14}$$

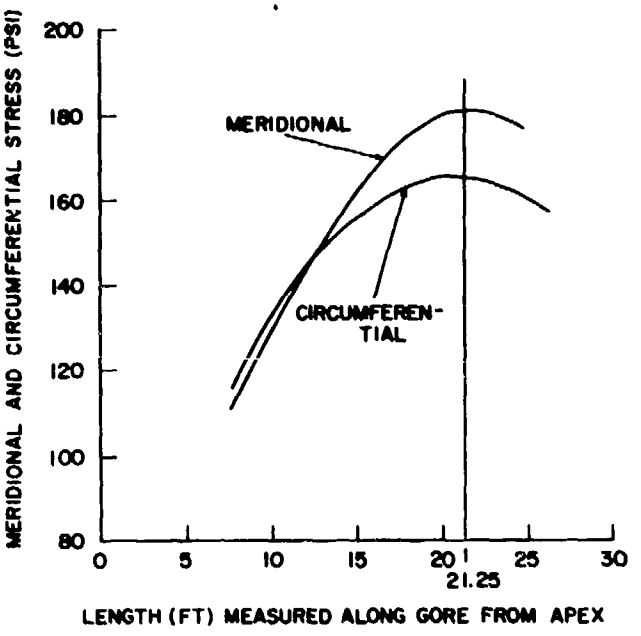

Figure D5. Gore Panel Stress Analysis of a Model SV-001 Balloon With a 488-lb Payload at Launch, According to Alexander[D1]. The 21.25-ft location corresponds to the value 0.174 S_e

References

D1. Alexander, H., and Agrawal, P. (1374) Gore Panel Stress Analysis of High Altitude Balloons, Scientific Report No. 2, Contract F19628-72-C-0100, AFCRL-TR-74-0597, AD A009627.

D2. Webb, L. D. (1978) Mechanical Behavior of Balloon Films, Scientific Report No. 2, Contract F19628-76-C-0082, AFGL-TR-79-0026, AD A098937.

D3. Rand, J. L. (1978) Design and Analysis of Single Cell Balloons, Scientific Report No. 1, Contract F19628-76-C-0082, AFGL-TR-78-0258, AD A072828.

D4. Smalley, J. H. (1963) Determination of the Shape of A Free Balloon, Scientific Report No. 2, Contract AF 19(628)-2783, AFCRL-64-734, AD 610125.

D5. Smalley, J. H. (1966) Balloon Shapes and Stresses Below the Design Altitude, NCAR-TN-25.

D6. Dwyer, J. F. (1973) Balloon Apex Pressure Differential, AFCRL-73-0632, AD 774399.

D7. Upson, R. H. (1939) Stresses in a partially inflated free balloon, J. Aero. Sci. 6(4):153-156.

D8. Dwyer, J. F. (1965) Some Polyethylene Balloon Statistics, Proceedings AFCRL Scientific Balloon Workshop, AFCRL-66-309, AD 634765.

D9. Kerr, A. D., and Alexander, H. (1967) On a Cause of Failure of High Altitude Plastic Balloons, Scientific Report No. 2, Contract F19628-67-C-0241, AFCRL-67-611, AD 667192.

Appendix E

A Practical Stratofilm® Model

The dependency of polyethylene balloon film properties on temperature, rate of loading and history (temperature, stress, and strain) suggests the need for a comprehensive model such as proposed and studied by Webb.[E1] Restated, his Eq. 71 is:

$$\sigma = [(Ka_T)^n/(1-n)/D_1]\,\epsilon^{1-n} \quad , \tag{E1}$$

where

- σ is stress (lb/in.^{2})
- K is strain rate (in./in./min)
- a_T is the time temperature shift factor
- n is the exponent in the power law relaxation function (Webb's Eq. 61)
- D_1 is the coefficient in the power law relaxation function (Webb's Eq. 61)
- ϵ is the strain (in./in.)

Taking the natural log of both sides of Eq. (E1) yields three equations:

$$\ln\sigma = x_o + x_i \ln\epsilon \tag{E2}$$

E1. Webb, L.D. (1978) Mechanical Behavior of Balloon Films, Scientific Report No. 2, Contract No. F19628-76-C-0082, AFGL-TR-79-0026, AD A098937.

$$x_o = \ln [(Ka_T)^n/(1-n)/D_1] \quad \text{(E3)}$$

$$x_1 = 1-n \quad \text{(E4)}$$

Graphs of σ versus ϵ for 0.7 mil Stratofilm® at 23°C for the values of K = 2.0, 0.2, 0.02, and 0.002 in./in./min were obtained under the Texas A&M contract of Reference E1. The graphs were for both machine and transverse direction (MD and TD) film tests. Averaging (by sight) each MD and TD pair of curves, 19 equally spaced strain values (0.005 through 0.095) were then processed (using Eq. (E2)) by regression analysis for each K-value.

The trends in the values of x_o and x_1, for the given values of K, were not immediately obvious. However, the intention of using the results for a fixed temperature (23°C) and at low strain rate would diminish rather than magnify the errors of any reasonably inferred trends. Thus we have.

$$x_o = \ln (7222\ K^{0.0217}) \quad \text{(E5)}$$

$$x_1 = 1 - \ln (1.34\ K^{0.00869}) \quad . \quad \text{(E6)}$$

Therefore, we can express the secant modulus, $E(K, \epsilon)$ at 23°C as:

$$E(K, \epsilon) = \frac{7222\ K^{0.0217}}{\epsilon^{\ln(1.34\ K^{0.00869})}} \quad . \quad \text{(E7)}$$

Selection of a proper strain rate and reasonable relaxation effects must still be made. The stress levels and respective strain levels in the crown area continuously change (even after inflation is completed) up to the time when the bubble is released to the vertical (dynamic launch). Since we have selected this point as the design point, and since the time to reach this pseudo-static state is generally about 60 min, the strain rate K selected is the strain of the pseudo-static state divided by the time, 60 min. Obviously the rate will thus differ for the meridional and transverse directions, and K becomes an output while 60 min becomes an input.

Meridional creep in the crown area is accompanied by increased circumferential strain. Also, relaxation of the circumferential stress results in increased circumferential strain in the bowed out section of the gore panels. The apparent secant moduli resulting from these interactions are effectively reduced.

Comparing the model generated moduli for a variety of times and rates indicated a trend toward a limiting value, thus implying that the use of variable strain rates and constant time to achieve a pseudo-static state effectively accounts for any creep and relaxation.

The resultant model* becomes on substitution of $\epsilon/60$ for K:

$$E_{60}(\epsilon) = 6608\ \epsilon^{-(27+\ln\epsilon)/115} \quad . \tag{E8}$$

The stress strain relationship resulting from this model becomes:

$$\sigma_{60}(\epsilon) = 6608\ \epsilon^{(88-\ln\epsilon)/115} \quad . \tag{E9}$$

Equations (8) and (9) were used to produce the results shown in Table E1.

The models developed in this manner could have been, if required, more accurate and comprehensive. First, data could have been analyzed separately for the MD and TD directions and then, given a_T as a function of temperature, equations 3, 4, 5, and 6 could have been used to define D_1 as:

$$D_1 = \frac{(Ka_T)^{1-x_1}}{x_o x_1} \tag{E10}$$

*For use in Appendix D, $E_{60}(\epsilon)$ must be multiplied by 144 in^2/ft^2.

Table E1. Numerical representation of Eqs. (8) and (9). LGT(MOD) is the log base 10 of the modulus

STRAIN in/in	STRESS PSI	MODULUS PSI	LGT(MOD)
0.002	41	20318	4.308
0.004	74	18532	4.268
0.006	105	17494	4.243
0.008	134	16763	4.224
0.010	162	16201	4.210
0.012	189	15746	4.197
0.014	215	15364	4.187
0.016	241	15036	4.177
0.018	265	14749	4.169
0.020	290	14493	4.161
0.022	314	14264	4.154
0.024	337	14055	4.148
0.026	360	13864	4.142
0.028	383	13689	4.136
0.030	406	13526	4.131
0.032	428	13375	4.126
0.034	450	13233	4.122
0.036	472	13101	4.117
0.038	493	12976	4.113
0.040	514	12857	4.109
0.042	535	12745	4.105
0.044	556	12639	4.102
0.046	577	12538	4.098
0.048	597	12441	4.095
0.050	617	12349	4.092
0.052	638	12261	4.089
0.054	658	12176	4.086
0.056	677	12095	4.083
0.058	697	12017	4.080
0.060	716	11941	4.077
0.062	736	11869	4.074
0.064	755	11798	4.072
0.066	774	11731	4.069
0.068	793	11666	4.067
0.070	812	11602	4.065
0.072	831	11540	4.062
0.074	850	11480	4.060
0.076	868	11422	4.058
0.078	887	11366	4.056
0.080	905	11311	4.054
0.082	923	11258	4.051
0.084	941	11206	4.049
0.086	959	11156	4.047
0.088	977	11107	4.046
0.090	995	11059	4.044
0.092	1013	11012	4.042
0.094	1031	10966	4.040
0.096	1048	10921	4.038
0.098	1066	10876	4.037
0.100	1084	10835	4.035

Appendix F

Duct Design Considerations

Researchers at the University of Minnesota (U M) developed the standard pressure relief duct to vent the excess lifting gas needed for ascent. It replaced the open base appendix which, although it also prevented balloon burst due to excess overpressure as the balloon system entered float, had the distinct disadvantage of ingesting air. This ingestion of air, caused by the negative pressure at the base of the partially inflated (ascending or descending) balloon, increased the venting back pressure and presented thermodynamic problems.

The back pressure created as a result of the venting process was related to the bursting pressure of a sphere with a diameter equivalent to the constructed diameter of the balloon.[F1] For a given ascent rate, allowable film stress, inflatant, and constant atmospheric scale height, the relationship reduced to:

$$A = cD^2\sqrt{\frac{G}{t}} \quad , \tag{F1}$$

where

- A is the total effective duct area (ft^2)
- D is the balloon diameter (ft)
- G is the weight of the displaced air (lb)

F1. University of Minnesota (1954) Progress Report on High Altitude Balloons, Vol IX, Contract No. NONR-710(01).

t is the film thickness (mil)

c is a constant .

This model may have provided needed safety margins in the days when polyethylene balloon seams were weak and frequently unreliable, but today the film and seam strengths are high, and reasonably indistinguishable. Further, the applicability of a spherically equivalent stress situation at the maximum horizontal diameter is precluded by the meridional stiffness of the seams. Even without load tape fibers the seam, backup tape, and tape casing significantly influence the stress and the stress distribution in both chamber test models[F2] and in computer aided balloon stress analyses.* Obviously then the U M model cannot accurately represent the stresses (due to venting) in today's large, tape-reinforced tailored polyethylene balloons.

Ignoring the U M stress model and concentrating on the overpressure itself, we find that the U M relationship yields:

$$\Delta P = \frac{V^2 v_o^2 \rho}{2gh_o^2 A^2} \qquad \text{(F2)}$$

where

ΔP is the venting overpressure (lb/ft^2)

V is the balloon volume (ft^3)

v_o is the ascent rate (ft/sec)

ρ is the specific weight of the inflatant (lb/ft^3)

g is the gravitational constant (32.1741) (ft/sec^2)

h_o is the atmospheric scale height (ft)

A is the total effective duct area .

For very small venting overpressure and equal air and gas temperature, the specific lift of the gas, b, is proportional to the specific weight of the gas and Eq. (F2) becomes:

$$\Delta P = 0.12608 \frac{V^2 v_o^2 b}{2gh_o^2 A^2} \quad . \qquad \text{(F3)}$$

*Rand, J. L., private conversation.

F2. Alexander, H., and Weissmann, D. (1972) A Compendium of the Mechanical Properties of Polyethylene Balloon Films, Scientific Report No. 2, Contract F19628-69-C-0069, AFCRL-72-0068, AD 746678.

Differential pressure at the maximum horizontal diameter of a fully inflated natural shape balloon is the product of the specific lift and the distance between the height of the plane of this maximum diameter and the base of the balloon. This latter distance is proportional to the cube root of the balloon volume. The proportionality factor, k_Σ, is dependent upon the value of Σ applicable to the in-flight deformed volume. This yields the relationship:

$$\Delta P = \alpha k_\Sigma b V^{1/3} \quad , \tag{F4}$$

where α is the ratio of valving back pressure to the pressure at the maximum diameter.

Without yet considering the stress, we can relate the effective valving area to the fractional back pressure by eliminating ΔP between Eqs. (F3) and (F4) to yield:

$$A = \sqrt{\frac{0.12608}{2g \alpha k_\Sigma}} \left(\frac{v_o}{h_o}\right) V^{5/6} \quad . \tag{F5}$$

A dynamic model was developed to evaluate the results of Eq. (F5). The U M appendix flow model was used in conjunction with the hydrostatic equation to develop the dynamic model. Further, it was assumed that the ascent rate would be constant, the air and gas temperature differential would be constant, and the atmospheric temperature and pressure would be in accordance with the 1962 U. S. Standard Atmosphere model. These seemed reasonable on the basis of preliminary work that indicated that the pressure would peak within about 15 sec after the start of valving. The following equations constitute the dynamic model:

$$\dot{P}_2 = (P_2/T_2)\dot{T}_2 - \frac{A}{V}\sqrt{(2gR_u/M_2)(P_2T_2(P_2 - P_1))} \tag{F6A}$$

$$\dot{P}_1 = -(M_1/R_u)(P_1/T_1)v_o \tag{F6B}$$

$$\dot{T}_1 = v_o L \tag{F6C}$$

$$\dot{T}_2 = v_o L \quad . \tag{F6D}$$

where

P is pressure (lb/ft^2)

T is temperature (^{o}R)

L is atmospheric temperature lapse rate (^{o}R/ft)

A is effective duct area (ft^2)

V is balloon volume (ft^3)

v_o is the ascent rate, constant (ft/sec)

g is the gravitational constant, 32.1741 (ft/sec^2)

R_u is the universal gas constant, 1545.31 (ft $lb_f/^{o}R/(lb\text{-}mol)$)

M is molecular weight .

The symbol . denotes a time derivative.

Subscripts 1 and 2 refer to air and gas respectively.

Equation F6 (A-D) was solved for duct area for a fixed α value over the following ranges and intervals:

altitude - 70,000 (10,000) 180,000 ft

system weight - 2,000 (1,000) 9,000 lb

ascent rate - 10 (5) 20 ft/sec

The resulting valving areas were compared with areas computed from Eq. (F5). Here it is important to note that the atmospheric scale height h_o at an altitude Z is the distance upward from that altitude to the point where the atmospheric pressure is reduced by one half of its value at altitude Z, and that h_o is not constant in the standard atmosphere model (see Table F1). This variation was included in Eq. (F5) computations and the ratios were constant to within 5 percent.

Table F1. Ratio R of Currently Used Duct Design Coefficient to Effective Coefficient Derived Using Eq. F7. Z is balloon altitude in feet; h_o is atmospheric scale height; θ is atmospheric temperature in ^{o}C

Z	h_o	θ	R
80000	14230	-52.209	3.99
90000	14430	-49.185	3.99
100000	14620	-46.165	3.98
110000	14720	-40.714	3.90
120000	14690	-32.273	3.70
130000	15000	-23.840	3.62
140000	15520	-15.415	3.55
150000	16060	-6.998	3.46
160000	16720	-2.500	3.47
170000	17780	-2.500	3.69

Thus while the U M stress model is probably conservative, the back pressure model appears consistent with the more complex dynamic model when the variable atmospheric scale height is introduced. One apparent question is what are the consequences of admitting changes in the other input variables. This analysis follows.

The current duct design model follows directly from Eq. (F1) (Eq. 12 on page II-36 of reference F1). The value of the Eq. (F1) constant now in use is C = 2.76E - 05. It appears to represent the following assumption:

F = 1, the fractional bursting pressure
M = 28.8, ingested air is being valved
h_o = 2.0E + 04, the atmosphere scale height (ft)
v_o = 0.7, the ascent rate (kilo-ft/min)
T = 1600, film strength (lb/in^2) .

The equivalent of Eq. (F1) then becomes:

$$A = 5.75 \left[\frac{v_o}{h_o} \sqrt{\frac{M}{FT}} \right] D^2 \sqrt{\frac{G}{t}} \qquad \text{(F7)}$$

where

D is the balloon maximum diameter (ft)
G is the gross inflation (lb)
t is the film thickness (mil) .

Balloons today, with the standard duct design, seldom ingest a significant volume of air; this suggests that the value of M should be 4 (helium) rather than 28.8 (air). Further at the higher altitudes in the troposphere, the ascent rate into float is generally on the order of 500 ft/min. Without changing F, we are left to determine the contribution of the term $1/\sqrt{T h_o^2}$.

Both the film strength T and the scale height h_o are functions of altitude, h_o directly and T because it is a function of temperature that varies with altitude. Substituting the values of 1, 0.5, and 4 for F, v_o, and M respectively, and approximating tensile strength by the model [F2]:

$$T = 1793.75 - 30.9375\theta \quad , \qquad \text{(F8)}$$

where θ is the atmospheric temperature in degrees centigrade, we can compare the equivalent value of C with the current value, 2.76E - 05. Table F1 gives the results. It shows that with the conservative stress analysis based on the assumption of sphericity, the present duct areas are about 3.75 times the minimum

effective area. This corresponds to an effective duct diameter that is about one half of the constructed duct diameter (a recommendation found in the U M work). The U M recommendations are applicable to duct diameters of a few feet and may be too conservative when using diameters of 14 ft.

How conservative the present U M model is we do not know, but a sound engineering basis for duct design must ultimately depend on a sound analysis of the stresses and strains in the balloon shell and the tapes at ceiling altitude. Needless to say, adequate tape and biaxial film characterization are implicit in any such model.

Whether or not significant saving in weight can be made, the use of many small ducts as opposed to significantly fewer large ducts means potential degradation of very thin film balloons due to excessive production handling during the hand installation of the ducts. The use of 150 ft^2 ducts in place of 40 and 50 ft^2 ducts on the very large balloons now using 8 to 10 ducts can reduce the number of ducts in some cases by four or more; for example, model SV-022 has eight 40 ft^2 ducts. Four ducts of 110 ft^2 each would provide one duct in excess of the required area at a saving of four ducts; the balloon shell was 0.45 mil thick.

Tables F2 and F3 compare some existing balloon duct designs with the results of Eq. (F1) (for C = 2.76E - 05) and Eq. (F7) increased by a factor of 3.75.

Table F2. Duct Area Comparisons. "WEIGHT" is the weight of the balloon. Under "TOTAL DUCT AREA", I represents the as built area, II represents the solution using Eq. F1, and III represents the solution using Eq. F7

MODEL NO	VOLUME ft^3	WEIGHT lbs	TOTAL DUCT AREA I ft^2	II ft^2	III ft^2
SV-001A	5033809	1340	120	107	98
SV-002	2661176	1070	120	66	61
SV-004	30272377	1530	500	372	362
SV-005	10578059	1335	160	169	158
SV-006	26600000	2695	400	452	427
SV-007	6677900	2470	180	189	172
SV-008	8740000	2400	300	208	191
SV-009	10578059	2150	200	180	166
SV-010	37736556	1910	600	475	463
SV-011	45380000	2890	600	563	546
SV-012	21770000	1700	300	285	273
SV-014	15600000	1890	300	294	274
SV-015	21680000	2145	400	375	354
SV-016A	11620000	1240	200	215	203
SV-017B	5142712	1600	120	120	111
SV-018	3685868	560	80	82	75
SV-019	5136000	1470	120	117	108
SV-020	11617429	1240	200	221	207
SV-021	47815660	1772	600	588	579
SV-022	28694910	1460	320	373	358
LTV-001	13486530	1425	200	171	162
LTV-002	4849664	740	100	67	62
LTV-003C	2945571	1110	75	51	47
LTV-005	642729	356	40	10	9
LTV-006	5033809	1120	120	91	83
LTV-007	2012003	800	60	35	33
LTV-008	273600	239	18	6	6
LTV-009	516000	340	20	10	9
LTV-010B	859000	440	40	15	13
LTV-011A	1840000	525	60	31	29
LTV-012	4890000	925	71	65	61
LTV-013A	2900135	995	60	52	48
LTV-014	2003675	1080	50	40	37
LTV-018	355000	260	20	9	8
LTV-019	628000	360	30	13	12
LTV-020	145026	135	10	3	3
LTV-021	264985	200	20	6	5
LTV-022	449183	200	20	9	8
LTV-023	1575005	440	40	28	26
LTV-024	1110000	505	50	20	18

Table F3. Duct Area Comparisons. "WEIGHT" is the weight of the balloon. Under "TOTAL DUCT AREA", I represents the as built area, II represents the solution using Eq. F1, and III represents the solution using Eq. F7

MODEL NO	VOLUME ft^3	WEIGHT lbs	TOTAL DUCT AREA I ft^2	II ft^2	III ft^2
LTV-026	2369069	800	50	47	43
SP-001	3016600	318	60	57	53
SP-003	711460	780	40	25	21
SV-500	26085893	2588	500	469	441
SV-501	27988324	3416	600	532	494
SV-502	29008952	2470	625	529	502
SV-503	33325200	3041	625	575	547
SV-504	25690000	2113	500	456	433
SV-505	25980000	2607	500	476	448
SV-506	28048674	4507	600	580	533
SV-507	25840000	1939	500	491	383
SV-508	28463000	2853	600	535	501
SV-509	30390000	4650	600	590	542
SV-510	31210000	2733	600	598	566
SV-511	31154200	2376	600	520	495
SV-512	30820000	2541	500	481	458
SV-513	33120000	2425	600	582	553
SV-514	31150000	2800	500	529	503
SV-515	33500000	4300	600	580	534
SV-516	31650000	2116	600	475	454
SV-517	34090000	3732	600	575	540
SV-518	34311500	4306	750	668	620
SV-519	37780000	2070	700	600	576
SV-520	36100000	2235	600	506	488
SV-521	39590000	5064	800	760	704
SV-523	45840000	3089	800	789	751
SV-524	47012000	4064	1000	966	914
SV-525	70700000	2974	1200	1128	1093
SV-527	30500000	2498	500	476	453
SV-528	36700000	2478	500	568	544
SV-529	50310000	2956	800	732	703
SV-530	52600000	3228	900	839	802
SV-531	26400000	2706	500	448	422
SV-532	35850000	2083	400	465	450
SV-533	36360000	2600	500	577	552
SV-535	46090000	2937	700	686	658
SV-536	30160000	1355	400	359	347
SV-522	42500000	5000	750	744	700
SV-526	33100000	3660	600	514	483
SV-534	33858500	2000	500	490	473

Appendix G

Program "DESIGN-II"

G1. DESCRIPTION

This program takes balloon mission requirements and develops therefrom a balloon system including the balloon design, the required ballast weight, and the size and weight of the required parachute. Values of pre-launch static stresses and the "shock index" (see dynamic loading index, Section 5.2) are output for comparison with current design allowables, and the option to redesign and change film thicknesses, load tape factor, and maximum gorewidth is offered. If the loadings are acceptable, the design and stress analysis data and a table of payload and altitude are output.

G2. METHOD

The program assumes a balloon weight, computes the shape from the relationship between the shape (Σ) and the balloon weight-payload weight ratio, recomputes the balloon weight from the input and the computed shape, compares the two balloon weights and reiterates the process if the weights are not within tolerance. In the reiteration, the computed balloon weight is substituted for the assumed weight. The shape characteristics are computed using, for the most part, sixth degree polynomials derived from Smalley's tables.

The analyses of stresses are based on variations of Alexander's approach (Appendix D) and refinements of Webb's materials characterization (Appendix E).

G3. SPECIAL CONSIDERATIONS

The following assumptions underly the solution process:

a. 1962 U.S. Standard Atmosphere
b. 500 ft/min ascent rate when venting through ducts
c. $23^{\circ}C$ launch temperature
d. 1004 lb/in^2 safe stress level
e. 60-min stress-strain relaxation time
f. 12 percent free lift
g. 0.0659 lb/ft^3 specific lift of helium at launch
h. 0.005 lb/ft^2/mil balloon film weight factor

G4. SYSTEM

This program is written in BASIC programming language and is configured to run on an HP9830A (3808 word, Read-Write Memory) with an HP9871A impact printer.

G5. OPERATION

The program is stored in two parts on cassette number 4, files 21 and 22. File 21 contains the input and design and analysis sections and file 22 the output statements. The two files are connected by a "link" command that is automatically activated by the program.

a. Press: LOAD, type: 21, press: EXECUTE
b. Press: RUN EXECUTE
c. The display reads: ALT? Type in the design floating altitude in feet, for example, 100000, press: EXECUTE
d. The display reads: MIN, DSGN, MAX? Type in the minimum payload, the design payload and the maximum payload, each in pounds, for example, 1000, 2000, 5000, press: EXECUTE . Note that the design payload can be assumed to include the weights of ballast and parachute, in which case the entry must be an integer. If it is required that the design payload be instrumentation only and that ballast and a parachute be computed, then the design payload should be entered

as the integer part of a mixed number, such that, where P9 is the code for the design payload, P9 ≠ INT(P9). The function INT (X) computes the integer part of the number X. If the design payload was entered as an integer, then the machine will skip (e) and respond according to (f) following.

e. The display reads: % BLST, CHUTE VEL? Type in the total ballast as a fraction of the system weight (see Section 2.3) and the allowable terminal velocity of the recovery parachute in ft/sec, for example, 0.25, 20, press: EXECUTE

f. The display reads: SHELL, CAP? Type in the shell film thickness and the cap film thickness each in mils, for example, 1.5, 0, press: EXECUTE. If the cap thickness entry is 0, then the design will proceed to yield an uncapped balloon.

g. The display (after a brief computation time) reads: LO(5), QO(101)? Type in the ratio of total load tape strength to tape load at the apex at float altitude for the maximum payload (normally five for the first estimate) and the allowable maximum gorewidth in inches (normally 101), for example, 5, 101, press: EXECUTE. After a significant computation time, the printer will output the following names and their corresponding values: SIGMA, SHOCK INDEX, STRAIN (meridional and circumferential), STRESS (meridional and circumferential in lb/in^2), % TAPE STRENGTH (for pre-launch loading), LO, QO, T6 (shell thickness in mils), and T7 (cap thickness in mils).

h. The display reads: SHELL (OK=0) & CAP? Type in the new thicknesses in mils for the shell and the cap, for example, 1.2, 0, press: EXECUTE. Any entry for shell thickness, other than 0, causes the program to reiterate and requires new inputs beginning at (g). Thus, the film thicknesses can be changed or they can remain the same (re-entered under this step) and the stresses reduced by increasing the value of LO or reducing the value of QO, (or both) under the reiterated step g. If the entry for the shell thickness is 0 and the entry for the cap thickness is any arbitrary number, file 22 is automatically linked and the design and loading analysis data output. In addition, a performance table of payload and altitude and the design point [for use with Eq. (2)] is output.

```
1000 REM "DESIGN-II(A)" (CF 4.21 82JUL29)


1010 REM TEMP=23C, STRAIN TIME=60 MIN
1020 REM FLOAT ENTRY SPEED=500FPM, FREE LIFT=12%
1030 DIM A[8],E[9,2],U[4,7]


1040 REM (Acap/A)=FCN(SIGMA,R)
1050 DATA -0.195390893,-0.952989499,0.819023889,0.581211894,-1.633868387
1060 DATA 1.118915175,-0.248342045,0.19664587,4.644428949,-3.24841125
1070 DATA -3.472893627,7.232507341,-4.259334618,0.785900199,3.383282482
1080 DATA -6.630204025,4.076038773,5.564315562,-10.05391706,5.404091207
1090 DATA -0.859152769,-2.398958901,2.952718136,-1.645782348,-2.706391858
1100 DATA 4.499006036,-2.28485346,0.325235255
1110 REM STD. ATM.
1120 DATA 9,1013.25,0,288.15,11,216.65,20,216.65,32,228.65,47,270.65
1130 DATA 52,270.65,61,252.65,79,180.65
1140 REM SIGMA=FCN(W/P)
1150 DATA 0,0.375469014941,-0.061  44739632,0.0179374540922
1160 DATA -1.83972293864E-03,2.25926217923E-04,-1.46417871814E-05,6
1170 REM (V/S^3)=FCN(SIGMA)
1180 DATA 0.12605508,0.061374109851,-8.63907397454E-03,-0.09 740353
1190 DATA 0.080087807233,-6.0680228217E-03,-0.0101107457963,6
1200 REM (A/S^2)=FCN(SIGMA)
1210 DATA 1.235984785,0.3889874254,-0.048794261,-0.374649865
1220 DATA 0.1451693335,0.196113802,-0.1170171769,6
1230 REM (T/G)=FCN(SIGMA)
1240 DATA 1.560420909,-0.798290024,-0.036815992,0.640557679,-0.318218061
1250 DATA 0.012582683,0,5
1260 REM (R1/S9)=FCN(SIGMA)
1270 DATA 0.28202,0.13557,0.7319,-3.34086,6.20111,-5.42733,1.81098,6


1280 MAT READ U
1290 MAT READ E
1300 FORMAT B
1310 FORMAT 2B
1320 WRITE (15,1310)27,84;
1330 RAD
1340 B=0.0659
1350 D0=0
1360 S0=1004
1370 N1=0.679
1380 T0=9.8
1390 W0=0.005
1400 W9=1000
1410 D7=P8=V0=0
1420 DISP "ALT.";
1430 INPUT H0
1440 DISP "MIN, DSGN, MAX ";
1450 INPUT P0,P9,P
1460 P3=P
1470 P5=P0
1480 IF P9 >= P0 THEN 1510
1490 P9=0
1500 GOTO 1530
```

```
1000 REM "DESIGN-II(A)" (CF 4.21 82JUL29)


1510 IF P9=INTP9 THEN 1560
1520 P5=INTP9
1530 DISP "& BLST, CHUTE VEL ";
1540 INPUT F8,V0
1550 D7=0.090278-0.0028*V0^2
1560 DISP "SHELL, CAP ";
1570 INPUT T6,T7
1580 T8=T6+T7
1590 B8=FNAH0
1600 C8=1793.75-30.9375*H2


1610 K3=K4=K9=R7=0
1620 K6=1280
1630 K2=FNA(H0-5)-FNA(H0+5)
1640 F=H0-15000
1650 K1=FNAF-2*B8
1660 K7=FNL(-K1)
1670 IF K6<10 THEN 1690
1680 IF K7=2 THEN 1650
1690 Z8=H0-F


1700 W1=W5=0
1710 P8=INTP9
1720 DISP "L0(5),Q0(101)";
1730 INPUT L0,Q0
1740 W8=W9
1750 IF P9>0 AND P9=INTP9 THEN 1820
1760 W5=F8*(W8+P5)/(1-F8)
1770 IF V0=0 THEN 1810
1780 R7=(1.5694-SQR(2.4632-4*D7*(52.778+P0+W5)))/D7/2
1790 W1=0.090278*R7^2-1.5694*R7+52.778
1800 W5=F8*(W8+P5+W1)/(1-F8)
1810 P8=P5+W1+W5
1820 RESTORE 1150
1830 Y9=W8/(P0+W1)
1840 Z1=FNE(LOG(1+Y9))
1850 V1=FNEZ1
1860 RESTORE 1150
1870 Z2=FNE(LOG(1+W8/P8))
1880 V2=FNEZ2
1890 IF P>0 THEN 1910
1900 P3=P8
1910 RESTORE 1150
1920 Z3=FNE(LOG(1+W8/P3))
1930 V3=FNEZ3
1940 S8=(((W8+P0+W1)/V1+(P8-P0-W1)/0.12605)/B8)^(1/3)
1950 R=3*(1.12*V3*B8/8)^(1/3)
1960 R8=0.007+(V1-0.095*SQR(V1/0.13))^(1/3)
1970 RESTORE 1210
1980 S=FNEZ1
1990 W7=W0*T7*FNC(R)*S*S8^2
2000 W6=W0*T6*S*S8^2
```

```
1000 REM "DESIGN-II(A)" (CF 4.21 82JUL29)


2010 Q=1+INT(24*PI*S8*R8/Q0)
2020 L=25*INT(1+L0*FNEZ3*(W8+P3)/Q/25)
2030 W2=INT(0.5+(0.00279879+0.0000098 37*L)*Q*S8)
2040 A5=97.36*((R8*S8)^2)*SQR((P+W8)/C8/T8)/Z8
2050 P7=W8/Y9
2060 U=((W8+P7)/V1+(P-P7)/0.12605)/S8^3
2070 V8=(W8+P)/U
2080 M0=150
2090 Q1=2+INT(A5/M0)
2100 IF Q1-1 <= 6 THEN 2130
2110 M0=2.25*M0
2120 GOTO 2090
2130 M0=A5
2140 A5=10*INT(1+A5/10/(Q1-1))
2150 X8=0.425*S8
2160 W4=1.1*Q1*T6*W0*X8*SQR(4*P1*A5)
2170 W3=0.0475*S8
2180 U9=(Q*S8*W0/12)*(T6+R*T7)
2190 L8=U8=0
2200 IF S8<315 THEN 2230
2210 L8=1+INT(S8*(1-R)-5)
2220 U8=8*W0*L8
2230 W9=30+U8+U9+W2+W3+W4+W6+W7
2240 IF ABS(W9-W8)>0.01*W8 THEN 1740
2250 W8=W9


2260 W9=2*PI*S8*R8/Q
2270 T=T8/12000
2280 G=1.12*(W8+P3)
2290 RESTORE 1150
2300 Z=FNE(LOG(1+W8/(G-W8)))
2310 V=FNEZ
2320 S9=S8*(0.897455-0.232485*LGT((S8^3)^B*V/G))
2330 RESTORE 1270
2340 R1=S9*FNEZ
2350 P=(EXPZ-EXP(-P1))*((G-W8)^(1/3))*(B^(2/3))
2360 W=2*P1*0.17*S9/Q
2370 RESTORE 1240
2380 Y=FNEZ
2390 U2=S8*(G-W8)/T0/T6
2400 F0=0.716*Y^3


2410 K9=K4=K3=0
2420 K2=0.000000001
2430 A1=L*T0/T/W
2440 A2=A1*D0+Z0/Q/T/W
2450 A4=P*R1/T
2460 E0=A2/A1
```

```
1000 REM "DESIGN-II(A)" (CF 4.21 82JUL29)


2470 K6=0.999998*E0/10
2480 E1=0.000001*E0
2490 F1=A2-A1*E1
2500 E3=144*6608*E1^(-(27+LOGE1)/115)
2510 E2=((1-N1^2)*F1-E1*E3)/N1/E3
2520 IF E2>0 THEN 2550
2530 K1=1
2540 GOTO 2630
2550 E4=144*6608*E2^(-(27+LOGE2)/115)
2560 F6=(A4-F1)/(E4*R1*(E2+N1*F1/E3))
2570 F7=(1+E1)*F6*W/2
2580 F9=F7*(1+E2)/(1+E1)
2590 F7=ATN(F7/SQR(1-F7^2))
2600 IF K9>0 THEN 2620
2610 F2=SGN(F7-F9)
2620 K1=F2*(F9-F7)
2630 F=E1
2640 K7=FNLK1
2650 E1=F
2660 IF K7=2 THEN 2490


2670 R2=1/F6
2680 S1=F1
2690 S2=E4*(E2+N1*S1/E3)
2700 U1=E3*(E1+N1*S2/E4)
2710 U1=ABS((U1-S1)/S1)
2720 B1=T0*(E1-D0)


2730 FIXED 5
2740 PRINT "SIGMA:              "Z1
2750 PRINT "SHOCK INDEX:        "U2/1E+06
2760 PRINT "STRAIN (M & C):     "E1,E2
2770 FIXED 0
2780 PRINT "STRESS (M & C):     "S1/144,S2/144
2790 PRINT "% TAPE STRENGTH:    "100*B1
2800 FIXED 2
2810 PRINT "L0="L0"Q0="Q0"T6="T6"T7="T7
2820 PRINT


2830 DISP "SHELL(OK=0) & CAP ";
2840 INPUT C1,C2
2850 IF C1=0 THEN 2900
2860 T6=C1
2870 T7=C2
2880 T8=T6+T7
2890 GOTO 1720
2900 WRITE (15,1300)12
2910 LINK 22,1330,1330
```

```
1000 REM "DESIGN-II(A)" (CF 4.31 82JUL29)


2920 DEF  NL(K1)
2930 REM BINARY CHOP
2940 K9=K9+1
2950 IF ABSK1 <= K2 THEN 3050
2960 IF K1>0 THEN 2990
2970 K3=K5=1
2980 GOTO 3010
2990 K5=-1
3000 K4=1
3010 K6=K6/(K3+K4)
3020 F=F+K5*K6
3030 RETURN 2
3040 STOP
3050 K3=K4=0
3060 RETURN 1


3070 DEF FNA(A)
3080 REM ATMOSPHERE
3090 C1=6356766
3100 C2=0.3048037
3110 C3=34.163195
3120 C4=0.0217484
3130 C5=0.8618105
3140 H1=E[1,2]
3150 X=C2*A
3160 X=0.001*C1*X/(C1+X)
3170 FOR I=2 TO E[1,1]
3180 J=I
3190 F1=0
3200 IF E[I+1,2]#E[1,2] THEN 3220
3210 F1=0.0001
3220 F3=(F1+E[I+1,2]-E[1,2])/(E[I+1,1]-E[I,1])
3230 IF X<E[I+1,1] THEN 3260
3240 H1=H1*((E[I,2]/(F1+E[I+1,2]))^(C3/F3))
3250 NEXT I
3260 H2=E[J,2]+F3*(X-E[J,1])
3270 H1=H1*((E[J,2]/H2)^(C3/F3))
3280 H4=C4*H1/H2
3290 H3=C5*H4
3300 H1=2.08858*H1
3310 H2=H2-273.16
3320 RETURN (H3)
3330 STOP


3340 DEF FNE(X)
3350 REM POWER SERIES
3360 MAT READ A
3370 Y=A[1]
3380 FOR I=1 TO A[8]
3390 Y=Y+A[I+1]*X^I
3400 NEXT I
3410 RETURN Y
3420 STOP
```

```
1020 REM "DESIGN-II(A)" (CF 4.21 82JUL29)


3430 DEF FNC(R)
3440 REM CAP AREA SUBROUTINE
3450 U=0
3460 X=1-R
3470 FOR I=1 TO 4
3480 C=0
3490 FOR J=1 TO 7
3500 C=C+U[I,J]*Z1^(J-1)
3510 NEXT J
3520 U=U+C*X^(I-1)
3530 NEXT I
3540 U=1-U
3550 RETURN U
3560 END
```

```
1330 REM "DESIGN-II(B)" (CF 4.22 82JUL30)

1340 REM BALLOON DESIGN, LAUNCH STRESS ANALYSIS AND
1350 REM PERFORMANCE TABLE FOR EST. BALLOON WEIGHT.

1360 PRINT "Output from 'DESIGN-II(A)' (CF 4.21)"
1370 FIXED 0
1380 PRINT
1390 PRINT "TARGET MIN. PAYLOAD "P0+W1
1400 PRINT "MAXIMUM PAYLOAD     "P3
1410 PRINT "DESIGN PAYLOAD      "P8
1420 PRINT "ALT. FOR DSGN. PAY. "H0
1430 PRINT
1440 FIXED 5
1450 PRINT "SIGMA               "Z1
1460 FIXED 2
1470 PRINT "SHELL THICKNESS     "T6
1480 PRINT "CROWN THICKNESS     "T6+T7
1490 PRINT "DUCT AREA           "A5
1500 FIXED 0
1510 PRINT "NUMBER OF DUCTS     "Q1
1520 FIXED 0
1530 PRINT "DUCT LOWER LIP      "X8
1540 PRINT
1550 PRINT "VOLUME (MAX.)       "V1*S8^3
1560 PRINT "VOLUME (MIN.)       "V8
1570 PRINT
1580 PRINT "BALLOON WEIGHT      "W8
1590 PRINT "SHELL WEIGHT                        "W6
1600 IF T7=0 THEN 1620
1610 PRINT "CAP WEIGHT                          "W7
1620 PRINT "TAPE WEIGHT                         "W2
1630 PRINT "SEAM WEIGHT                         "U9
1640 PRINT "DUCT WEIGHT                         "W4
1650 PRINT "MISCELLANEOUS WEIGHTS               "30+U8+W3
1660 FIXED 2
1670 PRINT
1680 PRINT "GORELENGTH          "S8
1690 PRINT "GORE WIDTH          "W9
1700 PRINT "MAX. DIA.           "2*R8*S8
1710 PRINT
1720 FIXED 0
1730 IF L8=0 THEN 1750
1740 PRINT "SLEEVE LENGTH       "L8
1750 IF T7=0 THEN 1780
1760 FIXED 2
1770 PRINT "CAP LENGTH          "R*S8
1780 FIXED 0
1790 PRINT "NUMBER OF GORES     "Q
1800 PRINT "TAPE STRENGTH       "L
```

```
1330 REM "DESIGN-II(B)" (CF 4.22 82JUL30)


1810 IF R7=0 THEN 1850
1820 PRINT "CHUTE DIA.          "2*R7
1830 PRINT "CHUTE WEIGHT        "W1
1840 PRINT "CHUTE SPEED         "V0
1850 IF F8=0 THEN 1870
1860 PRINT "BALLAST             "W5
1870 PRINT
1880 PRINT
1890 PRINT
1900 PRINT
1910 PRINT


1920 PRINT "                      MERID.        CIRC."
1930 PRINT
1940 FIXED 5
1950 PRINT "STRAIN (DIM):     "E1,E2
1960 FIXED 0
1970 PRINT "SEC. MOD. (PSI): "E3/144,E4/144
1980 FIXED 2
1990 PRINT "RADIUS (FT):      "R1,R2
2000 FIXED 0
2010 PRINT "STRESS (PSI):     "S1/144,S2/144
2020 FIXED 2
2030 PRINT "% SAFE STRESS:    "S1/S0/1.44,S2/S0/1.44
2040 PRINT
2050 FIXED 3
2060 PRINT "SHOCK INDEX (FT*LB/IN^2):"U2/1E+06
2070 FIXED 0
2080 PRINT "TAPE LOAD (LB):           "B1*L
2090 FIXED 2
2100 PRINT "% MAX TAPE LOAD:          "100*B1
2110 PRINT
2120 PRINT
2130 FLOAT 3
2140 PRINT "REL. ERROR IN STRESS:     "U1
2150 PRINT
2160 PRINT


2170 P7=W8/Y9
2180 B2=B7=(P7+W8)/(V1*S8^3)
2190 GOSUB 2800
2200 PRINT "DESIGN POINT"
2210 PRINT "PAYLOAD=    "P7
2220 PRINT "ALTITUDE=   "Y0
2230 PRINT "SP. LIFT=   "B2
2240 WRITE (15,1300)I2
```

```
1330 REM "DESIGN-11(B)" (CF 4.22 82JUL30)


2250 FIXED 0
2260 PRINT "PAYLOAD        ALTITUDE"
2270 PRINT " (lbs)          (feet)"
2280 PRINT P7,K0
2290 P0=100*(1+INT(P7/100))
2300 FOR P=P0 TO P3 STEP 100
2310 B2=B7+(P-P7)/(S8^3)/0.12605
2320 GOSUB 2800
2330 PRINT P,K0
2340 NEXT P
2350 WRITE (15,1300)12
2360 STOP


2370 DEF FNL(K1)
2380 REM  BINARY CHOP
2390 K9=K9+1
2400 IF ABSK1 <= K2 THEN 2500
2410 IF K1>0 THEN 2440
2420 K3=K5=1
2430 GOTO 2460
2440 K5=-1
2450 K4=1
2460 K6=K6/(K3+K4)
2470 F=F+K5*K6
2480 RETURN 2
2490 STOP
2500 K3=K4=0
2510 RETURN 1


2520 DEF FNA(A)
2530 REM  STANDARD ATMOSPHERE.
2540 C1=6356766
2550 C2=0.3048037
2560 C3=34.163195
2570 C4=0.0217484
2580 C5=0.8018105
2590 H1=E[1,2]
2600 X=C2*A
2610 X=0.001*C1*X/(C1+X)
2620 FOR I=2 TO E[1,1]
2630 J=I
2640 F1=0
2650 IF E[I+1,2]#E[I,2] THEN 2670
2660 F1=0.0001
2670 F3=(F1+E[I+1,2]-E[I,2])/(E[I+1,1]-E[I,1])
2680 IF X<E[I+1,1] THEN 2710
2690 H1=H1*((E[I,2]/(F1+E[I+1,2]))^(C3/F3))
2700 NEXT I
2710 H2=E[J,2]+F3*(X-E[J,1])
2720 H1=H1*((E[J,2]/H2)^(C3/F3))
2730 H4=C4*H1/H2
2740 H3=C5*H4
2750 H1=2.08858*H1
2760 H2=H2-273.16
2770 RETURN (H3)
2780 STOP
```

```
1330 REM "DESIGN-II(B)" (CF 4.22 82JUL30)


2790 REM ALT=FCN(SP LIFT)
2800 K3=K4=K9=0
2810 K6=1280
2820 F=80+20000
2830 K2=FNA(F-10)-FNA(F+10)
2840 K1=FNAF-82
2850 K7=FNL(-K1)
2860 IF K6<10 THEN 2880
2870 IF K7=2 THEN 2840
2880 K0=F
2890 RETURN
2900 END
```

Appendix H

Table of Existing Designs Used in Study

In the following listings, the headings are to be interpreted as follows:

Heading	Dimension	Meaning
Model	-	AFGL Assigned Model No.
Volume	FT^3	Balloon Maximum Volume
Rated	LB	Maximum Payload/rater
Flown	LB	Maximum Tested Payload (Successful)
Flt no.	-	Reference for "Flown" Assigned in AFGL Records
Gorlen	FT	Gorelength
Sigma	-	Natural Shape Number
Ref	-	Sigma Table Source
Area	FT^2	Duct Area (each)
DLEN	FT	Distance from Nadir to Duct Ellipse
DNO	-	Number of Ducts
Tapes	LB	Rated Tape Strength
Gores	-	Number of Gores
Wall	MIL	Gore Film Thickness

Heading	Dimension	Meaning
CP? EN	FT	Longest Cap Length
KRWN	MIL	Total Crown Thickness
CN	-	Number of Caps
BLNWT	LB	Total Balloon Weight
AWT	LB	Apex Fitting Weight
BWT	LB	Base Fitting Weight

In Tables H1 and H2 the payloads and altitudes are the effective design points associated with Eq. (2), Section 4.

Table H1. Design Point Conditions for Balloon Data Base

Model No.	Volume (ft^3)	Payload (lb)	Altitude (ft)	Model No.	Volume (ft^3)	Payload (lb)	Altitude (ft)
SV-001A	5033809	531	119170	LTV-001	13486500	565	139830
SV-002	2661176	699	106910	LTV-002	4849664	293	131430
SV-004	30272377	303	161610	LTV-003C	2945571	440	111770
SV-005	10578059	529	135730	LTV-005	642729	423	94130
SV-006	26600000	1309	139430	LTV-006	5033809	444	123070
SV-007	6677900	4470	97390	LTV-007	2012003	420	108810
SV-008	8740000	3841	105430	LTV-008	273600	240	86370
SV-009	10578059	853	125050	LTV-009	516000	335	92510
SV-010	37736553	435	160930	LTV-010B	859000	389	98970
SV-011	45380000	580	155530	LTV-011A	1840000	351	113890
SV-012	21770000	578	147890	LTV-012	4890000	333	127210
SV-014	15600000	917	135270	LTV-013A	2900135	913	107130
SV-015	21680000	1505	136780	LTV-014	2003675	2035	88870
SV-016A	11620000	331	141850	LTV-018	355000	575	80210
SV-017B	5142712	1331	110110	LTV-019	628000	643	88310
SV-018	3685788	481	125150	LTV-020	145026	254	77490
SV-019	5136000	1620	108970	LTV-021	264985	255	86790
SV-020	11617429	850	135270	LTV-022	449183	238	98750
SV-021	47815660	265	170910	LTV-023	1575005	231	116250
SV-022	28604910	1000	152670	LTV-024	1110000	754	95530

Table H2. Design Point Conditions for Balloon Data Base

Model No.	Volume (ft^3)	Payload (lb)	Altitude (ft)
LTV-026	2369069	1507	98790
SP-001	3016600	531	125410
SP-002	12441783	47	162530
SP-003	711460	1632	72650
SV-500	26085893	1964	135970
SV-501	27988324	2623	131140
SV-502	29008952	1561	141210
SV-503	33325200	1424	142060
SV-504	25690000	1339	142010
SV-505	25980000	1814	136530
SV-506	28048674	4066	123430
SV-507	25840000	319	152210
SV-508	28463000	2589	133890
SV-509	30390000	3690	125780
SV-510	31210000	2156	138450
SV-511	31154200	1175	145860
SV-512	30820000	862	146610
SV-513	33120000	1770	143390
SV-514	31150000	1013	144190
SV-515	33500000	4492	126860
SV-516	31650000	616	152520
SV-517	34090000	2769	133930
SV-518	34311500	3478	130030
SV-519	37780000	837	155310
SV-520	36100000	351	157190
SV-521	39590000	4568	128470
SV-523	45840000	1895	146990
SV-524	47012000	2851	139890
SV-525	70700000	1023	163440
SV-527	30500000	1123	144910
SV-528	36700000	647	152850
SV-529	50310000	1146	153900
SV-530	52600000	1609	150980
SV-531	26400000	1937	135790
SV-532	35850000	513	156890
SV-533	36360000	919	149750
SV-535	46090000	1029	152590
SV-536	30160000	571	160210
SV-522	42500000	3118	133910
SV-526	33100000	2810	133370
SV-534	33858500	293	158670

Table H3. Balloon Data Base

MODEL	VOLUME	RATED	FLOWN	REF.NO.	GORLEN	SIGMA	REF	AREA	DLEN	DNO	TAPES	GORES	WALL	CPLEN	KNN	CN	BLMWT	AMT	BMT
SV-001A	5033809	4500A	4956	H-74-062	324.00	0.400	U/M	40.00	146.0	3	500	120	1.00	110.0	2.00	1	1340	33	6
SV-002	2061176	4000	2001	H-68-075	265.00	0.300	U/A	40.00	90.0	3	500	120	1.00	108.0	2.00	1	1070	33	6
SV-004	30272377	75[illegible]	445	H-69-059	586.91			50.00	116.0	10	100	165	0.45	101.0	1.15	1	1530	33	6
SV-005	10578059	21[illegible]0M	1658	H-71-015	415.00	0.400	U/A	40.00	176.0	4	300	120	0.70	90.0	1.40	1	1335	33	6
SV-006	20000000	42000M	3946	MF-71-026	571.73			100.00	190.0	4	400	154	0.70	144.0	2.40	2	2685	33	6
SV-007	6677900	6000M	6303	H-74-023	367.40			60.00	122.0	3	800	95	1.00	193.0	3.50	2	2470	17	6
SV-008	8740000	7000M	5166	H-75-030	399.93			100.00	130.0	3	600	104	1.00	186.0	3.00	2	2400	33	6
SV-009	10578059	3500	3437	H-69-025	415.00	0.400	U/A	40.00	135.0	5	500	120	1.00	140.0	2.50	1	2150	33	6
SV-010	3773[illegible]56	725M	674	H-72-056	634.62			100.00	205.0	6	100	172	0.45	110.0	1.25	1	1910	33	4
SV-011	45380000	9000M	8990	H-74-020	674.63			100.00	287.0	6	150	189	0.60	135.0	1.60	1	2880	33	6
SV-012	21770000	10500M	10038	H-[illegible]-052	530.75			100.00	225.0	5	150	146	0.60	125.0	1.30	1	1700	33	6
SV-014	15000000	3400M	2312	H-75-039	476.05			100.00	132.5	3	300	126	0.60	159.0	2.00	2	1890	33	6
SV-015	21000000	5100M	2357	H-77-056	534.76			100.00	180.0	4	250	144	0.60	152.0	2.00	2	2145	33	6
SV-016A	11020000	2400M	2156	C-75-004	428.07			100.00	184.0	2	300	120	0.50	136.0	1.40	1	1240	25	6
SV-017B	5142712	5000M	4199	H-72-001	333.07			40.00	147.0	3	500	120	1.00	146.0	2.30	1	1600	33	6
SV-018	3068588	1300M	1738	H-81-015	296.55			40.00	130.0	2	200	80	0.50	103.0	1.20	1	560	17	6
SV-019	5130000	5000M	2020	H-71-016	331.43			40.00	112.0	3	500	90	1.00	146.0	[illegible]30	1	1470	17	6
SV-020	11017429	2400	1313	H-81-004	434.25	0.300	JHS	100.00	187.0	2	300	115	0.50	136.0	1.40	1	1240	33	6
SV-021	4781560	500M	509	C-72-021	682.71			100.00	237.0	6	60	197	0.35	128.0	1.20	2	1772	33	4
SV-022	2009491[illegible]	9000	432	H-68-062	587.00	0.300	JHS	40.00	100.0	8	100	155	0.45	90.0	1.15	1	1460	33	4
LRV-001	1348650[illegible]	1000	750	AS-013U	450.00	0.400	U/A	50.00	120.0	4	100	125	0.75	0.0	0.75	0	1425	10	6
LRV-002	4849664	600A	911	H-66-066	320.00	0.400	U/A	25.00	179.0	4	100	88	0.75	0.0	0.75	0	740	10	6
LRV-003	2943571	4900M	30[illegible]	C-67-005	271.00	0.400	U/A	25.00	190.0	3	650	75	1.50	0.0	1.50	0	1110	17	6
LRV-005	642729	750	0		167.00	0.200	U/M	20.00	42.0	2	250	60	1.50	0.0	1.50	0	356	17	6
LRV-006	5033809	3000A	3000	AS-0058	324.00	0.400	U/M	40.00	146.0	3	500	120	1.00	0.0	1.00	0	1120	33	6
LRV-007	2012003	2300M	2165	H-78-052	241.00	0.350	JHS	20.00	100.0	3	500	64	1.50	0.0	1.50	0	800	17	6
LRV-008	473600	1200M	1106	H-79-011	120.51			8.75	63.0	2	200	52	1.50	0.0	1.50	0	239	17	6
LRV-009	510000	1200M	949	H-80-025	155.42			10.00	75.0	2	200	54	1.50	0.0	1.50	0	340	17	6
LRV-010B	859000	1100M	952	H-75-029	183.37			20.00	78.0	2	200	56	1.50	0.0	1.50	0	440	17	6
LRV-011A	1840000	1200M	1145	H-79-019	235.54			20.00	103.0	3	150	85	1.00	0.0	1.00	0	525	17	6
LRV-012	4890000	950M	1237	H-79-047	323.73			23.75	108.0	3	150	93	1.00	0.0	1.00	0	925	17	6
LRV-013A	4900135	3000M	4602	H-77-034	274.81	0.250	JHS	40.00	122.0	2	500	73	1.50	0.0	1.50	0	995	17	6
LRV-014	2003675	4000M	3091	C-74-002	245.88	0.150	JHS	25.00	83.0	2	600	64	2.00	0.0	2.00	0	1080	17	6
LRV-018	355000	1875M	1330	H-77-010	139.19			10.00	61.5	2	400	36	1.50	0.0	1.50	0	260	17	6
LRV-019	628000	1650M	1441	H-80-016	167.61			15.00	80.0	2	300	43	1.50	0.0	1.50	0	360	17	6
LRV-020	145026	750M	803	C-74-007	102.47	0.150	JHS	5.00	31.0	2	250	26	1.50	0.0	1.50	0	135	17	6
LRV-021	2649[illegible]	900M	892	H-72-072	124.48	0.200	JHS	10.00	35.0	2	250	33	1.50	0.0	1.50	0	200	17	6
LRV-022	449183	600M	554	C-72-012	148.20	0.200	U/M	10.00	50.0	2	250	39	1.00	0.0	1.00	0	200	17	6
LRV-023	1575005	1440M	712	[illegible]3-030	222.11	0.350	JHS	20.00	75.0	2	250	67	1.00	0.0	1.00	0	440	17	6
LRV-024	1110000	1650M	1525	H-80-015	201.80			25.00	89.0	2	250	52	1.50	0.0	1.50	0	505	17	6

Table H3. Balloon Data Base (Contd)

MODEL	VOLUME	RATED	FLOWN	FLT.NO.	GURLEY	SIGMA	REF	AREA	DLEN	DNO	TAPES	CORES	WALL	CPLEN	KNEE	CH	BLNWT	AMT	BWT
SPV-026	23e9069	3400W	1311	H-79-034	260.00	0.150	JHS	25.00	110.0	2	500	67	1.50	0.0	1.50	0	800	17	6
SP-001	301e630	700W	413	C-72-020	278.91			20.00	90.0	3	100	75	0.35	74.0	1.05	2	318	17	4
SP-002	12441783	100W	93	H-71-036	435.14			40.00	148.0	4	50	125	0.35	91.0	0.70	1	681	14	4
SP-003	7114e0	5000W	3856	H-72-057	174.87			20.00	58.0	2	500	83	1.50	174.9	3.00	1	780	17	6
SV-500	26085893	3800W	3004	MF-80-001	569.29			125.00	200.0	4	300	154	0.60	168.0	2.30	2	2588	33	10
SV-501	27988324	5400W	3686	MF-80-002	583.15			150.00	193.0	4	400	157	0.70	184.0	2.90	2	3416	33	10
SV-502	29008952	3400W	2287	MF-80-003	588.80			125.00	196.0	5	300	160	0.50	165.0	2.20	2	2470	32	6
SV-503	33325200	3900W	3102	MF-80-004	614.43			125.00	205.0	5	300	168	0.60	172.0	2.30	2	3041	33	10
SV-504	23690000	3000W	2786	MF-78-005	566.50			100.00	188.0	5	200	152	0.50	157.0	1.90	2	2113	33	6
SV-505	25980000	4000W	3786	MF-74-006	569.43			100.00	189.0	5	300	154	0.60	164.0	2.20	2	2607	33	6
SV-506	26048674	7250W	5800	MF-79-007	585.93			150.00	196.0	4	600	156	0.80	215.0	3.40	3	4507	33	10
SV-507	25840000	2000W	2003	76-001	560.26			100.00	186.0	5	200	157	0.50	139.0	1.60	2	1939	33	6
SV-508	28463000	4500W	3697	MF-80-008	582.53			150.00	196.0	4	300	157	0.60	175.0	2.50	2	2853	33	10
SV-509	36390000	7500W	0		603.68			100.00	200.0	6	500	160	0.90	205.0	3.40	2	4650	33	10
SV-510	31210000	4000W	0		606.40			100.00	200.0	6	300	162	0.50	212.0	2.30	3	2733	33	6
SV-511	31154200	2700W	2029	MF-80-011	600.80			150.00	200.0	4	200	164	0.50	155.0	2.00	2	2376	33	6
SV-512	30820000	2800W	2305	MF-75-012	596.64			100.00	198.0	5	300	163	0.60	155.0	2.00	2	2541	33	6
SV-513	33120000	3400W	2690	MF-77-013	619.02			100.00	195.0	6	250	164	0.50	163.0	2.20	3	2425	33	6
SV-514	31150000	3800W	3420	77-006	598.00			100.00	200.0	5	300	166	0.60	162.0	2.20	2	2800	33	6
SV-515	33500000	6000W	6068	75-002	620.48			100.00	205.0	6	400	166	0.90	191.0	3.10	2	4300	33	6
SV-516	31650000	2000W	1528	MF-77-014	601.20			100.00	200.0	6	150	165	0.50	141.0	1.70	2	2116	33	6
SV-517	34090000	5050W	4800	MF-78-015	624.03			100.00	208.0	6	400	170	0.80	171.0	2.80	2	3732	33	10
SV-518	34311500	6000W	4813	MF-79-016	625.28			150.00	207.0	5	500	167	0.70	208.0	3.10	3	4306	33	10
SV-519	37780000	2000W	1995	MF-76-017	641.35			100.00	213.0	7	150	176	0.40	137.0	1.60	2	2670	33	6
SV-520	36100000	1600W	1364	75-007	624.84			100.00	210.0	6	150	174	0.50	137.0	1.60	2	2235	33	6
SV-521	39590000	7500W	6593	MF-80-018	658.08			100.00	218.0	8	500	175	0.80	203.0	3.50	3	5064	33	10
SV-523	45840000	3900W	0		686.31			100.00	225.0	8	250	185	0.50	168.0	2.40	3	3089	33	6
SV-524	47012000	6300W	0		693.06			200.00	225.0	5	400	187	0.50	205.0	3.20	2	4064	33	10
SV-525	70700000	2500W	0		785.78			200.00	260.0	6	200	220	0.35	165.0	2.05	3	2974	33	6
SV-527	30500000	2800W	2749	MF-72-022	595.02			100.00	160.0	5	300	163	0.60	144.0	2.00	2	2498	33	6
SV-528	36700000	2420W	1877	73-004	630.26			100.00	210.0	5	250	176	0.50	149.0	1.90	2	2478	33	6
SV-529	50310000	2000W	1609	74-005	703.56			100.00	233.0	8	200	193	0.50	152.0	1.90	2	2956	33	6
SV-530	52000000	3200W	1905	MF-75-023	715.94			100.00	240.0	9	250	195	0.50	155.0	2.20	2	3228	33	6
SV-531	2e400000	4000W	0		571.81			100.00	195.0	5	300	154	0.70	164.0	2.40	2	2706	32	6
SV-532	35850000	1000W	1149	72-010	624.41			100.00	225.0	4	150	174	0.50	121.0	1.40	1	2083	17	w
SV-533	36360000	2400W	1960	MF-75-024	630.84			100.00	225.0	5	200	174	0.50	151.0	1.90	2	2600	33	6
SV-535	46090000	2000W	1834	72-012	681.99			100.00	225.0	7	200	188	0.50	151.0	1.90	2	2937	33	6
SV-536	30160000	800W	896	MF-71-025	587.93			100.00	185.0	4	80	163	0.45	88.0	1.15	1	1355	15	4
SV-522	42500000	5900W	4751	MF-80-019	668.97			150.00	223.0	5	400	181	0.80	211.0	3.30	3	5000	33	10
SV-526	33100000	4500W	3615	72-003	616.69			100.00	212.0	6	300	165	0.90	167.0	2.70	2	3660	33	6

Table H3. Balloon Data Base (Contd)

MODEL	VOLUME	RATED	FLOAN	FLT.NO.	GORLEN	SIGMA	REF	AREA	DLEN	DNO	TAPES	GORES	WALL	CPLEN	KMAN	CN	BLMWT	AWT	BWT
SV-534	33858500	1e00W	1423	70-011	611.38			100.00	165.0	5	200	171	0.45	124.0	1.45	2	2000	34	4